MONTHLY NOTICES

OF THE

ROYAL ASTRONOMICAL SOCIETY.

VOL. LXXXVIII. NOVEMBER 11, 1927. No. 1

Rev. T. E. R. PHILLIPS, PRESIDENT, in the Chair.

Ram Behari, M.A., Lecturer in Mathematics, St. Stephen's College, Delhi, India, and Sidney Sussex College, Cambridge ;
Alfred Allinson Bourne, M.A., Prestwich Lodge, Cheltenham, Glos ;
Theodor S. Jacobsen, Assistant in the Lick Observatory, Cal., U.S.A. ;
Hamilton M. Jeffers, Assistant Astronomer in the Lick Observatory, Cal., U.S.A. ;
Ernest Alfred Letcher, 815 Higgins Building, Los Angeles, Cal., U.S.A. ;
Allen D. Maxwell, James M. Goewey Fellow in the University of California, Berkeley, Cal., U.S.A. ;
Joseph H. Moore, Astronomer in the Lick Observatory, Cal., U.S.A. ;
Frank Robinson, A.I.N.A., Cunard Steamship Co., Ltd., and 78 Welbeck Street, Princes Avenue, Hull ;
Wyman W. Storer, Fellow in the Lick Observatory, Cal., U.S.A. ;
Robert J. Trumpler, Associate Astronomer in the Lick Observatory, Cal., U.S.A. ;
Cromwell Hall Warren, 23 Florence Park, Redland, Bristol ;
Howard Welch, B.Sc., 35 Century Road, Oldbury, Worcs ;
William H. Wright, Assoc. R.A.S., Astronomer in the Lick Observatory, Cal., U.S.A. ; and
Ch'ing-Sung Yü, Martin Kellog Fellow in the Lick Observatory, and University of Amoy, China,

were balloted for and duly elected Fellows of the Society.

The following candidates were proposed for election as Fellows of the Society, the names of the proposers from personal knowledge being appended :—

Herbert Brown, The Haven, 11 Walsingham Road, Enfield, Middlesex (proposed by W. H. Steavenson) ;

Lt.-Col. George Dudley MacMahon, The Orchard, Church Crookham, Hants (proposed by P. A. MacMahon) ;

Mrs. Louise Victoria Mathieson, 6 Park Circus Place, Glasgow (proposed by P. A. MacMahon) ; and

Frederick Gordon Wood, M.A., Headmaster, Caldicott School, Hitchin, Herts (proposed by T. M. Cherry).

One hundred and ninety-three presents were announced as having been received since the last meeting, including, amongst others :—

Peter Doig : An Outline of Stellar Astronomy.

S. A. Mitchell and C. G. Abbot : The Fundamentals of Astronomy.

Catania Observatory, Astrographic Catalogue, vol. 3, parte 2 (fasc. 18).

San Fernando Observatory, Astrographic Charts, zone $-3°$ (10 charts).

Enlarged and framed photograph of a Chinese Planisphere (*for particulars see M.N.*, **69**, 435), presented by Mr. E. B. Knobel.

Total Solar Eclipse, 1927 June 29 : Enlarged print of corona, photographed at Giggleswick (presented by the Astronomer Royal).

———— One print of inner corona and three prints of outer corona, photographed by the Hamburg Observatory Expedition at Jokkmokk, Lapland (presented by Prof. R. Schorr).

Celestial Photographs.

The following have been added to the list of Celestial Photographs reproduced by the Society for sale to the Fellows :—

R.A.S. Ref. No.

392. Solar Corona, 1927 June 29, Giggleswick. 6-in. Refr., F.L. 45 ft. Exp. 19 secs. J. Jackson.

393. Solar Corona, 1927 June 29, Jokkmokk. 11-m. Refl., Ap. 35 cm. Exp. 1 sec. Hamburg Observatory Expedition.

394. Solar Corona, 1927 June 29, Jokkmokk. Refr., Ap. 10 cm., F.L. 3·65 m. Exp. 25 secs. Hamburg Observatory Expedition.

The Motion of Gases in the Sun's Atmosphere. By S. R. Pike.

(*Communicated by Prof. E. A. Milne, F.R.S.*)

Introduction.—The conclusion appears to be now generally accepted that the upper parts of the sun's atmosphere are supported almost entirely by radiation pressure.* If an atom reaches a height of more than 6000 or 7000 km., we may safely conclude that the radiation pressure acting upon it under normal circumstances is equal to its own weight. At such heights the gas pressure is very small, probably 10^{-9} atm. at 6000 km., and 10^{-11} atm. at 10,000 km., so that collisions between atoms will be a matter of some rarity. In the case of hydrogen the average intervals between collisions at these pressures and at 6000° A. are 36 seconds and 1 hour respectively, whilst for Ca the intervals are $7\frac{1}{2}$ minutes and $12\frac{1}{2}$ hours. Thus, in the absence of electrical forces, the motion of the atoms should be controlled almost entirely by the radiation from the sun's disc.

In the present paper an attempt is made to calculate the magnitude of the accelerations and velocities which may be expected to arise from this cause, and to examine how far the known facts can be accounted for in this way alone without the aid of any additional hypotheses. The motions which have been observed are sometimes very large and violent, as evidenced, for example, by Pettit's work † on prominences and the observations of Hale ‡ on hydrogen flocculi. We shall refer to these in detail later on.

The problem to be solved is to calculate the acceleration of an atom situated at any height above an infinite radiating surface, not necessarily uniform, with the condition that when the surface is uniform and at a given temperature T, the atom is to be in equilibrium.

In considering this problem there are two main principles which have to be taken into account.

(a) *Effect of a Particular Area.*—If a particular area is raised to a temperature above or below the normal value T, then the equilibrium of the atom will be upset ; a rise in temperature will give it an upward acceleration § and also repel it away from the area in question, whilst a fall in temperature will cause it to sink, and to move horizontally || towards this area.

In general, of course, the area may be quite irregular in shape, and detailed calculation of the actual vertical and horizontal forces will not be possible ; but we can get a good idea of their magnitude from the results for a particular geometrical shape. Calculations have been carried out for the case of a square or rectangle, and are given in § 1.

(b) *Doppler Effect.*—It has already been shown by Milne in a well-

* Milne, *M.N.*, **84**, 354 ; **85**, 111 ; **86**, 8.

† *Publications of the Yerkes Observatory*, **3**, pt. iv.

‡ *Astr. Journ.*, **28** (1908), 100 ; *Proc. Nat. Ac. Sci.*, **11** (1925), 691 ; *Nature*, **119** (1927), 708 ; and other papers.

§ Sur, *Astrophys. Journ.*, **63**, 111.

|| Pike, *M.N.*, **87**, 56.

known paper * that the equilibrium of an atom under radiation pressure in a V-shaped absorption line is unstable for upward displacements. If the atom acquires a rapid vertical motion it absorbs at a shorter wave-length than that corresponding to the point of the V, *i.e.* it absorbs in a region of increased intensity, and so will be continuously accelerated outwards.

There are two other points of importance in this connection, however, which do not seem to have been previously pointed out, viz. that a large *horizontal* velocity will also cause vertical instability due to the Doppler effect, and that a *vertical* velocity will produce a net horizontal force different from zero. These results are a consequence of the fact that the radiations from the outer part of the sun's disc are received at an angle inclined to the vertical, and so both vertical and horizontal velocities affect the wave-length received by the atom. Exact expressions are worked out in § 2, but it must be pointed out that calculations of this sort only hold good so long as the number of atoms involved is small enough to have no effect on the contour of the absorption line. Owing to the low density of the chromosphere, however, this condition is likely to be fulfilled in nearly every case.

§ 1. *Radiation Pressure exerted by any Part of the Sun's Disc.*

We consider an atom in equilibrium at a height h above the sun's disc, *i.e.* above an infinite radiating plane. The atom only absorbs light of frequency between ν and $\nu + d\nu$, and has an absorption coefficient k_ν; that is to say, if the radiation incident in a direction θ, ϕ, and contained in the solid angle

$$d\omega = \sin\theta d\theta d\phi,$$

has energy density

$$\mathrm{I}(\nu, \theta, \phi)d\nu d\omega,$$

then the force on the atom in this direction is, by definition,

$$k_\nu \,.\, \mathrm{I}(\nu, \theta, \phi).$$

The vertical component of this force is

$$k_\nu \mathrm{I}(\nu, \theta, \phi)d\nu d\omega \cos\theta,$$

and the total vertical component, which must be equal to $mg_\odot$, the weight of the atom, is

$$k_\nu d\nu \int_0^{2\pi}\int_0^{\pi/2} \mathrm{I}(\nu, \theta, \phi)\cos\theta \sin\theta d\phi d\theta.$$

If the surface is at a uniform temperature T, then $\mathrm{I}(\nu, \theta, \phi)$ is independent of θ, ϕ, and the condition for equilibrium becomes

$$mg_\odot = \pi k_\nu \mathrm{I}(\nu)d\nu \quad . \quad . \quad . \quad . \quad (1)$$

Milne has shown that this equation may be applied to determine the mean " life " τ in the excited state of any atom which absorbs all its

* *M.N.*, **86**, 474.

energy on one wave-length, such as Ca+ ; and thence the value of τ may be found from the equation

$$k_\nu d\nu = e/8\pi\nu^2\tau.$$

Milne's value $\tau = 1{\cdot}8 \times 10^{-8}$ sec. gives $k_\nu d\nu = 10^8$.

There are also horizontal forces due to each half of the plane acting separately ; these, of course, cancel out if the surface brightness follows a symmetrical law, but not otherwise.

The force along $\phi = 0$, due to the semi-infinite plane bounded by $\phi = \pm\frac{\pi}{2}$, is easily found to be

$$\tfrac{1}{2}\pi k_\nu \mathrm{I}_\nu d\nu = \tfrac{1}{2}mg_\odot.$$

The problem which we require to solve is to find the vertical and horizontal forces at a given point due to any selected area of the sun's surface ; our subsequent intention being, of course, to find the effect of a sudden change in the temperature of this area to some definite value above or below that of the rest of the photosphere.

It is convenient to introduce a quantity

$$\sigma_0 = k_\nu \mathrm{I}_\nu d\nu$$

which measures the radiation pressure on a given atom under standard conditions. Our problem then becomes formally identical with an electrostatic problem in which the surface density of electrification is given by

$$\sigma = \sigma_0 \cos\theta$$

at a point lying in a direction θ, as seen from the atom under consideration.

This expression applies only to a uniform radiating disc, but if we wish to take account of the law of solar darkening (as we shall have to do), then the "surface density" becomes

$$\sigma = \sigma_0 \cos\theta(1 - a_\nu + a_\nu \cos\theta) = \sigma_0(\beta \cos\theta + a\cos^2\theta) \qquad (2)$$

Force exerted by a Disc.—The simplest case is that of an atom situated on the axis of a circular disc of radius a. The vertical force is found to be

$$\pi\sigma_0\left\{\beta\left(1 - \frac{h^2}{h^2 + a^2}\right) + \tfrac{2}{3}a\left(1 - \frac{h^3}{(h^2 + a^2)^{3/2}}\right)\right\} \qquad (3)$$

If $\beta = 1$, $a = 0$ (no darkening), this agrees with a result already given by Sur.*

Taking $a = \infty$, we get the vertical force exerted by the whole of the sun's disc, viz.

$$\pi\sigma_0(\beta + \tfrac{2}{3}a) = \pi\sigma_0(1 - \tfrac{1}{3}a),$$

and consequently equation (1) must be replaced by

$$mg_\odot = \pi\sigma_0(1 - \tfrac{1}{3}a) \qquad (4)$$

* *Loc. cit*

The horizontal force due to half the disc is, similarly,

$$\sigma_0\left\{\beta\left(\tan^{-1}\frac{a}{h}-\frac{ah}{h^2+a^2}\right)+\tfrac{2}{3}\alpha\frac{a^3}{(h^2+a^2)^{3/2}}\right\} \quad . \quad (5)$$

but to find the forces at a point off the axis is not so simple. We cannot expand the potential in the ordinary way as a series of Legendre coefficients, as a potential function in the ordinary sense of the term does not appear to exist, and it is simpler to begin *ab initio* and integrate the forces directly.

It so happens that a square or rectangle presents fewer mathematical

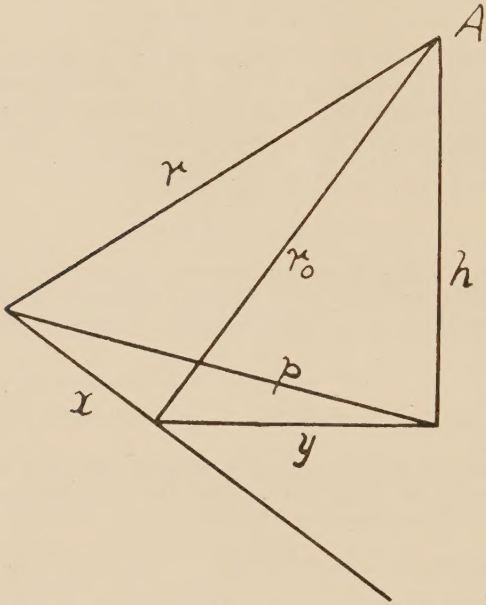

Fig. 1.

difficulties than a circle, and we shall therefore calculate the forces exerted by a figure of this shape. The actual shape of any sunspot is, of course, irregular, and would not in any case lend itself conveniently to calculation ; and all that we can hope to do, therefore, is to estimate the magnitude of the forces acting in any particular case, for which purpose one geometrical figure is as good as another.

Force exerted by a Filament.—Consider a straight filament on the surface of the sun, distant y from the foot of the perpendicular from A, and of width dy (fig. 1).

The vertical force exerted at A by any element dx of this filament is

$$dV = \sigma_0 dy dx h^2\left(\frac{\beta}{(r_0{}^2+x^2)^2}+\frac{\alpha h}{(r_0{}^2+x^2)^{5/2}}\right)$$

where $$r_0^2 = h^2 + y^2$$

and the horizontal force resolved along the direction of y is

$$dH = \frac{y}{h} dV.$$

Thus, if the filament extends from $x = a$ to $x = b$, we have

$$V = \sigma_0 h^2 dy \left[\frac{\beta}{2r_0^3} \left(\tan^{-1} \frac{x}{r_0} + \frac{xr_0}{x^2 + r_0^2} \right) + \frac{\alpha h}{3r_0^4} \left(\frac{3x}{(x^2 + r_0^2)^{1/2}} - \frac{x^3}{(x^2 + r_0^2)^{3/2}} \right) \right]_b^a$$

and

$$H = yV/h \quad . \quad . \quad . \quad . \quad (6)$$

Force exerted by a Lamina.—We can now find by direct integration between suitable limits the force exerted by any rectangular area, and it is most convenient to take the case of a square whose side is bisected by y. As already explained, the loss of generality is of no importance.

By inserting the limits $\pm a$, we have then the expressions

$$V = \sigma_0 h^2 \int_{y_1}^{y_1 + 2a} \beta dy \left[\frac{1}{(y^2 + h^2)^{3/2}} \tan^{-1} \frac{a}{\sqrt{y^2 + h^2}} + \frac{a}{(y^2 + h^2)(y^2 + h^2 + a^2)} \right]$$

$$+ \sigma_0 h^3 \int_{y_1}^{y_1 + 2a} \alpha dy \left[\frac{2a}{(y^2 + h^2)^2 (y^2 + h^2 + a^2)^{1/2}} - \frac{2a^3}{3(y^2 + h^2)^2 (y^2 + h^2 + a^2)^{3/2}} \right]$$

or

$$V = \sigma_0 \beta (I_1 + I_2) + \sigma_0 \alpha (I_3 - I_4)$$

where

$$I_1 = \int \frac{h^2}{(y^2 + h^2)^{3/2}} \tan^{-1} \frac{a}{\sqrt{y^2 + h^2}} dy$$

$$= \frac{h}{a} \tan^{-1} \frac{h}{y} + \frac{y}{\sqrt{y^2 + h^2}} \tan^{-1} \frac{a}{\sqrt{y^2 + h^2}} - \frac{\sqrt{h^2 + a^2}}{a} \tan^{-1} \frac{1}{\sqrt{m^2 + n^2}}$$

$$I_2 = \int \frac{ah^2 dy}{(y^2 + h^2)(y^2 + h^2 + a^2)} = \frac{h}{a} \tan^{-1} \frac{y}{h} - \frac{h^2}{a\sqrt{h^2 + a^2}} \tan^{-1} \frac{y}{\sqrt{h^2 + a^2}}$$

between limits ; and

$$I_3 = \int \frac{2ah^3 dy}{(h^2 + y^2)^2 \sqrt{a^2 + h^2 + y^2}}$$

$$= \frac{a^2 - h^2}{a^2} \tan^{-1} \left(\frac{ay}{h\sqrt{y^2 + h^2 + a^2}} \right) + \frac{h}{a} \cdot \frac{y\sqrt{y^2 + h^2 + a^2}}{(y^2 + h^2)}$$

$$I_4 = \int \frac{2a^3 h^3 dy}{3(y^2 + h^2)(y^2 + h^2 + a^2)^{3/2}}$$

$$= \frac{2h^3 y}{3a(a^2 + h^2)\sqrt{y^2 + h^2 + a^2}} + \frac{a^2 - h^2 - 4h^4}{3a^2(a^2 + h^2)} \tan^{-1} \frac{ay}{h\sqrt{y^2 + h^2 + a^2}}$$

$$+ \frac{h}{3a} \cdot \frac{y\sqrt{y^2 + h^2 + a^2}}{(y^2 + h^2)},$$

so that

$$I_3 - I_4 = \tfrac{2}{3}\left[\tan^{-1}\frac{ay}{h\sqrt{y^2+h^2+a^2}} + \frac{h}{a}\frac{y\sqrt{y^2+h^2+a^2}}{(y^2+h^2)} - \frac{h^3}{a(a^2+h^2)}\frac{y}{\sqrt{y^2+h^2+a^2}}\right]$$

between the same limits.

These integrals give the value of the vertical force due to a square of side $2a$ at any point (y, h), where the axis of y bisects the side of the square; and their values at various heights and distances have been found and tabulated.

The most convenient proceedure is to measure y and h in terms of a; thus let

$$y = ma, \qquad h = na,$$

where m, n may have any value.

Then we can construct two tables, corresponding to the α term and the β term respectively, using the equations

$$I_\beta = I_1 + I_2 = \left[\begin{array}{l} n\tan^{-1}\frac{m}{n} + n\tan^{-1}\frac{n}{m} + \frac{m}{\sqrt{m^2+n^2}}\tan^{-1}\frac{1}{\sqrt{m^2+n^2}} \\ -\frac{n^2}{\sqrt{1+n^2}}\tan^{-1}\frac{m}{\sqrt{1+n^2}} - \sqrt{1+n^2}\tan^{-1}\frac{\sqrt{1+n^2}}{m} \end{array}\right]_m^{m+2} \quad (7)$$

$$I_\alpha = \tfrac{2}{3}\left[\tan^{-1}\frac{m}{n\sqrt{1+m^2+n^2}} + \frac{nm}{m^2+n^2}\sqrt{1+m^2+n^2} - \frac{n^3}{1+n^2}\cdot\frac{m}{\sqrt{1+m^2+n^2}}\right]_m^{m+2} \quad (8)$$

In Tables I. and II. are given the numerical values of these expressions corresponding to

$$n = 1, 2, 3, 4, 6,$$

and

$$m = 0, 1, 2, 4, 6, 8.$$

TABLE I.

Values of I_β.

$m=$	0.	1.	2.	4.	6.	8.
$n=1$	1·05	·299	·049	·0078	·001	·0009
2	·794	·257	·104	·0205	·0065	·0028
3	·330	·212	·110	·0346	·0093	·0066
4	·219	·163	·091	·0400	·0128	·0095
6	·101	·080	·070	·0384	·0199	·012

TABLE II.

Values of I_α.

$m=$	0.	1.	2.	4.	6.	8.
$n=1$	·837	·118	·0175	·0015	·000	·000
2	·503	·194	·057	·0123	·000	·000
3	·307	·177	·0835	·0174	·001	·000
4	·202	·139	·0801	·0247	·0047	·0027
6	·0997	·0833	·0663	·0330	·0117	·0077

Similarly, we have for the horizontal force

$$J = \sigma_0\beta\int\frac{hydy}{(y^2+h^2)^{3/2}}\tan^{-1}\frac{a}{(y^2+h^2)^{1/2}} + \sigma_0\beta\int\frac{aydy}{(y^2+h^2)(y^2+h^2+a^2)}$$
$$+ \sigma_0\alpha\int\frac{2ah^2ydy}{(y^2+h^2)^2\sqrt{y^2+h^2+a^2}} - \sigma_0\alpha\int\frac{2a^3h^2ydy}{3(y^2+h^2)^2(y^2+h^2+a^2)^{3/2}}$$

between the limits y and $y+2a$; or, splitting this up into an α term and a β term,

$$J = \sigma_0\beta J_\beta + \sigma_0\alpha J_\alpha, \qquad (9)$$

we find

$$J_\beta = -\left[\frac{h}{\sqrt{y^2+h^2}}\tan^{-1}\frac{a}{\sqrt{y^2+h^2}}\right]_y^{y+2a}$$

$$J_\alpha = -\left[\frac{2ah^2}{3(y^2+h^2)}\cdot\frac{1}{\sqrt{y^2+h^2+a^2}}\right]_y^{y+2a}$$

Putting $y = ma$, $h = na$, the horizontal force exerted by a square patch may then be found from tables of the functions

$$J_\beta = \left[-\frac{n}{\sqrt{m^2+n^2}}\cdot\tan^{-1}\frac{1}{\sqrt{m^2+n^2}}\right]_m^{m+2} \qquad (10)$$

and

$$J_\alpha = \left[-\frac{2n^2}{3(m^2+n^2)\sqrt{1+m^2+n^2}}\right]_m^{m+2} \qquad (11)$$

Values for $n = 1, 2, 3, 4, 6,$
$m = 0, 1, 2, 4, 6, 8,$

are given in Tables III. and IV.

TABLE III.

Values of J_β.

$m=$	0.	1.	2.	4.	6.	8.
$n=1$	·597	·339	·130	·031	·012	·0055
2	·224	·226	·142	·049	·020	·010
3	·097	·127	·107	·052	·025	·013
4	·048	·073	·073	·047	·028	·014
6	·016	·028	·034	·032	·023	·016

TABLE IV.

Values of J_α.

$m=$	0.	1.	2.	4.	6.	8.
$n=1$	·417	·172	·045	·0063	·0017	·0006
2	·187	·163	·082	·021	·0035	·0022
3	·087	·104	·077	·027	·0101	·0041
4	·045	·064	·058	·030	·014	·0061
6	·016	·027	·030	·024	·015	·0085

Force at great Distances.—Finally, at great distances we have

$$I_\beta = Ah^2/R^4, \qquad I_\alpha = Ah^3/R^5$$
$$J_\beta = Ahy/R^4, \qquad J_\alpha = Ah^2y/R^5$$

where $A = 4a^2$ is the area of the spot, and

$$R^2 = y^2 + h^2.$$

Then

$$\left.\begin{aligned} V &= \sigma_0 A\left(\frac{\beta h^2}{R^4} + \frac{\alpha h^3}{R^5}\right) \\ H &= \sigma_0 A\left(\frac{\beta hy}{R^4} + \frac{\alpha h^2 y}{R^5}\right) \end{aligned}\right\} \quad . \quad . \quad . \quad (12)$$

and these equations are evidently true, whatever be the shape of the spot, so long as its area is A.

Effect of altering the Temperature.—We are now in a position to find the force exerted on an atom by any square region of the photosphere whose temperature differs from that of its surroundings. For, confining our attention to radiation of a particular frequency ν, we have

$$\frac{\sigma_1}{\sigma_0} = \frac{e^{h\nu/kT_0} - 1}{e^{h\nu/kT_1} - 1},$$

where σ_0, T_0 refer to the normal parts of the photosphere, σ_1, T_1 to the particular area under consideration.

Now, when this area is at T_0, the atom is in equilibrium under radiation pressure and gravity; and so the net force exerted on the atom, following on the change of temperature, is

$$V_1 = (\sigma_0 - \sigma_1)(\beta I_\beta + \alpha I_\alpha) = xV_0 \quad . \quad . \quad (13)$$

$$H_1 = (\sigma_0 - \sigma_1)(\beta J_\beta + \alpha J_\alpha) = xH_0 \quad . \quad . \quad (14)$$

where $x = 1 - \sigma_1/\sigma_0$. Forces directed towards the area are reckoned positive.

TABLE V.

Values of x.

T=	4000.	4500.	5000.	5500.	6000.	6500.	7000.	7500.
λ=6564	0·842	0·708	0·524	0·287	0·000	0·25	0·73	1·13
4861	0·915	0·807	0·628	0·364	0·000	0·46	1·03	1·71
3950	0·952	0·868	0·696	0·424	0·000	0·59	1·37	2·37
1215	1·000	0·999	0·996	0·833	0·000	0·67	1·81	4·09
912	1·000	1·000	0·995	0·907	0·000	6·4	41	188

In Table V. values are given of σ_1/σ_0 and x at various different temperatures and wave-lengths, taking $T_0 = 6000°$ A. The most important temperatures are 4500° A. and 7500° A., corresponding to sun-

spots and faculæ respectively. The relevant wave-length, on the other hand, depends upon the element chosen for consideration. If we are dealing with Ca+ vapour, for instance, we take for λ the mean of the H and K lines, viz. 3950 Å.U. In the case of hydrogen, however, we are confronted with the difficulty that we do not know which line, if any, is responsible for the main bulk of the absorption, or whether the work is more or less evenly shared amongst a large number of lines. Fortunately this uncertainty is not very serious at the lower temperatures; for instance, at 4500° A. it is evident from the table that x cannot be very different from 0·85, whatever lines are involved, and, in any case, must lie between 0·71 and 1·00.

At 7500°, however, the value of x rises rapidly at the shorter wave-length.

As an example of the use of the foregoing methods we will calculate the actual accelerations of a calcium atom at different distances from a sunspot of definite area, assuming the temperature of the latter to be 4500° A.

Combining equation (4) with equation (13) we have

$$\frac{V}{mg_\odot} = \frac{x(\beta I_\beta + \alpha I_\alpha)}{\pi(1 - \frac{1}{3}a)},$$

and we take the darkening coefficient a as $\frac{2}{5}$, so that

$$\frac{V}{mg_\odot} = \frac{x(2I_\beta + 3I_\alpha)}{4\pi}.$$

Similarly,

$$\frac{H}{mg_\odot} = \frac{x(2J_\beta + 3J_\alpha)}{4\pi}.$$

The value of x is 0·868, and we may take to represent the dimensions of a medium-sized spot

$$a = \tfrac{1}{2} \times 10^4 \text{ km.}$$

In Tables VI. and VIA. are given the accelerations of a Ca+ atom towards the spot at different heights and distances; these are expressed in terms of $g_\odot$ as unit where

$$g_\odot = 0{\cdot}271 \text{ km./sec.}^2.$$

TABLE VI.

Vertical Accelerations of Ca+ Atom.

	y.	0.	5×10^3.	10^4.	2×10^4.	4×10^4.	10^5 km.
h	5×10^3	·319	·066	·010	·0014	2×10^{-4}	$4{\cdot}8\times10^{-6}$
	10^4	·170	·076	·026	·0054	·0004	$1{\cdot}7\times10^{-5}$
	$1{\cdot}5\times10^4$	·109	·066	·032	·0084	·0009	$3{\cdot}6\times10^{-5}$
	2×10^4	·073	·050	·030	·0106	·0020	$6{\cdot}6\times10^{-5}$
	3×10^4	·028	·024	·019	·0099	·0028	$1{\cdot}5\times10^{-4}$

TABLE VIa.

Horizontal Accelerations of Ca+ Atom.

	y.	0.	5×10^3.	10^4.	2×10^4.	4×10^4.	10^5. km.
h	5×10^3	·169	·083	·027	·0056	9×10^{-4}	$7{\cdot}4\times10^{-6}$
	10^4	·083	·066	·036	·011	·0018	$1{\cdot}6\times10^{-5}$
	$1{\cdot}5\times10^4$	·032	·039	·031	·013	·0028	$2{\cdot}4\times10^{-5}$
	2×10^4	·016	·023	·022	·013	·0042	$3{\cdot}3\times10^{-5}$
	3×10^4	·0057	·0095	·0109	·0095	·0040	$5{\cdot}0\times10^{-5}$

Thus, for example, an atom at a height 15,000 km. above this sunspot and distant 20,000 km. from it horizontally will have an acceleration downwards of

$$230 \text{ cm./sec.}^2$$

and a horizontal acceleration towards the spot of

$$350 \text{ cm./sec.}^2.$$

As an indication of the order of magnitude involved it may be pointed out that this atom will acquire vertical and horizontal velocities of 1 km./sec. in about 7 minutes and 5 minutes respectively, during which time it will have descended about 220 km. and moved 140 km. nearer to the spot.

The foregoing applies in the first instance only to a Ca+ atom; but the same accelerations, within about 20 per cent., will be experienced by all other atoms which are found in the chromosphere, such as hydrogen, helium, strontium, etc.

If we replace the spot by a facula of the same area and at a temperature of 7500° A., the Ca+ atom will be repelled with accelerations which are about two and a half times those given in Tables VI. and VIa. This figure, however, does not apply to other atoms unless they have their absorption lines in the same part of the spectrum as H and K: if their principal lines lie more to the red, the accelerations will be less; if more to the violet, they will be greater.

Maximum Values.—Another point worth noticing is that the various functions I_β, I_α, J_β, J_α expressing the forces on an atom pass through a maximum if we keep y constant and alter h. At some distance from a spot or facula the forces may be negligible at the base of the chromosphere, but quite appreciable at great heights. If we call θ the angle between the line joining the atom to the centre of the spot and the vertical, then it is easily verified that the directions in which the various maxima occur are as follows:—

$$I_\beta, \quad \theta = 45^\circ$$
$$I_\alpha, \quad \theta = 39^\circ\ 14'$$
$$J_\beta, \quad \theta = 60^\circ$$
$$J_\alpha, \quad \theta = 50^\circ\ 46'.$$

If we take, as usual, $\alpha = \frac{3}{5}$, $\beta = \frac{2}{5}$, then V is a maximum when

$$\theta = 41^\circ\ 45'$$

and H when $$\theta = 55^\circ\ 2'.$$

The total force reaches a maximum in between, viz. at

$$\theta = 49^\circ\ 9'.$$

The actual values of the maxima are :

$$\left.\begin{aligned} V_{max} &= 0{\cdot}209\,\frac{A}{y^2} = 0{\cdot}836/m^2 \\ H_{max} &= 0{\cdot}235\ A/y^2 = 0{\cdot}939/m^2 \\ \text{and} \\ F_{max} &= 1{\cdot}186/m^2 \end{aligned}\right\} \quad . \quad . \quad (15)$$

Of course these formulæ only apply at considerable distances.

To take the case which we dealt with before, namely, that of a Ca+ atom above a sunspot at 4500° A., the maximum accelerations are given by

$$\frac{V_{max}}{mg_\odot} = \frac{0{\cdot}320}{m^2}, \qquad \frac{H_{max}}{mg_\odot} = \frac{0{\cdot}324}{m^2},$$

and occur when the radius vector has the directions already specified.

One interesting conclusion is that a large spot may have a considerable influence high up above the chromosphere, whilst affecting the lower regions very little ; thus, for example, a spot 50,000 km. across will produce accelerations

860 cm./sec.^{2} vertically

and

870 cm./sec.^{2} horizontally

at y = 250,000 km., h = 220,000 km. (this being roughly the direction of the maximum) ; whilst at the base of the chromosphere itself (say, h = 5000 km., y = 250,000 as before) the accelerations will hardly exceed twenty or thirty cm./sec.^{2}.

§ 2. *Doppler Effect of the Whole Disc.*

Consider an atom whose natural frequency is ν_0, and which is in equilibrium under gravity and the pressure of the radiation at the point B in its absorption line (fig. 2). Then equilibrium will only persist if the atom has no appreciable vertical or horizontal velocity. As soon as it begins to move an asymmetry is introduced ; a horizontal motion will produce a vertical acceleration, and a vertical motion will produce both horizontal and vertical accelerations.

Suppose now that the atom is moving vertically upwards with velocity u, and horizontally along $\phi = 0$ with velocity v. For a given value of ϕ between $\frac{\pi}{2}$ and $-\frac{\pi}{2}$ the frequency absorbed by the atom will be ν, where

$$\nu - \nu_0 = \frac{\nu_0}{c}[v \cos\phi \sin\theta - u \cos\theta]$$

and the " representative point " of the atom will be at P, say. Here θ is, as usual, the angle between the vertical and the line joining the atom to any particular area of the sun's surface.

Then from $\theta = 0$ to $\theta = \theta'$ where

$$\tan \theta' = \frac{u}{v} \sec \phi \quad . \quad . \quad . \quad . \quad (1)$$

P will be to the left of B, and the intensity at any point will be given by

$$I_\nu = -b(\nu - \nu_0) + I' \quad . \quad . \quad . \quad . \quad (2a)$$

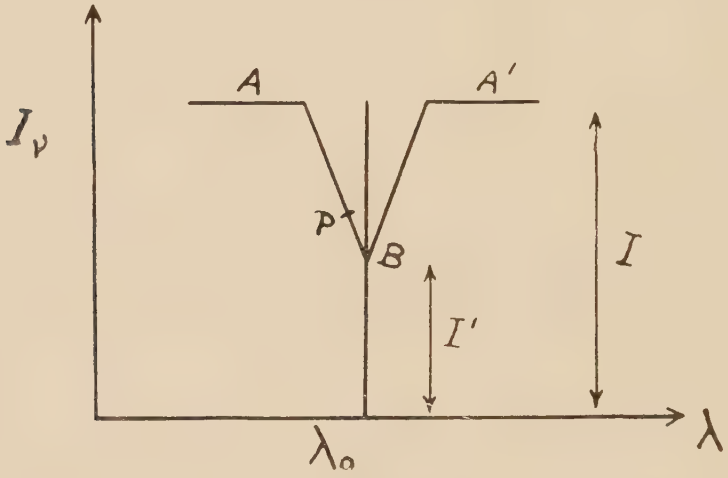

FIG. 2.

From $\theta = \theta'$ to $\theta = \frac{\pi}{2}$ P will be to the right of B, and we shall have

$$I_\nu = b(\nu - \nu_0) + I' \quad . \quad . \quad . \quad . \quad (2b)$$

This applies to the region in front of the atom, viz. $\phi = -\frac{\pi}{2}$ to $\frac{\pi}{2}$; in the region behind, viz. $\phi = \frac{\pi}{2}$ to $\frac{3\pi}{2}$, the absorption takes place wholly along BA.

We can now calculate the horizontal and vertical forces for any given values of u and v, for we have

$$\frac{H}{k_\nu d\nu} = \int_0^{\frac{\pi}{2}} \int_{-\frac{\pi}{2}}^{\frac{3\pi}{2}} I_\nu \cos\phi(\beta \sin^2\theta + \alpha \cos\theta \sin^2\theta) d\theta d\phi$$

$$\frac{V}{k_\nu d\nu} = \int_0^{\frac{\pi}{2}} \int_{-\frac{\pi}{2}}^{\frac{3\pi}{2}} I_\nu(\beta \sin\theta \cos\theta + \alpha \sin\theta \cos^2\theta) d\theta d\phi$$

where

$$I_\nu = \pm \frac{b\nu_0}{c}(v \cos\phi \sin\theta - u \cos\theta) \quad . \quad . \quad (3)$$

The horizontal force from the front, resisting the motion of the atom, is thus

$$\begin{aligned}\frac{H_f}{k_\nu d\nu} &= 2\int_0^{\frac{\pi}{2}}\int_0^{\theta'} \frac{b\nu_0}{c}[v\cos^2\phi(\beta\sin^3\theta + \alpha\cos\theta\sin^3\theta) \\ &\qquad - u\cos\phi(\beta\sin^2\theta\cos\theta + \alpha\cos^2\theta\sin^2\theta)]d\phi d\theta \\ &\quad - 2\int_0^{\frac{\pi}{2}}\int_{\theta'}^{\frac{\pi}{2}} \frac{b\nu_0}{c}[v\cos^2\phi(\beta\sin^3\theta + \alpha\cos\theta\sin^3\theta) \\ &\qquad - u\cos\phi(\beta\sin^2\theta\cos\theta + \alpha\cos^2\theta\sin\theta)]d\phi d\theta \\ &\quad + 2\int_0^{\frac{\pi}{2}}\int_0^{\frac{\pi}{2}} I'(\beta\sin^2\theta + \alpha\cos\theta\sin^2\theta)\cos\phi d\phi d\theta \\ &= \frac{2b\nu_0}{c}\left[\frac{\pi}{2}\left(-\frac{1}{3}\beta + \frac{1}{8}\alpha\right)v + \left(\frac{1}{3}\beta + \frac{\pi}{16}\alpha\right)u + \frac{2}{3}\beta\sin^{-1}\frac{u}{w} - \frac{a\pi}{8}\frac{uv}{w}\right] \\ &\qquad + I'\left(\frac{\pi}{2}\beta + \frac{2}{3}\alpha\right) \quad (4)\end{aligned}$$

where

$$w^2 = u^2 + v^2.$$

The force from behind, urging the atom on, may be found quite simply by putting $\theta' = \frac{\pi}{2}$. We have then

$$\frac{H_r}{k_\nu d\nu} = \frac{2b\nu_0}{c}\left[\frac{\pi}{2}\left(\frac{1}{3}\beta + \frac{1}{8}\alpha\right)v + \left(\frac{1}{3}\beta + \frac{\pi}{16}\alpha\right)u\right] + I'\left(\frac{\pi}{2}\beta + \frac{2}{3}\alpha\right) \quad (5)$$

and so the net force on the atom in the direction of its motion is

$$H = H_r - H_f = \frac{2b\nu_0 k_\nu d\nu}{c}\left[\frac{1}{3}\beta\sin^{-1}\frac{u}{w} + \frac{a\pi}{16}\cdot\frac{u}{w}\right]\cdot v \quad . \quad (6)$$

In the same way we find for the vertical force

$$\begin{aligned}V &= \frac{2b\nu_0 k_\nu d\nu}{c}\left[\frac{2}{3}\beta\left(v + u\sin^{-1}\frac{u}{w}\right) + \frac{a\pi}{8}\left(w + \frac{u^2}{w}\right)\right] \\ &\qquad + 2\pi I' k_\nu d\nu\left(\frac{1}{2}\beta + \frac{1}{3}\alpha\right) \quad (7)\end{aligned}$$

The I′ term balances gravity (*vide* equation (4), § 1), so that the remainder represents a vertical acceleration.

When $v = 0$

$$V - mg_\odot = \frac{b\nu_0 k_\nu d\nu}{c}\cdot\frac{\pi}{2}\left(\frac{4}{3}\beta + \alpha\right)u.$$

When $u = 0$

$$V - mg_\odot = \frac{2b\nu_0 \cdot k_\nu d\nu}{c}\left(\frac{2}{3}\beta + \frac{a\pi}{8}\right)v,$$

so that there is a vertical acceleration even when there is no vertical velocity.

Numerical Values.—In order to estimate the numerical magnitude of the expressions which we have just obtained, we must know the intensity distribution in the absorption line. For Ca+ we have Schwarzschild's * measurements on the H and K lines, which give for the half width

$$\Delta\nu \equiv 10 \text{ Å.U.}$$

and for the residual intensity

$$r = I'/I = 0{\cdot}11$$

approximately, but for other lines there are no suitable measurements available.

In general,

$$b = \frac{I - I'}{\Delta\nu} = \frac{1 - r}{r} \cdot \frac{I'}{\Delta\nu},$$

and since

$$mg_\odot = 2\pi I' k_\nu d\nu(\tfrac{1}{2}\beta + \tfrac{1}{3}\alpha)$$

we have, for the horizontal and vertical accelerations,

$$f_h = \frac{\nu_0}{c\Delta\nu} \cdot \frac{1 - r}{\pi r} \cdot \frac{1}{3\beta + 2\alpha}\left[2\beta \sin^{-1}\frac{u}{w} + \alpha \cdot \frac{3\pi}{8} \cdot \frac{u}{w}\right]v \quad . \qquad (8)$$

$$f_v = \frac{\nu_0}{c\Delta\nu} \cdot \frac{1 - r}{\pi r} \cdot \frac{1}{3\beta + 2\alpha}\left[4\beta \sin^{-1}\frac{u}{w} \cdot u + 4\beta v + \alpha \cdot \frac{3\pi}{8}\left(w + \frac{u^2}{w}\right)\right] \qquad (9)$$

or, putting $\alpha = \frac{3}{5}$, $\beta = \frac{2}{5}$,

$$f_h = \frac{\nu_0}{c\Delta\nu} \cdot \frac{1 - r}{12\pi r}\left(4 \sin^{-1}\frac{u}{w} + \frac{9\pi}{8} \cdot \frac{u}{w}\right)v,$$

$$f_v = \frac{\nu_0}{c\Delta\nu} \cdot \frac{1 - r}{12\pi r}\left[8 \sin^{-1}\frac{u}{w} \cdot u + 8v + \frac{9\pi}{8}\left(w + \frac{u^2}{w}\right)\right].$$

Taking now the data given above for the H, K lines, we obtain the following figures :—

$$v = 0, \quad f_v = {\cdot}0024u;$$
$$u = 0, \quad f_v = {\cdot}0043v;$$
$$v = u, \quad f_h = {\cdot}0016v, \quad f_v = {\cdot}0068v;$$

u, v being expressed in km./sec., and f as a fraction of $g_\odot$.

Hence, if v is only a few km./sec., the accelerations will not be large ; † but if v is of the order of 50 km./sec., they will then be from $\frac{1}{10}$ to $\frac{1}{4}$ of $g_\odot$, *i.e.* round about 5×10^3 cm./sec.^{2}. Thus an atom which is moving

* *Sitz. d. preuss. Ak.*, 1914, p. 1183.

† The equilibrium is actually stable for *small* vertical velocities, as Milne has shown, and the same argument must apply to horizontal motion, so that the acceleration will be zero for velocities below a certain limit, depending upon the bluntness of the V.

horizontally, but which has no vertical velocity at all to start with, will soon acquire an appreciable vertical velocity as well, if its original horizontal motion is fast enough. The effect is cumulative, and the atom will ultimately travel right away from the sun with a limiting velocity of many hundreds of km./sec. This process is practically the same as that discussed by Milne in his paper "On the Escape of High-speed Atoms from the Sun," the only difference being that in the present case the atom not only moves radially away from the sun, but has also a tangential velocity. The amount of the latter will be roughly of the same order as the radial velocity, so that the ultimate direction of motion will make a large angle with the vertical.

§ 3. *Doppler Effect of a Given Area.*

We have already calculated the acceleration produced at any distance by a given area of the sun, on the assumption that it has a "surface intensity" $\sigma_0(\beta \cos\theta + \alpha \cos^2\theta)$; in this way any alteration of temperature and any assumed law of darkening can be allowed for. A further complication, however, is introduced by the fact that this expression only applies when the absorbing atom is at rest. As soon as the atom has acquired an appreciable velocity towards or away from the area in question, the value of σ is modified by the Doppler effect, and in a narrow line may change rapidly with ν. We thus get additional terms in the expression for the acceleration which depend on $\frac{v}{c}$, and which will always differ from zero except when the contour of the line is parallel to the axis of ν; in particular, the line need not be unsymmetrical or displaced in any way in order that an effect may be produced.

We will confine ourselves to the case in which the line has a simple V-shaped structure (displaced or undisplaced) and the velocity of the atom is small enough to keep its absorption wholly within that line. (For the H, K lines the latter restriction merely means $v < 500$ km./sec.; and even for a line 1 Å.U. wide the limit is 50 km./sec.) Calculations are quite possible in other cases, of course, but the results are too unwieldy to be much use until we have more accurate data as to line structure.

We make the convention that velocities upwards and horizontally away from a given area are reckoned positive, and confine ourselves to the cases in which both velocities have the same sign.

Writing

$$I_\nu = \pm b(\nu - \nu_0) + I'$$

we have, for an atom moving downwards with velocity $|u|$ (u is then negative), and horizontally with velocity $|v|$ (where v is also negative):

$$\nu - \nu_0 = \frac{\nu_0}{c}(|v| \cos\phi \sin\theta + |u| \cos\theta) \qquad (10)$$

in front; and hence

$$I_\nu = I' + \frac{b\nu_0}{c}(|v| \cos\phi \sin\theta + |u| \cos\theta).$$

Thus the " effective surface intensity " is

$$\begin{aligned}\sigma &= k_\nu I_\nu d\nu(\beta\cos\theta + \alpha\cos^2\theta)\\ &= \sigma_0(\beta\cos\theta+\alpha\cos^2\theta) + \sigma_2[\,|\,v\,|\cos\phi\,(\beta\cos\theta\sin\theta + \alpha\cos^2\theta\sin\theta)\\ &\qquad + |\,u\,|(\beta\cos^2\theta + \alpha\cos^3\theta)]\end{aligned}$$

where

$$\sigma_2 = \frac{b\nu_0}{c}\,.\,k_\nu d\nu.$$

If we take, as before, a square region of side $2a$, and consider an atom situated at a height h and at a distance y from the centre of one side, we find

$$\begin{aligned}V = -\sigma_2 v\Bigg[&\tfrac{2}{3}\beta\Big(3ah^2\int\frac{ydy}{(y^2+h^2)^2\sqrt{y^2+h^2+a^2}} - a^3h^3\int\frac{ydy}{(y^2+h^2)^2(y^2+h^2+a^2)^{3/2}}\Big)\\ &+\tfrac{3}{4}\alpha\Big(h^3\int\frac{ydy}{(y^2+h^2)^{5/2}}\tan^{-1}\frac{y}{\sqrt{y^2+h^2}} + ah^3\int\frac{ydy}{(y^2+h^2)^2(y^2+h^2+a^2)}\\ &+\tfrac{2}{3}ah^3\int\frac{ydy}{(y^2+h^2)(y^2+h^2+a^2)^2}\Big)\Bigg]\\ -\sigma_2 u\Bigg[&\tfrac{2}{3}\beta\Big(3ah^3\int\frac{dy}{(y^2+h^2)^2\sqrt{y^2+h^2+a^2}} - a^3h^3\int\frac{dy}{(y^2+h^2)^2(y^2+h^2+a^2)^{3/2}}\Big)\\ &+\tfrac{3}{4}\alpha\Big(h^4\int\frac{dy}{(y^2+h^2)^{5/2}}\tan^{-1}\frac{y}{\sqrt{y^2+h^2}} + ah^4\int\frac{dy}{(y^2+h^2)^2(y^2+h^2+a^2)}\\ &+\frac{2ah^4}{3}\int\frac{dy}{(y^2+h^2)(y^2+h^2+a^2)^2}\Big)\Bigg]\\ &+\sigma_0(\beta I_\beta + \alpha I_\alpha),\end{aligned}$$

the integrals being taken between the limits y and $y+2a$,

$$= -\sigma_2 v(\beta I_\beta' + \alpha I_\alpha') - \sigma_2 u(\beta I_\beta'' + \alpha I_\alpha'') + \sigma_0(\beta I_\beta + \alpha I_\alpha) \quad . \qquad (11)$$

where

$$\left.\begin{aligned}I_\beta' &= -\tfrac{2}{3}\Big[\frac{ah^2}{(y^2+h^2)\sqrt{y^2+h^2+a^2}}\Big]_y^{y+2a} = J_\alpha\\ I_\alpha' &= -\tfrac{1}{4}\Big[\frac{h^3}{(y^2+h^2)^{3/2}}\tan^{-1}\frac{ay}{h\sqrt{y^2+h^2}} + \frac{ah^3}{(y^2+h^2)(y^2+h^2+a^2)}\Big]_y^{y+2a}\\ I_\beta'' &= \tfrac{2}{3}\Big[\tan^{-1}\frac{ay}{h\sqrt{y^2+h^2+a^2}} + \frac{ahy(y^2+2h^2+a^2)}{(a^2+h^2)(y^2+h^2)\sqrt{y^2+h^2+a^2}}\Big]_y^{y+2a} - I_\alpha\\ I_\alpha'' &= \tfrac{1}{4}\Big[\frac{a(2a^2+3h^2)}{3(a^2+h^2)^{3/2}}\tan^{-1}\frac{y}{\sqrt{a^2+h^2}} + \frac{y(2y^2+3h^2)}{3(y^2+h^2)^{3/2}}\tan^{-1}\frac{a}{\sqrt{y^2+h^2}}\\ &\qquad + \frac{ah^2y(y^2+2h^2+a^2)}{3(a^2+h^2)(y^2+h^2)(y^2+h^2+a^2)}\Big]_y^{y+2a}\end{aligned}\right\} \qquad (12)$$

Values of I_α' and I_α'' are given in Tables VII. and VIII.

TABLE VII.

Values of I_α'

$m=$	0.	1.	2.	4.	6.	8.
$n=1$	·304	·091	·016	·0013	·00024	·00007
2	·158	·119	·048	·0072	·0016	·00049
3	·079	·086	·055	·0145	·0041	·0011
4	·044	·056	·047	·019	·0068	·0026
6	·015	·025	·027	·019	·0099	·0049

TABLE VIII.

Values of I_α''.

$m=$	0.	1.	2.	4.	6.	8.
$n=1$	·209	·036	·0097	·0049	·0017	·0012
2	·126	·053	·021	·0059	·0027	·0018
3	·077	·045	·023	·0061	·0053	·0020
4	·050	·035	·022	·0064	·0054	·0021
6	·025	·021	·019	·0049	·0043	·0024

Similarly, we find

$$H = -\sigma_2 v(\beta J_\beta' + \alpha J_\alpha') - \sigma_2 v(\beta J_\beta'' + \alpha J_\alpha'') + \sigma_0(\beta_\beta J + \alpha J_\alpha) \quad (13)$$

where

$$\left.\begin{aligned} J_\beta' &= \tfrac{2}{3}\left[\tan^{-1}\frac{ay}{h\sqrt{y^2+h^2+a^2}} - \frac{ahy}{(y^2+h^2)\sqrt{y^2+h^2+a^2}}\right]_y^{y+2a} \\ J_\alpha' &= \tfrac{1}{4}\left[\frac{y^3}{(y^2+h^2)^{3/2}}\tan^{-1}\frac{a}{\sqrt{y^2+h^2}} + \frac{a}{\sqrt{a^2+h^2}}\tan^{-1}\frac{y}{\sqrt{a^2+h^2}} - \frac{ah^2y}{(y^2+h^2)(y^2+h^2+a^2)}\right]_y^{y+2a} \\ J_\beta'' &= I_\beta' = J_\alpha \\ J_\alpha'' &= I_\alpha'. \end{aligned}\right\} \quad (14)$$

Values of J_β' and J_α' are given in Tables IX. and X.

TABLE IX.

Values of J_β'.

$m=$	0.	1.	2.	4.	6.	8.
$n=1$	·346	·273	·121	·030	·012	·0051
2	·103	·153	·113	·045	·019	·010
3	·035	·069	·072	·044	·023	·013
4	·014	·032	·043	·036	·023	·014
6	·0035	·0093	·015	·020	·018	·013

TABLE X.

Values of J_{α}'.

$m=$	0.	1.	2.	4.	6.	8.
$n=1$	·227	·137	·040	·020	·0014	·0000
2	·085	·103	·064	·017	·0053	·0023
3	·023	·054	·059	·023	·0093	·0042
4	·014	·028	·033	·023	·011	·0056
6	·0033	·0089	·017	·012	·011	·0074

We can now write down the complete expressions for the forces exerted on an atom by a square sunspot or facula, including the effect of the rest of the sun, which is supposed to be radiating at its usual temperature. It is convenient to separate the two cases, since the motion will, in general, be upwards and away from a facula, but downwards and towards a spot.

Sunspot (u, v *negative*).—The quantities σ_0 and σ_2 become reduced to σ_1 and σ_3 respectively where

$$\frac{\sigma_1}{\sigma_0} = \frac{\sigma_3}{\sigma_2} = \frac{e^{h\nu/kT_0} - 1}{e^{h\nu/kT} - 1} = 1 - x$$

and the total horizontal force urging the atom towards the sunspot is

$$\mathrm{H} = (\sigma_0 - \sigma_1)[\beta \mathrm{J}_{\beta} + \alpha \mathrm{J}_{\alpha}] + (\sigma_2 - \sigma_3)[v(\beta \mathrm{J}_{\beta}' + \alpha \mathrm{J}_{\alpha}') + u(\beta \mathrm{J}_{\beta}'' + \alpha \mathrm{J}_{\alpha}'')] - \sigma_2 v\left[\frac{4}{3}\beta \sin^{-1}\frac{u}{w} + \frac{\pi}{8}\cdot\alpha\cdot\frac{u}{w}\right];$$

or, since

$$mg_{\odot} = 2\pi\sigma_0(\tfrac{1}{2}\beta + \tfrac{1}{3}\alpha) = q\sigma_0)$$

say

$$\frac{\mathrm{H}}{mg_{\odot}} = \frac{x}{q}[\beta \mathrm{J}_{\beta} + \alpha \mathrm{J}_{\alpha}] + \frac{x}{q}\cdot\frac{\sigma_2}{\sigma_0}\cdot[v(\beta \mathrm{J}_{\beta}' + \alpha \mathrm{J}_{\alpha}') + u(\beta \mathrm{J}_{\beta}'' + \alpha \mathrm{J}_{\alpha}'')] - \frac{\sigma_2}{q\sigma_0} v\left[\frac{4}{3}\beta \sin^{-1}\frac{u}{w} + \frac{\pi\alpha}{8}\cdot\frac{u}{w}\right] \quad (15)$$

Similarly, for the downward force

$$\frac{\mathrm{V}}{mg_{\odot}} = \frac{x}{q}\cdot(\beta \mathrm{I}_{\beta} + \alpha \mathrm{I}_{\alpha}) + \frac{x}{q}\cdot\frac{\sigma_2}{\sigma_0}[v(\beta \mathrm{I}_{\beta}' + \alpha \mathrm{I}_{\alpha}') + u(\beta \mathrm{I}_{\beta}'' + \alpha \mathrm{I}_{\alpha}'')] - \frac{\sigma_2}{q\sigma_0}\cdot\left[\frac{4}{3}\beta\left(u \sin^{-1}\frac{u}{w} + v\right) + \frac{\alpha\pi}{8}\left(w + \frac{u^2}{w}\right)\right] \quad (16)$$

The first term in each expression is given in Table VIA. or VIB., but the other terms are extra. They may be positive or negative, according to circumstances; indeed, if x is small or w large we may have $\mathrm{H} = 0$, $\mathrm{V} = 0$, *i.e.* a limiting velocity w exists.

Facula (u, v *positive*).—The horizontal force *away* from the facula is

$$-\frac{\mathrm{H}}{mg_{\odot}} = \frac{x}{q}(\beta \mathrm{J}_{\beta} + \alpha \mathrm{J}_{\alpha}) + \frac{x}{q}\cdot\frac{\sigma_2}{\sigma_0}[v(\beta \mathrm{J}_{\beta}' + \alpha \mathrm{J}_{\alpha}') + u(\beta \mathrm{J}_{\beta}'' + \alpha \mathrm{J}_{\alpha}'')] + \frac{\sigma_2}{q\sigma_0}\left[\frac{4}{3}\beta \sin^{-1}\frac{u}{w} + \frac{\pi}{8}\alpha\cdot\frac{u}{w}\right]v \quad (17)$$

and the force vertically upwards

$$-\frac{V}{mg_\odot} = \frac{x}{q}\cdot[\beta I_\beta + \alpha I_\alpha] + \frac{x}{q}\cdot\frac{\sigma_2}{\sigma_0}[v(\beta I_\beta' + \alpha I_\alpha') + u(\beta I_\beta'' + \alpha I_\alpha'')]$$
$$+ \frac{\sigma_2}{q\sigma_0}\left[\frac{2}{3}\cdot\beta\left(u\sin^{-1}\frac{u}{w} + v\right) + \frac{\alpha\pi}{8}\left(w + \frac{u^2}{w}\right)\right] \quad (18)$$

So long as $w<10$ or 20 km./sec. the first term is likely to be the predominant one in both cases.

§ 4. *Comparison with Observation.*

We now come to the comparison of the preceding theory with observation; what we want to find out is how far the movements in the sun's upper atmosphere can be accounted for by the effects of radiation pressure alone. The observational data are to be found in various papers by Hale,* and in Pettit's monograph † "On the Forms and Motions of Solar Prominences." There are three types of motion which it is convenient to consider separately, viz. vertically upward, vertically downward, and lateral motions.

(1) *Upward Vertical Motion.*—Practically all the available evidence has been collected by Pettit. Prominences of all sizes are found moving upwards with velocities varying from 2 or 3 km./sec. up to 200 or 300 km./sec., or even more. They attain heights of the order of 10^5 to 10^6 km. above the sun's surface, and then fade out, usually with some suddenness. Pettit gives measurements of 18 eruptive prominences in which a velocity >50 km./sec. is attained (in 7 of them 200 km./sec. is exceeded); and under these conditions the vertical instability pointed out by Milne can hardly help setting in. At 3000 Å.U. 50 km./sec. corresponds to a shift of $\frac{1}{2}$ Å.U., so that the intensity acting upon a Ca+ atom moving with this velocity will be increased in the ratio 1·12 : 1 roughly; at 200 km./sec. the ratio will be 1·6 : 1, and for other atoms the effect will be of the same order. It would appear, therefore, that nothing can prevent these prominences from being shot right away from the sun with a limiting velocity of about 1000 to 2000 km./sec. Before this stage is reached, however, the prominence has been dissipated into space; and this is what we should expect from equation (6) § 2, for we saw there that the effect of a large vertical velocity was to produce a horizontal force acting in the direction of motion. Thus the random horizontal motions of the atoms in the prominence will be magnified when u is large, and so the cloud tends to spread out more and more rapidly, and finally to disperse altogether.

One great difficulty in this connection, however, is that Pettit finds the motion of the prominences to be carried out, not with an acceleration, but with a uniform velocity, which now and then changes its value abruptly. In other words, the motion is represented by a series of

* *Loc. cit.* For a convenient summary *vide* supplement to *Nature*, 1927 May 14.

† *Loc. cit.*

broken straight lines and not by a continuous curve. A constant *upward* velocity is very difficult to account for theoretically; but it appears from his figures that the broken straight lines could be replaced by smooth curves in nearly every case without any great loss in accuracy. In view of the difficulty of measuring exactly an object with such an indefinite structure as a prominence, it is perhaps permissible to regard the constant velocity law as unproven and to do the best we can with the figures on the assumption of a continuous acceleration.

In Table XI. are given rough values of the mean accelerations deduced in this way from Pettit's figures, together with the size of the facula that would be required to produce these accelerations in an atom whose absorption lines are at about 4000 Å.U. The atom is assumed to be on the edge of a square facula of side $2a$. If we assume instead that it is circular in shape and the atom situated on its axis, then the requisite diameter can be calculated from equation (3) § 1; this turns out to be practically equal to the values of $2a$ given in the table.

TABLE XI.

Vertical Acceleration of Prominences.

No.	Acceleration.	Mean Height.	$2a$.
		km.	km.
1	·01	$3{\cdot}5\times10^5$	$2{\cdot}4\times10^4$
2	·17	5×10^5	$2{\cdot}0\times10^5$
4	·01	$2{\cdot}5\times10^5$	$2{\cdot}4\times10^4$
5	·025	2×10^5	$3{\cdot}0\times10^4$
6	·025	$1{\cdot}5\times10^5$	$2{\cdot}0\times10^4$
8	·04	$1{\cdot}5\times10^5$	$2{\cdot}4\times10^4$
9	·31	$3{\cdot}0\times10^5$	$2{\cdot}4\times10^5$
11	·24	$3{\cdot}0\times10^5$	$1{\cdot}6\times10^5$
15	·48	2×10^5	$3{\cdot}0\times10^5$
22	·04	2×10^5	$3{\cdot}0\times10^4$

Accelerations expressed as fractions of $g_\odot$.

(2) *Downward Vertical Motion.*—Here the controlling factor is the half-width of the absorption line from which the atom derives its support. As soon as an atom begins to move downwards it becomes exposed to an increased intensity, and its motion is therefore resisted. In general an appreciable downward motion will be due to the "attraction" of a sunspot, *i.e.* the unbalanced component of the atom's weight in the direction of the spot, and a limiting downward velocity will be reached at which these two effects balance. The value of the limiting velocity in any particular case can be found from equation (16), but it depends on a large number of variables.

As an illustration of its order of magnitude at different distances we may take the case $v = u$; the limiting horizontal and vertical velocities found on this assumption are given in Tables XII. and XIIA.

TABLE XII.

Limiting Vertical Velocities in km./sec.

$m=$	0.	1.	2.	4.
$n=1$	82	11	1·5	0·2
2	33	13	4	0·8
3	16	10	6	1·3
4	12	4	3	1·5

TABLE XIIA.

Limiting Horizontal Velocities in km./sec.

$m=$	0.	1.	2.	4.
$n=1$	..	208	23	4
2	55	44	36	8
3	28	39	28	10
4	11	18	17	9

(3) *Lateral Motions.*—On our present theory there are three ways in which lateral motions can arise—by "attraction" towards a sunspot, by "repulsion" from a facula, or by a combination of these two forces. Pettit remarks (*loc. cit.*, p. 205) that in certain cases the motion of gas into a sunspot proceeds "as though along lines of magnetic force." If, as we are now supposing, the motion takes place under the joint action of bright and dark areas, this is precisely the sort of effect to be anticipated.

In general a disturbed area on the sun contains both spots and faculæ; and if the faculæ predominate, the motion of the gases will be upwards and laterally away from this area, and must *always* be an accelerated motion. If, however, the dark areas exceed the bright ones in importance (so that the total amount of light from the region is lessened), then there will be a general inflow of matter from the chromosphere. At any given height and distance from the dark areas the velocity of inflow will have a fixed limiting value, which increases as the spots are approached. The exact value of this limit is, of course, a complicated function of the position and shape of the various bright and dark regions; but its order of magnitude has been seen to be 50 to 100 km./sec. At great distances there will be inward and downward accelerations which can be more closely estimated; and the forces are then so small that the limiting velocities will also be much reduced.

Another important point to notice is that on the edges of even a large spot group there will be regions where the faculæ take control, and where the motion is consequently upwards and outwards instead of in the directions prevailing elsewhere. This applies especially to the lower regions of the chromosphere, where the effects of foreshortening become pronounced.

To illustrate this point we will consider a very much simplified case,

viz. a sunspot of side $4a$ in contact with a facula of side $2a$ (as shown in fig. 3), and will find the accelerations of a Ca+ atom at various points P along AA′, BB′. This can be done at once from Tables VIA. and VIB., using the appropriate values of m and n; the results are exhibited graphically in figs. 4 and 5.*

It will be seen that when h is small, the influence of the facula predominates and the atom moves upwards and to the right. Higher up the accelerations first fall to zero and then change sign, but not at the same point—there is an intermediate stage at which the atom is attracted inwards and repelled upwards at the same time, *e.g.* along the line AA′ the acceleration is away from the spot so long as $h<3a$, but

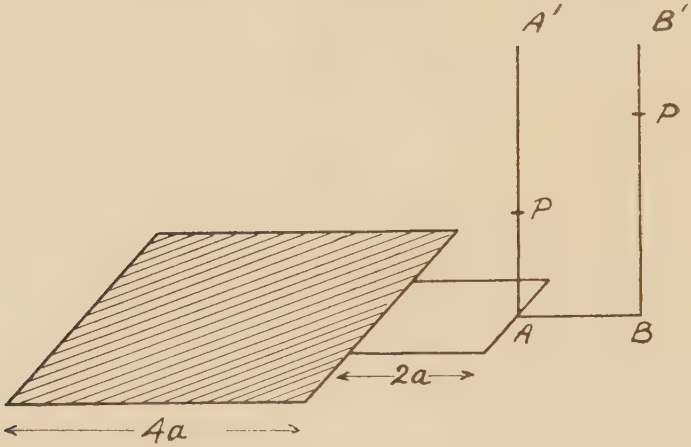

FIG. 3.

above that point it is inwards. The vertical acceleration, however, remains upwards until $h>6a$, and not until that height has been reached will the atom begin to move downwards as well as towards the spot. Along BB′ the limits are greater, viz. $4a$ and $7a$. We may therefore represent the lines of flow somewhat as in fig. 6.

All this fits in fairly well with the observational material available. Pettit classifies prominences under three headings as "Splash," "Tornado," and "Eruptive"; and of the "Splash" type he says:

"Normally this type consists of broken spikes projecting radially from the spot, together with one or a pair of wing-like prominences on either side, often raised into space. . . . The motion of these prominences, broken spikes, and loose knots of matter is into, not out from, the spot."

These prominences never occur except in association with an active

* The calculated accelerations thus refer only to an atom initially at rest; as soon as an appreciable velocity is acquired, the lines of flow will be modified by the Doppler effect. In most cases of this sort, however, the velocities do not exceed 10 km./sec. or so, and the Doppler effect will therefore not be large.

sunspot, *i.e.* a dark area bordered by bright regions. This is obviously just the kind of disturbance required, on our present theory, to produce the effects described above.

In particular, the great spot of 1917 August may be cited; this was associated with a "Splash" prominence, of which Pettit gives a plate and a pantograph drawing (*loc. cit.*, pl. xxiv. and fig. 12). The estimated area of all the spots in the group is 2×10^9 sq. km., corresponding to a value for a of $2{\cdot}2 \times 10^4$ km., whilst bright patches were also

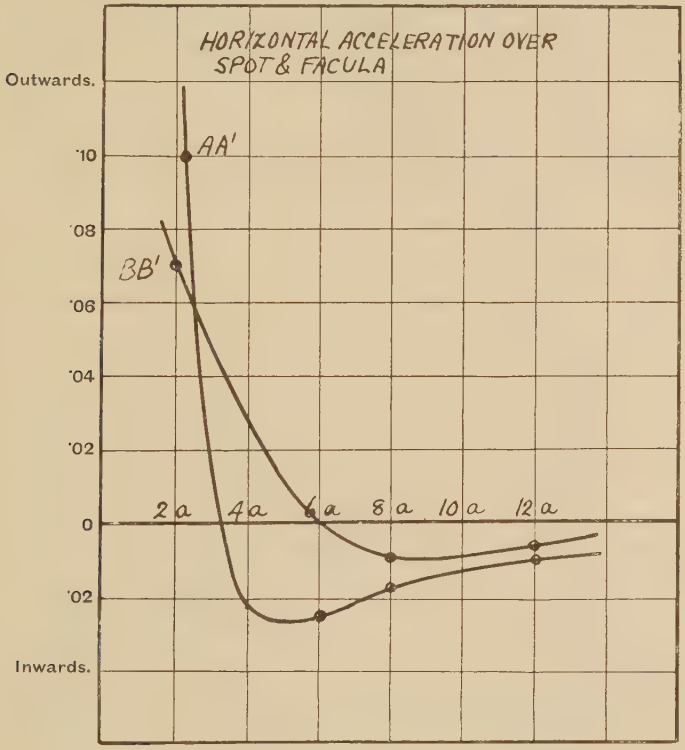

Fig. 4.

present in abundance. At a point given roughly by $m = 4$, $n = 2$, a velocity of inflow of 8 km./sec. was found; and on the other side, at $m = 3$, $n = 1$, an inflow of 1 km./sec. At some distance from the spot, viz. $m = 8$, $h = 0$ very roughly, there is an inflow of 7·4 km./sec. This is precisely the sort of effect that the preceding theory has predicted.

Another case in point, of which the details may be found in Pettit's monograph (*vide* pl. xxxvi.) is the prominence of 1919 September 22, which appeared over a spot on the limb. Here one streamer was actually seen describing a closed loop, first rising and then falling into the

chromosphere, where it was at once absorbed. Several other instances are given of the same sort of thing.

Observations of great interest, which also have a direct bearing on this matter, have been made by Hale with the spectrohelioscope, and are described in the supplement to *Nature* already referred to. He there gives measurements of the accelerated (vertical) inflow of hydrogen into a sunspot; the word "accelerated" meaning strictly that the

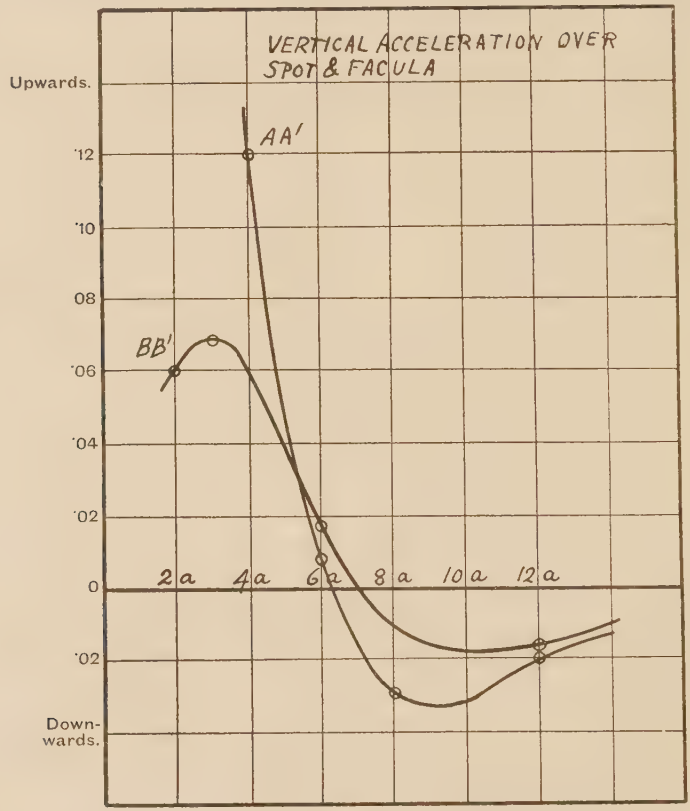

Fig. 5.

observed velocity of inflow at any point increases as the spot is approached. This again is precisely what the present theory demands. The velocities were of the order 50 km./sec.

Another important phenomenon discovered by Hale is that of "arched prominences," *i.e.* masses of gas which are found to rise from bright regions with a high velocity, then to pursue a more or less horizontal trajectory, and finally to fall back into the chromosphere with a velocity of the same order as that of the ascent. The author remarks:

" . . . I have observed many of these arches. In a bipolar spot group three or four may often be seen at once, rising from a region of bright flocculi and falling at a distance, sometimes on the penumbra of one of the spots, sometimes elsewhere."

These observations were made with the H_α line; and we should expect hydrogen to rise from the flocculi and fall into, or near, the spots, as usually appears to be the case. It constitutes, however, a very real difficulty that it should not *always* do so. Thus, in the first case given by Hale, the gas appears to have moved directly away from the neighbourhood of the spot. In itself, of course, this is not in conflict with our theory; but the subsequent motion should then be slightly upwards or at any rate horizontal. The large downward velocity over an apparently normal region of the photosphere is very difficult to explain. We might perhaps attribute it to the influence of some more distant spot, but this does not seem convincing. A more plausible explanation would be the ionization of the hydrogen at the higher levels, resulting in a loss of

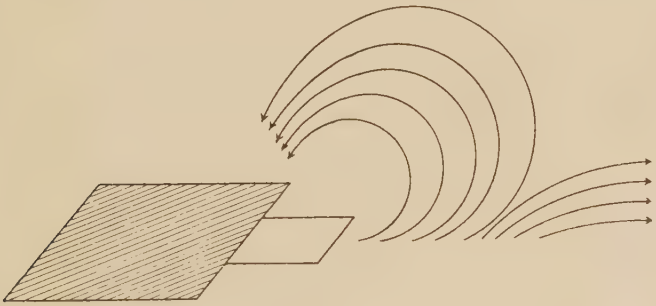

Fig. 6.

absorbing power. No appreciable fading of the cloud, however, is mentioned, such as should have been noticed if it had become transparent by ionization.

A further way out of the difficulty would be to attribute the descent of the flocculus to its effect upon the absorption line in its own immediate neighbourhood. If it contains enough matter to lower the residual intensity by an appreciable percentage, it will descend with an acceleration which is about the same percentage of solar gravity. If this explanation holds good, it removes the difficulty completely; but it seems doubtful whether a flocculus does actually produce extra absorption to the required extent. An observational test should be possible, and would, of course, settle the matter.

Another phenomenon dealt with by Pettit is the internal motion in prominences of knots and other recognisable markings; a study of this subject is, of course, invaluable in giving an idea of the forces acting in different regions of the prominence. Broadly speaking, it is found that when a spot is present near a prominence there is a general inflow of matter into it, at a velocity of 50 to 100 km./sec. in its immediate neighbourhood. At greater distances from the spot, however, the

motion of the knots and markings is upwards and away from it; at great heights the vertical component predominates, whilst lower down the motion is more nearly horizontal. This, of course, is in accordance with our theory.

In one case (the prominence of 1919 May 29) Pettit has plotted the velocity of inflow as a function of the distance from the spot, and finds that the velocities decrease according to an exponential law from 200 km./sec. at the level of the chromosphere to a nearly constant value at $h = 5 \times 10^5$ km. He then proceeds to compute the velocities which would be expected if the matter were falling freely towards the spot under gravity, and remarks:

"By way of anticipation, one might suppose that the velocities observed would exceed those computed, since it is quite certain that the centre of attraction, the spot, is exerting a force on the matter in the streamer which is the principal cause of the whole phenomenon."

Actually, the observed velocities turn out to be of the order of a quarter of the computed values, instead of exceeding them, as was expected; and Pettit concludes that—

". . . altogether, one is led to question whether gravity has anything to do with the motions of these knots."

This startling conclusion is not, however, an inevitable one, for it is based on the assumption that there is a real attractive force emanating from sunspots. On our present theory, however, this attractive force is only an apparent one; it is, of course, simply the component of gravity which is left unbalanced by the deficiency of radiation from the spot. Thus there is nothing paradoxical at all in the occurrence of downward motions smaller than would be caused by gravity alone.

Difficulties of the Theory.—There are one or two observations which clash rather seriously with our theory, and these must now be mentioned.

Hale has published an observation, already referred to, of a dark hydrogen (H_α) flocculus which remained quiescent for some days, and then was suddenly drawn into a neighbouring sunspot. The velocity was high, of the order 100 km./sec., and was attained very quickly.

Generally speaking, of course, this is just the type of event which we should expect; but in this particular case the insertion of numerical values reveals a large discrepancy.

The initial (horizontal) distance from the flocculus to the spot was about 150,000 km., and the area of the latter, roughly, $2{\cdot}2 \times 10^8$ sq. km., so that we may take

$$a = 7{\cdot}5 \times 10^3 \text{ km.}$$

The height of the flocculus cannot be estimated at all closely; it would certainly be between 10,000 and 20,000 km., however, which is all we need to know for our present purpose.

From Tables VIA. and VIB. it is evident that under these conditions the horizontal and vertical accelerations will be of the order

$$4 \times 10^{-6} \text{ km./sec.}^2,$$

and an atom subject to an acceleration of this amount would require three days to reach a velocity of 1 km./sec. Evidently, therefore, at the

distance of the flocculus the spot is almost without influence. Indeed, were it not so, it would be difficult to account for the quiescence of the flocculus for so long in that neighbourhood. Nevertheless, it ended up by being drawn (or perhaps pushed) into the spot ; and it is not easy to find a satisfactory origin for the forces which produced this result. The acceleration must have been very high, since a velocity of 100 km./sec. was acquired in a distance of less than 150,000 km. ; the minimum value is thus

$$f = 0{\cdot}033 \text{ km./sec.}^2 = 0{\cdot}123 g_{\odot}.$$

The spot alone is not capable of producing an acceleration so large as this at any point whose horizontal distance is greater than about 6000 km.

The only obvious way out of the difficulty seems to be to assume that a large facula suddenly developed in a line with the spot and the flocculus, and on the far side of the latter. This would have the effect of propelling the flocculus towards the spot, which would itself take control after a certain distance and draw the matter in. It is a very artificial assumption to make, however, and, moreover, it does not derive much support from the published photographs.

Another serious difficulty is presented by two prominences observed by Pettit * and named by him the " sigma " and " rocket " prominences respectively. In both cases a mass of gas was suddenly projected from a quiescent prominence, and, after describing a trajectory, was drawn into an obvious " point of attraction " on the surface. In the case of the " sigma " prominence the matter overshot the mark, and its horizontal velocity was actually reversed before it fell into the chromosphere.

On our theory, such a " point of attraction " can only be one thing, viz. a sunspot ; but Pettit notes specifically that in neither case was a spot present. This difficulty is similar to the one we have already met with in connection with Hale's observations of " arched prominences," but it is more acute, as there is a reversal of the horizontal motion to be accounted for also.

Conclusion.—The problem which we set ourselves was to find out whether the observed motions of gases in the sun's atmosphere could be accounted for by the effects of radiation pressure alone ; or whether it is necessary to postulate the existence of various attractive and repulsive forces of electrical or unknown origin, the suspension of the law of gravitation, and so on. The reader is now in a position to judge for himself how far the attempt has succeeded.

It should be emphasised that in any case the effects of radiation pressure which we have been discussing will certainly be present ; if other forces are acting too, their effects will simply be superposed. In general, however, it may fairly be said that radiation pressure alone is quite capable of accounting for all the observed facts, without the assistance of any other agency whatever.

Nevertheless there are one or two outstanding observations which seem to indicate that sometimes there are other forces acting as well. It is tentatively suggested that a study of the motions of flocculi, etc.,

* *Loc. cit.*, p. 218.

near the so-called " invisible " sunspots would help to resolve this difficulty ; for there the effects of radiation pressure will be automatically eliminated, and the unknown forces, if any, will be acting by themselves.

In conclusion, I should like to express my warmest thanks to Professor E. A. Milne for the interest which he has taken in the foregoing work, and for his valuable criticisms and advice.

Summary.

(1) Calculations are given of the radiative force exerted by a square area of the photosphere at any given temperature upon an atom at any given point in the chromosphere. Strictly speaking, the expressions found apply only to an atom of the Ca+ type ; but a great deal of the work holds good approximately for atoms of any type whatever, provided they are supported by radiation pressure.

(2) The vertical instability, due to the Doppler effect, which was first pointed out by Milne, is found to have a horizontal counterpart. An atom moving upwards is accelerated horizontally, resulting in a rapid dispersal of upward-moving clouds ; and an atom moving downwards and towards the sunspot is retarded, so that a limiting velocity is attained, of the order 50 to 100 km./sec.

(3) The observed motions of gases in the chromosphere are considered in the light of the preceding calculations ; and it is found that nearly all of them can be satisfactorily accounted for. There remain, however, one or two observations which it does not seem possible to explain by means of radiation pressure alone. It is suggested that if specified regions of the sun can exert forces of any other nature than this upon atoms in the chromosphere, then these forces should be found acting by themselves over " invisible " sunspots.

The University, Leeds
1927 September.

The Relative Intensity of the Principal Doublet (H, K) and the Diffuse Doublet (X) in the Spectrum of the Calcium Chromosphere. By C. Davidson. (Plate 1.)

(*Communicated by the Astronomer Royal.*)

From a consideration of the mechanics of the ionized calcium atom, Professor E. A. Milne has deduced that—

(1) The lines of the diffuse doublet in the infra-red are to be expected at every height at which the lines of the principal doublet in the violet appear.

(2) The infra-red lines should be more intense than H, K at low levels in the chromosphere, whilst at high levels they should be fainter.

A test of this prediction was part of the programme of observation at the eclipse of June 29 last, but the observation failed.

However, such results as were obtained suggested the possibility, with suitable apparatus, of obtaining some information, qualitative if

not quantitative, on the subject under ordinary conditions without an eclipse.

After return to Greenwich the spectrograph was again set up with necessary modifications. The prism of small dispersion was replaced by a plane diffraction grating 3·25 inches by 1·85 inches, ruled 14,438 lines to the inch. The scale in the Littrow spectrograph was 1 mm. = 18 A in the first order, and consequently 1 mm. = 9 A in the second order spectrum.

The first and second orders overlap, so that :

3968 in the second order coincides with 7937 in the first order, and

4271 „ „ „ 8542 „ „

3968 and 8542 thus fall only 34 mm. apart in the focal plane, and may be received on one plate in critical focus.

The overlapping spectra were intercepted by filters placed just inside the focal plane, a red filter over the half on which 8542 fell and a blue filter over the other half. The resulting photograph shows the violet in the second order on the one side and the infra-red in the first order on the other side.

The red line Hα fell well off the plate, and with an eyepiece let into the back of the camera could be viewed whilst the exposure was being made.

The solar image on the slit plate was 82 mm. in diameter, and was formed by a 15-inch mirror of 29-feet focus filled from a 16-inch cœlostat.

When the sun's image was brought tangential to the slit, Hα was visible as a bright line. It was held in this position during the exposure, and, using neocyanin plates, the infra-red Ca^+ lines were photographed with ease when the conditions were good. The principal difficulty of the observation was due to want of transparency in the sky, which gave a bright background, and also unsteadiness of the image, causing the photosphere to boil over into the slit. This made it impossible to keep the slit on the lowest level, and the brightest portions of the photographed bright lines must be taken to refer to an average height lying between 1000 and 2000 km. A number of photographs were taken, the best results being obtained on September 25 and October 3.

Normally the violet end of the solar spectrum would be recorded on the plate much more strongly than the infra-red, but the difference in dispersion and luminosity of the second and first order spectra, together with the increased atmospheric absorption at the lower altitudes of the sun, the relative absorption of the two filters, and the sensitivity gradient of the plate all combine in reducing the registered intensity in the violet and infra-red to approximate equality.

The photographed lines may be compared with the continuous solar spectrum in the immediate neighbourhood and by assuming a temperature for the sun, comparison can be made between the violet and infra-red lines.

For this purpose a series of graded exposures was made on the sun's limb.

For the continuous spectrum at wave-lengths 3968 and 8542, Planck's formula gives the relative intensities—

If $T = 5000°$, $I_{3968}/I_{8542} = 0{\cdot}94$
$T = 5500°$, $I_{3968}/I_{8542} = 1{\cdot}31$

In the reductions T was assumed to be 5000°.

Photographs of the chromosphere were taken with various exposures —15 seconds, 30 seconds, 60 seconds, and 120 seconds. They show the calcium lines as emission lines superposed on an absorption spectrum from the sun's limb. This, again, is superposed on an absorption spectrum from the sky, and, further, a slight darkening from internal reflections in the spectrograph.

With a transparent sky the spectrum from atmospheric scattering should have been 16 times as strong in the violet as in the infra-red; actually it is less than 4 times, indicating that the sky spectrum is chiefly due to reflection from a haze, only a portion being attributable to true molecular scattering.

The principal features may be seen on the accompanying plate.

The relative intensities of the infra-red calcium lines were compared in the following manner:—

A series of measures of density were made extending from the continuous spectrum on the blue side of the line to the continuous spectrum on the red side. These were converted into absolute light intensities, the contrast factors required for the purpose being obtained from the series of graded exposures referred to above. When plotted against wave-length, the result was a curve of absolute light intensity; the light in the neighbouring continuous spectrum free from absorption lines being taken as unit.

This plotted curve is a compound of the plot for the chromospheric line and of the plot for the absorption line in the superposed photospheric spectrum. The form of this latter curve was determined from measures made on a photograph of the solar spectrum and the plot of the chromospheric line then deduced.

In each case the plot of the chromospheric line comes out roughly as an error curve, but the outlying base portions are liable to considerable error. The area of the plot in that region above half its maximum height was in each case taken as representing the intensity of the line.

The relative intensities of 8498, 8542, and 8662 obtained in this way for the level at which they are strongest are respectively:

1·0 : 1·7 : 1·1.

This level is taken to be between 1000 and 2000 km.

The relative intensities of K, H, and Hϵ were deduced in a similar manner, and were found to be:

1·0 : 0·8 : 0·6.

8542 was then compared with H in the same way. In this case a correction had to be made for the sky spectrum, as different proportions of sky light were superposed on the photospheric light in the two regions.

8662
8542
8498
H
K

Corrections for this effect were obtained by taking additional measures of the sky spectrum well away from the limb, and the ratio of 8542 to H was found to be :

1·5 : 1·0.

This refers to a level between 1000 and 2000 km., as before.

The comparison of 8542 and H is naturally more difficult than comparisons between the members of the doublets, but it indicates that 8542 is of somewhat greater intensity than K.

As we pass to heights greater than 4000 km. the infra-red lines disappear rapidly, whilst H and K persist on the plates to more than 7000 km. This does not necessarily mean that the X group is absent. It may merely have fallen below H and K in intensity and have passed below the threshold sensitivity of the plate.

I am indebted to Mr. E. Martin for his assistance in taking the photographs, and to Mr. W. M. H. Greaves for advice and help in the measurement and reduction of the plates.

Summary.

The chromospheric spectrum has been photographed in the regions near H and K and the infra-red doublet of Ca^+ with a simultaneous exposure enabling a direct comparison to be made. The absolute intensity of 8542 is found to be somewhat greater than that of K at moderate levels.

A Statistical Study of the Effect of the Mass-Luminosity Relation on the Hypothetical Parallaxes of Binary Stars. By R. O. Redman, B.A.

(*Communicated by Prof. A. S. Eddington, F.R.S.*)

§ 1. *Summary.*

Some years ago five papers were published by Jackson and Furner,* in which a study was made of the hypothetical parallaxes of some hundreds of binary stars. We here seek to make some improvement by making the components of each star obey Eddington's mass-luminosity relation instead of adopting a standard mass for each star. The procedure is to determine (by trial and error) a parallax such that the mass and luminosity resulting from it conform to the mass-luminosity relation. If, by paying attention to its luminosity, we can make a closer estimate of the mass of an individual star than by taking the simple average for all stars, then these parallaxes should show some gain in accuracy over the ordinary dynamical parallaxes. A comparison is made of our parallaxes with trigonometric and spectroscopic parallaxes in § 3, although the improvement, if any, could scarcely appear in these tests.

* *M.N.*, **81**, 2 ; **83**, 4, 436, 441, 444.

The results are given in a " Russell diagram " (fig. 2), containing absolute magnitude and spectral types for 803 stars (bright components only). From this the course of the central line of the main series should be found with considerable accuracy (§ 4). Further, a measure of the scatter from the central line is found. The apparent scatter arises from three sources : (1) true scatter ; (2) inaccuracy of observational data ; (3) varying inclination which for non-orbit stars is unknown and replaced by an appropriate average value in the formulæ. The third scatter is calculated theoretically with the intention of estimating how much scatter can be attributed to (1) and (2).

For stars of known proper motion these parallaxes enable us to calculate the solar motion and mean peculiar motion for stars of each type. For dwarf stars the results are in accord with those usually accepted, but the results for giants are difficult to explain (§ 5).

In the case of non-orbit stars the most probable value of the parallax does not correspond to the most probable value of the absolute magnitude, since a different kind of averaging of the inclination factors is required. This point is investigated theoretically, and it is found that with the formulæ used the resulting mean absolute magnitude (of stars of any spectral type) requires a correction of about $-0^{m}\cdot3$; on the other hand, the mean linear velocity requires very little correction.

§ 2. *Evaluation of Parallaxes.*

The stars under consideration are divided into two groups : (1) those with determined orbits ; (2) those without determined orbits. In the first group individual results are expected to be tolerably accurate, but in the second the parallaxes are only statistically correct.

(a) *Stars with Determined Orbits.*

There are about 120 of these, perhaps the most useful and complete list being that recently given by van den Bos.*

If M_1, M_2 are the masses (in terms of the sun) of the components of a binary,
m_1, m_2 ,, ,, absolute bolometric magnitudes,
m_{01}, m_{02} ,, ,, apparent ,, ,,
a is the semi-major axis in seconds of arc,
π ,, ,, parallax,
P ,, ,, period in years,

we have

$$M_1 + M_2 = a^3/P^2\pi^3 \quad . \quad . \quad . \quad . \quad (1)$$

Jackson and Furner assume $M_1 + M_2 = 2$.
Instead, we have

$$M_1 = f(m_1) \quad M_2 = f(m_2) \quad . \quad . \quad . \quad (2)$$

* *B.A.N.*, **3**, No. 101.

where f denotes the mass-luminosity relation, and

$$\left.\begin{aligned} m_1 &= m_{01} + 5\log\pi + 5 \\ m_2 &= m_{02} + 5\log\pi + 5 \end{aligned}\right\} \quad . \quad . \quad . \quad (3)$$

Theoretically we can solve these equations simultaneously and so obtain π, M_1, M_2, m_1, m_2.

In practice the procedure was as follows :—The apparent visual magnitudes of the stars as given by Burnham, Aitken, or others were corrected in three ways : (i) so as to give a total magnitude equal to that in the Harvard Draper Catalogue ; (ii) from visual to bolometric magnitudes ; (iii) to bolometric magnitudes at an effective temperature 5200° C., so as to render possible an application of the mass-luminosity relation as given by Eddington.* Corrections (ii) and (iii) require a knowledge of the effective temperatures, and therefore the spectral types, of the components. The type of the principal star was taken from the Harvard Draper Catalogue, and the other, when not given, was estimated from the difference of magnitudes as though both components were on the main series of the Russell diagram. If, on evaluation of the parallax, the components were found to be well off the main series, this assumption was no longer justifiable and, in default of other evidence, the types were taken to be the same for both. The effective temperature was deduced by means of the table given by Miss Payne.† The correction from visual to bolometric magnitudes was taken from Hertzsprung's table as quoted by Eddington.‡ Correction (iii) equals $2\log_{10}\frac{T_e}{5200}$. Thus we obtain the apparent bolometric magnitudes of the components, corrected to an effective temperature 5200° C.

It may be pointed out that (ii) and (iii) are small corrections, except for red stars, where also they are of the same sign and thus reinforce each other. For these stars there is greatest distinction between giants and dwarfs, and should any stars have been corrected inappropriately it is least likely that it would happen among these, which are the only ones for which the total correction approaches 1^m in order.

Owing to the fact that the mass-luminosity relation cannot be expressed accurately in a simple formula convenient for direct algebraical solution of equations (1), (2), and (3), we have to proceed somewhat more indirectly. If a value of π is assumed we can deduce $M_1 + M_2$ in two ways, from equation (1) and from equations (2) and (3). The second deduction was carried out by the aid of a graph plotted from Eddington's values with ordinates and abscissæ m and log M respectively. The two values of $M_1 + M_2$ will not in general agree. Another value of π is tried, and so on until agreement is as good as possible. This gives the required parallax. After a little practice it was found that three or four trials were usually sufficient for each star.

Many of the orbit elements used are admittedly poor determinations, but, as Jackson points out, the value of a^3/P^2 derived from them should usually be a fair approximation.

The results are to be found in the table at the end of the paper.

* *The Internal Constitution of the Stars*, § 107 and Table 14.
† *Stellar Atmospheres*, p. 33. ‡ *Ibid.*, p. 139, Table 16.

(b) *Stars without Determined Orbits.*

For these, Jackson and Furner used a method first suggested by Russell and Hertzsprung, which, while of small value as far as individual parallaxes are concerned, appears to yield quite good statistical results. A fairly full discussion of their methods is given by Jackson and Furner in the first paper to which reference has been made. For most of their work they use two formulæ, of which the first is

$$\pi = \frac{\text{A cosec } i}{\sqrt[3]{(M_1 + M_2)}},$$

where A is a function of the radius vector and position angle whose value is obtained from the double star observations, and i is the angle between the true radius vector and the line of sight. For $(M_1 + M_2)^{-\frac{1}{3}}$ they take the value 0·855, which corresponds to $M_1 + M_2 = 1{\cdot}60$, and for cosec i a mean value 1·57 ($= \pi/2$) is taken. This assumes that the distribution of radii vectores is independent of the line of sight, for then the probability of occurrence of an angle i is sin i and the mean value of cosec i for a large number of stars will be

$$\frac{\int_0^{\frac{\pi}{2}} \sin i \,.\, \text{cosec } i \,.\, di}{\int_0^{\frac{\pi}{2}} \sin i \,.\, di} = \frac{\pi}{2}.$$

The second of their formulæ is

$$\pi = \frac{\text{B } \sqrt[3]{(\text{cosec } i_1 \,.\, \text{cosec}^2 i_2)}}{\sqrt{(M_1 + M_2)}},$$

where B is again a function of the observations, i_1 is the angle between the true radius vector and the line of sight, and i_2 is the angle between the true direction of motion and the line of sight. The mass is assumed the same as before while mean values are taken for $\sqrt[3]{\text{cosec } i_1}$, and $\sqrt[3]{\text{cosec}^2 i_2}$ respectively.

The probability of i_1 is sin i_1 and therefore the average value of $\sqrt[3]{\text{cosec } i_1}$ is

$$\frac{\int_0^{\frac{\pi}{2}} \text{cosec}^{\frac{1}{3}} i_1 \sin i_1 di_1}{\int_0^{\frac{\pi}{2}} \sin i_1 di_1} = \int_0^{\frac{\pi}{2}} \sin^{\frac{1}{3}} i_1 di_1 = \frac{\sqrt{\pi}}{2} \frac{\Gamma(\frac{5}{6})}{\Gamma(\frac{4}{3})} = 1{\cdot}120.$$

Similarly, assuming the true direction of relative motion to be independent of the line of sight, the mean value of $\sqrt[3]{\text{cosec}^2 i_2}$ is

$$\int_0^{\frac{\pi}{2}} \sin^{\frac{1}{3}} i_2 di_2 = \frac{\sqrt{\pi}}{2} \frac{\Gamma(\frac{2}{3})}{\Gamma(\frac{7}{6})} = 1{\cdot}294.$$

In either case for a given star the total mass varies as $1/\pi^3$. Thus we can find the total mass corresponding to any assumed parallax, since Jackson and Furner's parallax is that corresponding to $M_1 + M_2 = 1{\cdot}6\odot$. We use this in place of equation (1) above. Equations (2) and (3) still apply, so that we can deduce the required value of π by a method of trial similar to that used for orbit stars. The magnitudes of the components were corrected exactly as before. Parallaxes were found in this way for all the non-orbit stars given in Jackson and Furner's papers, nearly 700 in all.

It may be noted that we have (*a*) to see whether the above average values give the best mean absolute magnitude of a number of stars, and (*b*) to find whether they are the best to use for parallaxes employed in examining the linear motions of the stars. These two points will be discussed in due course.

§ 3. *Comparison of Parallaxes with Trigonometric and Spectroscopic Estimates.*

Spectroscopic or trigonometric parallaxes of about 140 of the stars under discussion have been published. Most of these appear in the *Greenwich Catalogue of Double Stars* (1893–1919). The spectroscopic parallaxes come from *Mt. Wilson Contributions*, Nos. 199 and 244, and from the *Publications of the Dominion Astrophysical Observatory, Victoria*, vol. iii., No. 1. Where both Mt. Wilson and Victoria give a spectroscopic parallax a mean was taken of the two.

Orbit Stars.—For these the individual parallaxes have some claim to accuracy. Thus the arithmetic means of the quantities

$$\frac{\text{trig or spec } \pi - \text{hypothetical } \pi}{\text{trig or spec } \pi}$$

were taken (neglecting signs), and also as a comparison the arithmetic mean of

$$\frac{\text{spec } \pi - \text{trig } \pi}{\text{spec } \pi}$$

is given. The figures in brackets indicate the corresponding values derived from Jackson and Furner's parallaxes.

$\frac{\delta\pi}{\pi}$.	No. of Stars.	Arithmetic Mean (without regard to Sign).
$\frac{(\text{Trig } \pi - \text{hyp } \pi)}{\text{trig } \pi}$	56	0·35 (0·35)
$\frac{(\text{Spec } \pi - \text{hyp } \pi)}{\text{spec } \pi}$	66	0·24 (0·27)
$\frac{(\text{Spec } \pi - \text{trig } \pi)}{\text{spec } \pi}$	..	0·46

The following geometrical means give some indication of the

statistical value of our results and also show any tendency to systematic difference from these other parallaxes :—

$$\text{G.M.}\ \frac{\text{hyp}\,\pi}{\text{trig}\,\pi} = 0{\cdot}93\ (0{\cdot}92).$$

$$\text{,,}\ \frac{\text{hyp}\,\pi}{\text{spec}\,\pi} = 1{\cdot}01\ (1{\cdot}01).$$

$$\text{,,}\ \frac{\text{trig}\,\pi}{\text{spec}\,\pi} = 1{\cdot}07.$$

Non-orbit Stars.—The parallaxes for these are expected to be correct statistically, but not individually. In consequence, comparison with other results was made by taking the geometric means of

$$\frac{\text{hyp}\,\pi}{\text{trig}\,\pi \text{ or spec}\,\pi}$$

as above. Jackson's values are again in brackets.

$$\text{G.M.}\ \frac{\text{hyp}\,\pi}{\text{trig}\,\pi} = 1{\cdot}33\ (1{\cdot}47).\quad 45 \text{ stars.}$$

$$\text{,,}\ \frac{\text{hyp}\,\pi}{\text{spec}\,\pi} = 1{\cdot}02\ (1{\cdot}19).\quad 59 \text{ stars.}$$

The first of these two results was affected by two stars with very small (and probably inaccurate) trigonometric parallaxes.

We see that (1) agreement with spectroscopic parallaxes is good ; (2) the revised parallaxes agree, for orbit stars as well and for non-orbit stars rather better, with other estimates than do Jackson's ; and that (3) for orbit stars both sets of hypothetical parallaxes differ less from the spectroscopic and trigonometric values than these do from each other.

§ 4. *The Spectral Type—Absolute Magnitude Diagram.*

Diagrams of this kind were first discussed by Russell,* who used parallaxes of double stars to a large extent, including hypothetical parallaxes of stars without determined orbits.

The absolute bolometric magnitudes (bright components only) obtained from our parallaxes were plotted on three diagrams : (*a*) using orbit stars only ; (*b*) using non-orbit stars only ; (*c*) using all stars. Diagram (*a*) contained too few stars to give more than a rough outline of the main sequence. There were only two or three giants in this group. In (*b*) and (*c*) there is a sufficient number of stars, but, owing to the variable cosecant term, for which we have taken an average value, they are scattered considerably. In spite of this it is possible to see that the stars tend to lie around the usual figure of the shape shown in fig. 1.

* *Publ. Amer. Astr. Soc.*, **3**, 42.

The scatter to be expected theoretically may be estimated and compared with that actually occurring in diagram (*b*). To obtain the observed scatter, a somewhat arbitrary boundary was drawn as indicated in fig. 2, and all stars within this were assumed to belong to the main series. It was ultimately found that probably a few of the "giants" left outside should have been included, but, as will be seen, these do not affect the main results. Each type from Fo to Ko was considered separately, means being taken of the absolute bolometric magnitudes of all stars within the boundary and standard deviations

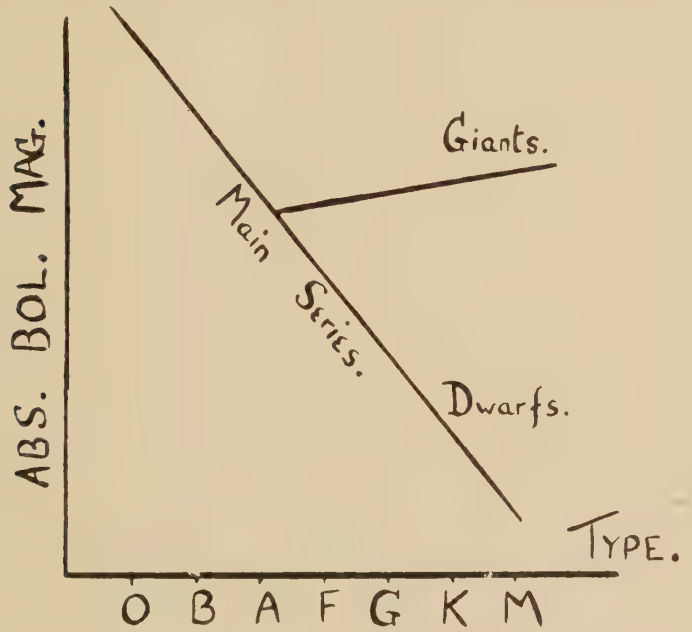

FIG. 1.

about these means were found. The theoretical standard deviations were calculated for the two cases (i), where the formula

$$\pi = \frac{\text{A cosec } i}{\sqrt[3]{(M_1 + M_2)}}$$

was used, and (ii), where

$$\pi = \frac{\text{B} \sqrt{(\text{cosec } i_1 \,.\, \text{cosec}^2 \, i_2)}}{\sqrt[3]{(M_1 + M_2)}}$$

was used (average values being taken for the cosecant terms in both cases). The method originally used for (i) is sketched very briefly here. It proved very cumbersome, and the simpler method which follows was found to be sufficient.

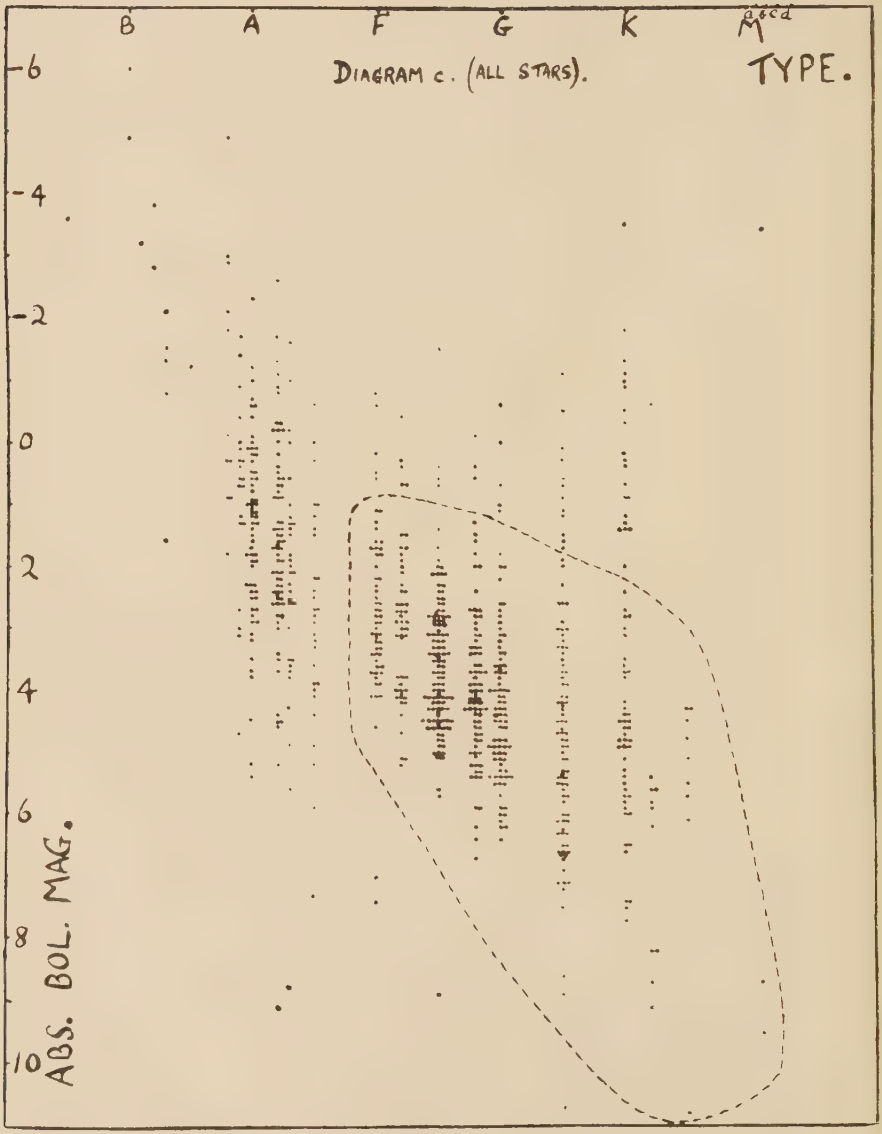

FIG. 2.

The empirical formula $M = 1{\cdot}22 \,.\, 10^5(m + 12{\cdot}25)^{-4{\cdot}14}$, where M is the mass and m the absolute bolometric magnitude of a star, was found to fit the mass-luminosity relation tolerably accurately over most of the range required.

If M_1, M_2 are the masses
m_1, m_2 ,, ,, absolute bolometric magnitudes } of the components of a binary,
and Δm = true − calculated magnitudes

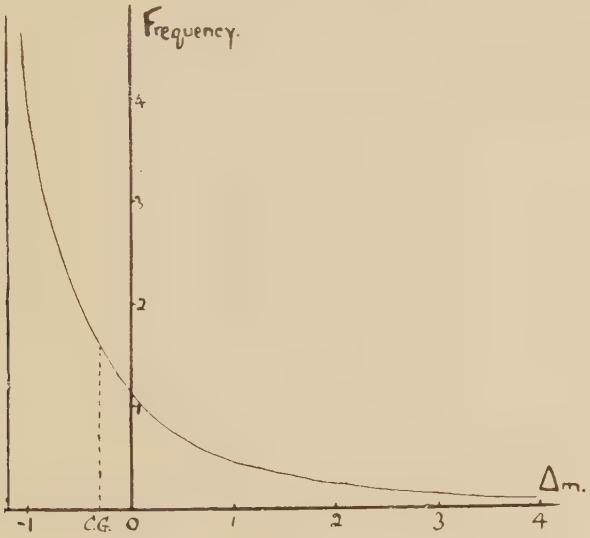

Fig. 3.

then, using the above formula, it can be shown that the probability that Δm lies between Δm and $\Delta m + d(\Delta m)$ is proportional to

$$\frac{10^{-0{\cdot}4\Delta m} \,.\, F \,.\, \left[\dfrac{\log_e 10}{5} - 1{\cdot}38\dfrac{(\mu_1 - \Delta m)^{-5{\cdot}14} + (\mu_2 - \Delta m)^{-5{\cdot}14}}{(\mu_1 - \Delta m)^{-4{\cdot}14} + (\mu_2 - \Delta m)^{-4{\cdot}14}}\right]}{\left[1 - \left(\dfrac{1}{1{\cdot}57}\right)^2 10^{-0{\cdot}4\Delta m} \,.\, F\right]^{\frac{1}{2}}}$$

where

$$\mu_1 = m_1 + 12{\cdot}25$$
$$\mu_2 = m_2 + 12{\cdot}25$$

and

$$F = \left[\frac{(\mu_1 - \Delta m)^{-4{\cdot}14} + (\mu_2 - \Delta m)^{-4{\cdot}14}}{\mu_1{}^{-4{\cdot}14} + \mu_2{}^{-4{\cdot}14}}\right]^{\frac{2}{3}}.$$

Taking mean values for m_1 and m_2 the frequency curves of Δm were drawn for each type (fig. 3). The centre of gravity of the area under the curve and the moment of inertia about the ordinate through the centre of gravity were found graphically. The results varied little

from type to type, and the following method, suggested to the writer by Professor Eddington, although apparently less rigorous, gives practically the same results with very little of the labour previously required.

Consider a binary with equal components. In the range required the mass-luminosity relation gives $L \propto M^4$ approximately, L being the luminosity of the star. We have

$$\pi \propto \frac{\operatorname{cosec} i}{M^{\frac{1}{3}}}$$

(the first of the formulæ quoted above) and, denoting calculated values (cosec $i_0 = 1{\cdot}57$) by a suffix 0,

$$\frac{L_0}{L} = \frac{\pi^2}{\pi_0{}^2} = \frac{\operatorname{cosec}^2 i}{\operatorname{cosec}^2 i_0} \frac{M_0{}^{\frac{2}{3}}}{M^{\frac{2}{3}}},$$

i.e.

$$\frac{LM^{-\frac{2}{3}}}{L_0 M_0{}^{-\frac{2}{3}}} = \frac{\operatorname{cosec}^2 i_0}{\operatorname{cosec}^2 i}$$

$$\left(\frac{L}{L_0}\right)^{\frac{2}{5}} = \frac{\operatorname{cosec}^2 i_0}{\operatorname{cosec}^2 i}$$

$$-\log \frac{L}{L_0} = \tfrac{1}{5}^2 \log \frac{\operatorname{cosec} i}{\operatorname{cosec} i_0},$$

thus

$$\Delta m = -\tfrac{5}{2} \log_{10} \frac{L}{L_0} = 2{\cdot}604 \log_e \frac{\operatorname{cosec} i}{\operatorname{cosec} i_0}.$$

Measure Δm in units of $2^{\mathrm{m}}{\cdot}60$; say $\mu = \Delta m / 2{\cdot}60$.
Then

$$e^{\mu} = \sin i_0 / \sin i.$$

When $\sin i_0 = 1/1{\cdot}57$ and $\sin i = 1$, $\mu = -0{\cdot}451$, *i.e.* $\Delta m = -1^{\mathrm{m}}{\cdot}17$. (The value for type Fo from the graphical method was $-1^{\mathrm{m}}{\cdot}20$.)

This gives an upper limit for Δm in one direction. We may simplify matters by measuring μ from the limit instead of from where

$$\sin i_0 = 1/1{\cdot}57.$$

Then

$$\sin i = e^{-\mu} \qquad . \quad . \quad . \quad . \quad (1)$$

$$\cos i di = -e^{-\mu} d\mu.$$

Frequency of i from i to $i + di$ is

$$\sin i di = -\frac{e^{-2\mu} d\mu}{\sqrt{(1 - e^{-2\mu})}}.$$

Frequency of μ from μ to $\mu + d\mu$ is

$$f(\mu) d\mu = \frac{e^{-2\mu} d\mu}{\sqrt{(1 - e^{-2\mu})}}.$$

This frequency curve is shown diagrammatically in fig. 3.

$$\int_0^\infty f(\mu)d\mu = 1.$$

Centre of gravity of area under curve is at

$$\mu = \frac{\int_0^\infty \mu f(\mu)d\mu}{\int_0^\infty f(\mu)d\mu}$$

$$= \int_0^\infty (e^{-2\mu} + \tfrac{1}{2}e^{-4\mu} + \ldots)\mu d\mu$$

$$= \frac{1}{2^2} + \frac{1}{2}\cdot\frac{1}{4^2} + \frac{1}{2}\cdot\frac{3}{4}\cdot\frac{1}{6^2} + \ldots$$

$$= 0{\cdot}295,$$

that is where $\Delta m = -0^{m}{\cdot}40$. (Graphical method gave $-0^{m}{\cdot}32$ for Fo.)

We may also find the standard deviation from the mean.

S.D. from limit is given by

$$\int_0^\infty \mu^2 f(\mu)d\mu \div \int_0^\infty f(\mu)d\mu$$

$$= \int_0^\infty (e^{-2\mu} + \tfrac{1}{2}e^{-4\mu} + \tfrac{1}{2}\cdot\tfrac{3}{4}\cdot e^{-6\mu} + \ldots)\mu^2 d\mu$$

$$= 2\left(\frac{1}{8} + \frac{1}{2}\cdot\frac{1}{4^3} + \frac{1}{2}\cdot\frac{3}{4}\cdot\frac{1}{6^3} + \ldots\right)$$

$$= 0{\cdot}268.$$

S.D. from mean is

$$\sqrt{[0{\cdot}268 - (0{\cdot}295)^2]} = 0{\cdot}425$$

or in magnitudes is $1^{m}{\cdot}11$. (Graphical method gave $1^{m}{\cdot}06$ as S.D. for Fo.)

For parallaxes derived from the formula

$$\pi = \frac{B\ \mathrm{cosec}^{\frac{1}{2}} i_1 \cdot \mathrm{cosec}^{\frac{3}{2}} i_2}{M^{\frac{1}{2}}}$$

we deduce in a manner similar to the above

$$\Delta m = 5 \log_{10}\frac{\pi}{\pi_0} = {\cdot}4343 \log_e \frac{\mathrm{cosec}^2 i_1 \cdot \mathrm{cosec}^4 i_2}{\mathrm{cosec}^2 i_{10} \cdot \mathrm{cosec}^4 i_{20}}.$$

Then

$$\frac{\mathrm{cosec}^2 i_1 \cdot \mathrm{cosec}^4 i_2}{\mathrm{cosec}^2 i_{10} \cdot \mathrm{cosec}^4 i_{20}} = e^{\frac{\Delta m}{{\cdot}4343}} = e^{\mu} \text{ say.}$$

Put $\mu = \mu_1 + \mu_2$, where μ_1 depends only on i_1 and μ_2 depends

only on i_2. Then as i_1, i_2 are independent we can consider μ_1, μ_2 separately.

$$e^{\mu_1} = \frac{\operatorname{cosec}^2 i_1}{\operatorname{cosec}^2 i_{10}}.$$

Measuring μ_1 from the limit, as before, we have $\sin i_1 = e^{-\frac{1}{2}\mu_1} = e^{-\mu'_1}$ say. This is an equation similar to (1) above. Proceeding as before we find the C.G. of the area under the curve to be where $\Delta m = -0^{m}\cdot039$ and the S.D. from this mean to be $0^{m}\cdot369$.

Similarly, considering

$$e^{\mu_2} = \frac{\operatorname{cosec}^4 i_2}{\operatorname{cosec}^4 i_{20}}$$

we find the C.G. of this second distribution is at $\Delta m = -0^{m}\cdot159$ and the S.D. from this mean is $0^{m}\cdot738$.

As i_1 and i_2 are independent, the C.G. of the combined distributions is at $\Delta m = -(0^{m}\cdot039 + 0^{m}\cdot159) = -0^{m}\cdot198$ and the S.D. is given by

$$\begin{aligned}\overline{\Delta m^2} = \overline{(\Delta m_1 + \Delta m_2)^2} &= \overline{\Delta m_1{}^2} + \overline{\Delta m_2{}^2} + \overline{2\,\Delta m_1}\,.\,\overline{\Delta m_2} \\ &= 0\cdot369 + 0\cdot738 + 2(\cdot159)(\cdot039) \\ &= 1\cdot11,\end{aligned}$$

i.e. S.D. is

$$\sqrt{(\overline{\Delta m^2})} = 1^{m}\cdot06.$$

Thus the theoretical standard deviation is about 1^{m} whichever way the parallax is derived. The following are the observational values (non-orbit stars only) obtained as explained above :—

Type (Dwarfs).	Fo.	F2.	F5.	F8.	Go.	G5.	Ko.
No. of stars	41	41	92	63	64	72	35
Mean abs. bol. mag.	2·89	3·24	3·67	4·00	4·33	4·91	4·92
Observed S.D.	0·94	1·03	0·93	1·17	1·09	1·75	1·40

It appears from this that the observed spread for F dwarfs is about equal to that to be expected as a result of the variable cosecant terms. From an examination of the frequency curves, we can see that we have probably excluded two or three stars of each type when drawing our boundary, *i.e.* a few dwarf stars of very small inclination for which the hypothetical parallax is so small that they appear to be giants. These do not materially alter our result, which suggests that the main series is comparatively narrow at its hotter end, *i.e.* the range of mass and absolute magnitude in F dwarfs of any given type (effective temperature) is small. On the contrary the orbit stars, which one would thus expect to have a very small standard deviation, are scattered so as to give an average S.D. nearly $0^{m}\cdot7$. Of course, these are relatively few in number, but owing to their comparatively well-determined parallaxes they must carry some weight. At the red end of the main series there is appreciably more scatter, for which the cosecant terms cannot fully account.

A point which may affect the above conclusions should be mentioned. The theoretical frequency curve for Δm is not symmetrical,

as may be seen from fig. 3. If one distinguishes between the two sides of the mean, one obtains two values for the standard deviation. These may be computed without trouble from the work done above, and the results are about $1^m{\cdot}74$ and $0^m{\cdot}63$. Now, if the observed scatters are measured they are found to be as follows, using the same data as that in the previous table:—

Fo.	F2.	F5.	F8.	Go.	G5.	Ko.
1·00	0·93	1·02	1·25	1·15	1·69	1·23
0·86	1·10	0·85	1·16	1·03	1·39	1·61

It is at once noticed that the values in the top line are not appreciably greater than those in the lower line, certainly the difference is not that between $1^m{\cdot}74$ and $0^m{\cdot}63$. Accidental scatter will tend to smooth out the theoretical scatter, but one does not expect this to be so marked as it turns out to be. We cannot explain matters by referring to the few stars excluded by our boundary (fig. 2). These may amount to half the "giants" in types F to Go, but there will be very few such "strays" in the later types in which our scatter accords no better with theory. We have to be content with the fact that the total deviation, above and below our central line, fits in with our calculations.

From the above calculations of the C.G. of the Δm frequency curve, we have found that the mean Δm has theoretical value $-0^m{\cdot}4$ or $-0^m{\cdot}2$ according to the way in which the parallax is obtained. This indicates that a correction of say $0^m{\cdot}3$ should be subtracted from our absolute magnitudes of non-orbit stars when finding mean absolute magnitudes for each type. The positions given in fig. 2 correspond to the uncorrected magnitudes. The mean absolute magnitudes for each type of dwarf star (non-orbit stars being corrected by $0^m{\cdot}3$) give the co-ordinates of the central line of the main series.

Type.	Fo.	F2.	F5.	F8.	Go.	G5.	Ko.
No. of stars	50	45	111	76	82	83	44
Mean abs. bol. mag.	2·72	2·87	3·38	3·78	4·12	4·89	4·66

(These values are not quite the same as those in the similar table above where non-orbit stars only were being considered.)

§ 5. *Solar Motion and Linear Motions of Stars.*

The parallaxes were used in connection with such proper motions as could be obtained to find the values of the solar motion and the average linear motions of various types of star. Proper motions were taken from Boss's *Preliminary General Catalogue*, the *Publications of the Cincinnatti Observatory*, No. 18, pt. 4, the *Greenwich* 1910 *Catalogue*, and from R. Schorr's *Einbewegungs-Lexikon*, which, incidentally, includes most of the proper motions contained in the others. In all, motions for about 500 stars were used. The position of the solar apex was assumed to be at $\alpha = 273°$, $\delta = 34°$. The reduction of the data was greatly facilitated by the use of diagrams published by Dr. Smart.*

* *M.N.*, **83**, 465.

Each proper motion was resolved into parallactic and transverse components, *i.e.* in directions towards the solar anti-apex and perpendicular to this. These components (expressed in seconds of arc per annum) were reduced to linear motion by dividing each by the corresponding hypothetical parallax. The transverse velocities should be independent of the solar motion, and, in fact, it was found that the residual motion obtained by averaging these velocities for all 500 stars was extremely small, being about 0·5 km./sec. The random cross-motion for various groups of stars was found by averaging (without regard to sign) these transverse motions.

To determine the solar motion the parallactic velocities were summed (with sign) for each group and divided by $\Sigma \sin \phi$, ϕ being the angle between the star and the solar anti-apex. Subtracting the solar motion multiplied by $\sin \phi$ from the parallactic motion and averaging (without sign) we get another value of the average peculiar motion of the stars in each group :

	Type.	No. of Stars.	Solar Motion.	Average Random Cross-motion.	Average Random Parallactic Motion (Solar Motion removed).
	–B6	12	−0·85 k.p.s.	8·25 k.p.s.	13·60 k.p.s.
	B8–A3	118	16·92	8·25	14·13
Dwarfs	A5–F2	71	14·74	12·23	13·03
Dwarfs	F5–G0	157	22·43	16·35	16·50
Dwarfs	G5–K2	98	24·78	20·95	21·13
Dwarfs	K5–	7	33·56	30·95	20·57
Giants	F–K	43	39·15	21·61	26·93
	All stars	506	21·67	15·24	17·23

The results are given in the adjoining table. It will be noticed that (i) the value for the solar motion obtained from all stars is reasonably good, and (ii) there is a steady increase of peculiar velocity with diminishing temperature among the dwarfs, which is in accordance with the usually accepted view. On the contrary, the giant velocities are unsatisfactory. If one divides by two the three velocities corresponding to this group so as to bring the solar motion about into line with that from the other stars, we find the random velocities are low compared with those of the corresponding dwarfs, as is usually found. It appears that our velocities are about twice as big as they should be. As was remarked above in connection with Russell's diagram, a few of these " giants " are probably spurious, *i.e.* they are dwarfs for which cosec i is large and have consequently been given so small a parallax as to appear to be giants. Using the frequency curves obtained, it appears probable that about one-half of the F–G0 giants are strayed dwarfs, but that a very much smaller proportion of those from G0 onwards are so. The total number of spurious giants is therefore probably small (most of these stars are of the G5 and K types) and our high velocities cannot be completely accounted for in this way. In fact the velocities for G5 and K giants alone, although little affected by this possible source of error, are practically the same as

for all giants. Other sources of error were tried, *e.g.* those stars which have a small separation, and for which observational errors are presumably greatest, were eliminated and velocities found for the remaining "good" giants, but these proved to be almost identical with those already obtained. Another possibility is that the mass-luminosity relation is in error at the giant end, but inspection shows that it would have to be incorrect to an improbable degree, which also would make it clash with evidence from eclipsing variables, etc. It may be that Jackson and Furner have by some means tended to correct their giant parallaxes which normally would be too big owing to their assumption of a total mass = 1·6⊙, which is rather low for dwarfs and is definitely too low for giants. If they have somehow obtained lower values (actually nearer the truth) than those corresponding to their assumed mass, then this would make our revised values too low. Whatever the reason, it seems fairly clear that our hypothetical parallaxes for giants are too low, differing from the true values by a factor of about 2.

On the whole the evidence from these linear motions goes to show that, except for giant stars, our hypothetical parallaxes are, statistically, tolerably correct. As was mentioned above, some investigation was made as to whether the average factors taken in place of the cosecant terms were the best for evaluation of parallaxes to be used in connection with proper motions.

From our first formula we have

$$\pi = \frac{A \operatorname{cosec} i}{M^{\frac{1}{3}}}$$

where we are considering the simplified case of two equal components and are using the same notation as before.

The mass-luminosity relation may be taken as $L \propto M^4$.

Then

$$\frac{\pi}{\pi_0} = \frac{\operatorname{cosec} i}{\operatorname{cosec} i_0} \frac{M_0^{\frac{1}{3}}}{M^{\frac{1}{3}}} = \frac{\operatorname{cosec} i}{\operatorname{cosec} i_0}\left(\frac{L_0}{L}\right)^{\frac{1}{12}} = \frac{\operatorname{cosec} i}{\operatorname{cosec} i_0}\left(\frac{\pi}{\pi_0}\right)^{\frac{1}{9}}$$

$$\therefore \left(\frac{\pi}{\pi_0}\right) = \frac{\operatorname{cosec} i}{\operatorname{cosec} i_0}$$

or

$$\pi/\pi_0 \,.\, \operatorname{cosec}^{\frac{8}{3}} i_0 = \operatorname{cosec}^{\frac{8}{3}} i.$$

Put L.H.S. $= x$. Then

$$x = \operatorname{cosec}^{\frac{8}{3}} i$$

$$dx = -\tfrac{8}{3} \operatorname{cosec}^{\frac{11}{3}} i \,.\, \cos i \,.\, di.$$

Thus

$$\sin i di = -\tfrac{5}{6}\, dx \frac{\sin^{\frac{16}{3}} i di}{\cos i}$$

$$= -\tfrac{5}{6} \frac{dx}{x^{\frac{8}{3}}\sqrt{(1 - x^{-\frac{8}{3}})}}$$

$$= f(x) \text{ say.}$$

As the probability of i is $\sin i$, $f(x) = 0$ is the frequency curve of x. Area under curve

$$= \int_1^\infty f(x)dx = 1.$$

C.G. of area is where

$$x = \tfrac{5}{6}\int_1^\infty \frac{xdx}{x^{\frac{8}{3}}\sqrt{(1-x^{-\frac{5}{3}})}} = \tfrac{5}{6}\int_1^\infty \frac{dx}{x^{\frac{5}{3}}\sqrt{(1-x^{-\frac{5}{3}})}} = \frac{\sqrt{\pi}}{2}\,\frac{\Gamma(\frac{2}{5})}{\Gamma(\frac{9}{10})} = 1{\cdot}840,$$

i.e. where

$$\frac{\pi}{\pi_0} = \frac{1{\cdot}840}{(1{\cdot}57)^{\frac{6}{5}}} = 1{\cdot}070.$$

Thus the mean value of $\dfrac{\pi}{\pi_0}$ for a large number of stars, where π_0 is derived from the formula

$$\pi_0 = \frac{\text{A } 1{\cdot}57}{\text{M}^{\frac{1}{5}}} \text{ is } 1{\cdot}070.$$

The other formula is

$$\pi = \frac{\text{B cosec}^{\frac{1}{5}} i_1 \,.\, \text{cosec}^{\frac{2}{5}} i_2}{\text{M}^{\frac{1}{5}}},$$

and, as before, we can treat the i_1 and i_2 parts separately, assuming i_1 and i_2 to be independent.

$$\frac{\pi}{\pi_0} = \frac{\text{cosec}^{\frac{1}{5}} i_1 \,.\, \text{cosec}^{\frac{2}{5}} i_2}{\text{cosec}^{\frac{1}{5}} i_{10} \,.\, \text{cosec}^{\frac{2}{5}} i_{20}}\,\frac{\text{M}_0^{\frac{1}{5}}}{\text{M}^{\frac{1}{5}}} \quad (\text{cosec}^{\frac{1}{5}} i_{10} = 1{\cdot}120,\ \text{cosec}^{\frac{2}{5}} i_{20} = 1{\cdot}294)$$

$$\left(\frac{\pi}{\pi_0}\right)^{\frac{5}{5}} = \frac{\text{cosec}^{\frac{1}{5}} i_1 \,.\, \text{cosec}^{\frac{2}{5}} i_2}{\text{cosec}^{\frac{1}{5}} i_{10} \,.\, \text{cosec}^{\frac{2}{5}} i_{20}}$$

or

$$\frac{\pi}{\pi_0} = \left(\frac{\text{cosec } i_1}{\text{cosec } i_{10}}\right)^{\frac{2}{5}}\left(\frac{\text{cosec } i_2}{\text{cosec } i_{20}}\right)^{\frac{1}{5}}.$$

Taking the i_1 part

$$\frac{\pi}{\pi_0}\,\text{cosec}^{\frac{2}{5}} i_{10} = \text{cosec}^{\frac{2}{5}} i$$

or, say,

$$x = \text{cosec}^{\frac{2}{5}} i.$$

The centre of gravity of the frequency curve of x may be found as before, and we find the mean π/π_0 is 1·003.

From the i_2 part we get the mean π/π_0 is 1·018.

Combining the two distributions, we find the mean π/π_0 is 1·021.

This indicates that for a large number of stars in which either formula may be used, the mean value of $\dfrac{\text{true parallax}}{\text{calculated parallax}}$ is about 1·05 or, say, 21/20, *i.e.* our parallaxes should be multiplied by 21/20 and the linear motions obtained above by 20/21. If we took this into account and neglected the "giants" our solar motion would become

19·3 k.p.s., which is possibly a better value than 21·67 k.p.s. Actually, however, we should apply a rather smaller correction, for the linear motions include those for about 100 orbit stars (about $\frac{1}{5}$ of the total), to which these arguments do not apply. It may be noted that the above work was also done on the assumption $L \propto M^3$, an approximation suitable for giant stars. The result differed very little from that already obtained, being just a trifle higher, and was insufficient to reduce appreciably our giant velocities. On the whole, owing to the number of sources of error both in observation of the binaries and in the proper motions, besides the various assumptions we have made in evaluating the parallaxes, the correction is of comparatively small importance.

§ 6. *Mean Absolute Magnitudes and Masses of the Stars.*

The following table gives the average absolute bolometric magnitudes, the corresponding masses, etc., of various groups of stars. The magnitudes of non-orbit stars have been corrected by $0^m{\cdot}3$, as seemed necessary from the work in § 4.

Type.		No. of Stars.	Mean Abs. Bol. Mag. (Princ. Components).	Corresponding Mass.	Mean Abs. Bol. Mag. (Secondary Components).	Corresponding Mass.	Total Mass.	Linear Velocity.	Corresponding K.E.
–B6		12	−2·77	8·4	−1·38	4·8	13·2	10·92 k.p.s.	787
B8–A3		193	1·14	2·2	2·21	1·6	3·8	11·19	238
A5–F2	Dwarfs.	126	2·73	1·5	3·64	1·2	2·7	12·63	215
F5–G0	Dwarfs.	269	3·71	1·2	4·47	1·0	2·2	16·42	297
G5–K2	Dwarfs.	135	4·89	0·98	5·55	0·83	1·8	21·04	398
K5–	Dwarfs.	11	6·00	0·82	6·73	0·70	1·5	25·66	494
Giant F–K		57	−0·11	3·8	1·40	2·3	6·1	24·27	1796
Sun		..	..	..	..	..	1·0	21·67	470

Most of this table agrees with the usually accepted views of mass, velocity, etc. It may be remarked that Jackson's assumption, $M_1 + M_2 = 1{\cdot}6$, was probably an underestimate for most types. The kinetic energies in the last column, although perhaps too much reliance should not be placed on them, seem to require the giant velocities to be halved. The data for stars earlier than B6 are based on only twelve systems and may not be a fair sample, otherwise the kinetic energy is rather high. The remainder of the table tends to support the theory of approximate equipartition of energy.

§ 7. *Conclusion.*

On the whole, it seems that the method here used is capable of giving good statistical results in the evaluation of hypothetical parallaxes. The greatest disadvantage is the amount of labour involved, which is considerable, even after parallaxes have been computed for a given assumed mass. However, parallaxes of any description are notoriously difficult to estimate with any degree of accuracy, and, this being so, our results may be regarded as valuable. Incidentally, we may have

added a little to the large amount of evidence in favour of the mass-luminosity relation.

This investigation was commenced at the suggestion of Professor Eddington, to whom the writer also owes grateful thanks for much valuable advice and guidance during his supervision of the work.

TABLE I.

Stars with Determined Orbits.

B.G.C.	Spec. Type.	Abs. Mag.	Hyp. Par.	B.G.C.	Spec. Type.	Abs. Mag.	Hyp. Par.
			″				″
21	A3	1·6	·012	5223	A2	−1·2	·007
104	Go	3·3	·013	5235	A2	1·0	·015
314	Go	3·9	·053	5734	Go	4·5	·137
335	Ko	4·6	·061	11h, 22	K5	6·9	·079
374	F8	4·7	·026	5805	F5	2·6	·013
426	F8	4·7	·162	5811	F5	3·2	·035
	K5	8·5		5951	F8	2·8	·016
479	Ao	1·2	·012	6028	F5	2 1	·010
482	Ko	2·9	·029	6158	A5	2·0	·014
1015	Go	3·8	·034	12h, 61	Ao	−0·1	·032
1036	A3	2·1	·031	6243	Fo	3·3	·085
1070	Ao	1·0	·015		Fo	3·3	
1144	Fo	2·9	·024	6406	F5	3·3	·059
1471	Fo	0·1	·009	6524	A5	3·2	·019
1761	A2	0·1	·007	6566	Fo	1·7	·023
2007	G5	6·1	·061	6578	F2	1·9	·019
2093	F8	4·5	·026	6641	K2	6·3	·065
2109	G5	6·3	·228	6711	F5	3·7	·015
2134	Go	3·6	·022	6832	F8	3·3	·016
2154	Go	5·0	·038	6842	Ao	2·4	·014
2187	Go	4·4	·022	6913	A2	1·8	·015
2381	F5	3·8	·023	14h, 59	Go	4·6	·730
2383	F5	3·8	·026		K5	6·0	
2535	Fop	3·0	·027	6955	A2	−0·6	·013
	A2 or 3	3·8		6999	F8	3·7	·020
3474	Go	3·6	·022	7001	F5	2·6	·012
3596	Ao	1·6	·428	7034	G5	5·5	·150
3876	F5	3·8	·029	7120	Go	4·5	·086
4122	Ao	1·4	·075	7251	Go	3·9	·059
	Ao	2·2		7259	Ko	3·7	·026
4187	F5	2·9	·303	7332	Ko	5·2	·049
4310	Go	4·6	·070	7368	Ao	0·1	·017
4414	G5	5·0	·026	7416	F2	2·5	·013
4477	Go	3·0	·043	7487	F8	2·2	·040
4771	F8	0·2	·022	7561	K5	6·3	·034
4923	F8	3·9	·065	7642	Ko	5·7	·053
5005	Ko	6·0	·055	7649	Ao	1·9	·041
5103	Go	2·3	·023	7717	Go	2·9	·094
9h, 40	F5	2·7	·064	7748	K5	5·5	·028

TABLE I.—*continued.*

B.G.C.	Spec. Type.	Abs. Mag.	Hyp. Par.	B.G.C.	Spec. Type.	Abs. Mag.	Hyp. Par.
			″				″
7783	F5	3·1	·021	9739	K0	4·4	·026
13364	A5	1·5	·017	9979	G5	3·2	·016
17h, 31	K0	6·4	·146	10363	F5	1·5	·036
7929	K2	6·5	·132	10559	F2	2·3	·018
8038	G5	4·5	·067	10643	F5	1·8	·020
8099	F8	4·1	·056	10829	F5	3·8	·068
8162	Mb	9·9	·111	10846	F0	2·4	·053
8303	F0	1·8	·024	11125	F8	4·3	·031
17h, 129	A3	2·0	·025	11222	F5	2·3	·041
8340	K0	5·6	·187	11761	Mb	11·0	·226
	K6	7·3		11763	F5	1·9	·019
8353	G0	4·6	·034	12143	F0	2·2	·021
8372	F8	4·3	·067	12290	G5	6·5	·038
8380	F2	2·2	·020	12404	F5	3·0	·014
8679	F8	3·5	·026	12696	G5	6·7	·041
8933	G0	4·4	·070	12701	G0	5·6	·087
8966	A2	1·1	·009	12755	G5	4·7	·053
8965	A2	1·1	·048	1h, 37	G5	7·0	·219
18h, 113	F8	3·4	·067	15h, 55	B3	−0·9	·017
9114	G5	4·1	·021	270	G5	6·7	·036
9319	F8	4·3	·020	2159	F0	3·0	·026
9605	A0	0·3	·029	2230	F0	3·0	·029
9643	A2	2·0	·026	2597	G0	−0·7	·065
9650	F5	2·5	·016	3291	A3	3·0	·015

Some Statistical Results from Counts of Double Stars in the Greenwich Astrographic Catalogue. By Dr. H. Groot.

(*Communicated by the Astronomer Royal.*)

In this paper a short account is given of some statistical results from my counts of double stars in the Zones of the Greenwich Astrographic Catalogue. I have searched this Catalogue, which contains 178,784 stars, for double stars of a separation less than 30″. Within this limit I have picked up 2953 pairs. All pairs with a separation less than 10″ in the Zones 64° to 69° have been remeasured at Greenwich on old and new plates with the intention of obtaining more trustworthy material, and it is planned to continue this work in future for the other Zones as well. At the same time the photographic magnitudes have been determined at the Greenwich Observatory, and the proper motions in these Zones are also being investigated. Full particulars will be given in the Catalogue, the first part of which will soon be published. It may suffice to state here that the magnitudes are somewhat mixed in value. Down to 9m·0 the probable error should be just under 0m·1. From 9m·0 to 12m·0 it might be put at 0m·2, and after 12m·0 the magnitudes

given are little more than indications. As to the distances, these may be trusted not to differ more than 1″ from the true value. The magnitude corrections to be applied to the Catalogue values are rather large, therefore I have confined the statistics, as far as they bear on magnitude, to the material from the Zones 64° to 69°.

The results have been collected in some tables, the first of which shows the connection between the number of double stars (T) and the separation (d). The number of double stars in the two first sections is so large that it is at once evident that it must contain a large percentage of true binary systems, especially when one bears in mind that the very close pairs ($d<1''$) cannot be measured on the plates and are therefore almost entirely absent from this number.

TABLE I.

	d.	0″–5″.	5″–10″.	10″–15″.	15″–20″.	20″–25″.	25″–30″.	0″–30″.
Greenwich 64°–90°	T	469	550	443	473	548	470	2953
	O	50	142	238	329	434	526	1721
	T : O	9·4	3·9	1·85	1·43	1·27	0·90	1·715
Vatican 60°–64°	T	170	254	154	190	177	204	1149
	O	15·9	47·6	73·9	110·9	142·7	174	571
	T : O	10·7	5·3	1·94	1·71	1·24	1·14	2·01

To get some indication of the quantitative proportions the second row was computed, which gives the number of optical double stars that might be expected on the hypothesis of a random distribution of the stars over the plates. This number (O) is computed by means of the well-known formula of W. Struve,

$$A = \frac{N(N-1)}{2} \cdot \frac{\pi d^2}{a^2},$$

which gives the number (A) of optical double stars of a separation $<d''$ on an area of a^2 square seconds when this area is covered by N stars.

For several reasons the true value of A may differ systematically from the calculated value. Father Stein has shown that a difference of 20 per cent. may originate, if the distribution of the stars over the considered area is not quite haphazard, *e.g.* when a portion of the area is covered by a star-cluster.* Other sources of error might be pointed out. Nevertheless, the figures of the third row (T : O) show convincingly the existence of a very large number of physical systems with separations up to 10″. It seems to me that one might predict safely that five or six out of each seven double stars of a separation less than 10″ will turn out true binaries. The limits laid down by Aitken in his well-known "working definition" of a double star certainly need to be enlarged if it is to include all true binaries.†

If all double stars were purely optical, the numbers of the succeeding sections ought to form the arithmetical succession 1 : 3 : 5 : 7 : 9 : 11, even if the numbers of all classes were systematically some 20 per cent. too large. From our figures it may be seen that the numbers T really show quite a different behaviour. This might have been foreseen for

* *Catalogo Astrografico*, Appendice III., Introducione, pp. viii–x.

† *A.N.*, **188**, 281, 1911.

the two first sections, and perhaps even for the third and fourth, but why the number of stars from the last section falls so much short of what we should expect is not at all clear, for it cannot be admitted that the number of true binaries of a separation from 20″ to 25″ is still so large as to spoil the proportion. In this connection it is of interest to compare our values with those of the Vatican Catalogue. Therefore in the fourth, fifth, and sixth rows the numbers T, O, T : O have been added, which have been found for the Vatican Zones 64° to 60° from plates containing less than 500 stars, which on a whole seem to be comparable with the material of the Greenwich Astrographic Catalogue. Here the numbers of the two last sections are respectively 177 and 204, the proportion of which is very nearly 9 : 11 as required.

I have tried to ascertain whether there is any indication of a declination effect by comparing the results of Zones 90° to 75° with those of Zones 74° to 64°. Table II. shows the results. If it is argued that T : O should be unity for the last section and that consequently the numbers for the Zones 74° to 64° are 20 per cent. too low, we can form the "reduced" values $(T : O)_{red.}$ The comparison then would seem to point out that the number of true binaries is somewhat lessened when nearing the Pole. But I would not lay any stress on this result, which most likely is purely accidental.

Table II.

	d.	0″–10″.	10″–20″.	20″–30″.
90°–75°	T	391	374	433
	O	87·5	258	436·5
	T : O	4·4	1·44	1·00
74°–64°	T	665	548	419
	O	115	309	524
	T : O	5·8	1·77	0·80
	$(T : O)_{red.}$	7·2	2·21	1·00

In Table III. we have subdivised the double stars of Zones 64° to 69° into magnitude classes. The magnitude given is the combined photographic magnitude of both components. It is readily seen that the behaviour of all classes is the same: a maximum for $5″ < d < 10″$ is succeeded by a more or less pronounced decrease for $10″ < d < 15″$. The number of stars of the last section is relatively too small for the magnitudes 13^m to 11^m. For the magnitudes 11^m to 8^m the proportion of stars from the fifth to that of the sixth section is 62 : 78, which is very nearly 9 : 11.

Table III.

	d. / *m.*	0″–5″.	5″–10″.	10″–15″.	15″–20″.	20″–25″.	25″–30″.	0″–30″.
64°–69°	12–13	20	28	20	22	32	19	141
	11–12	43	42	37	46	59	40	267
	10–11	49	53	42	38	35	37	254
	9–10	21	38	24	26	14	18	141
	8–9	7	18	11	14	9	16	75
	<8	1	3	11	3	4	7	29
		141	182	145	149	153	137	907

Table IV. gives the relation between d and Δm.

TABLE IV.

Δm. \ d.	0″–5″.	5″–10″.	10″–15″.	15″–20″.	20″–25″.	25″–30″.	0″–30″.	
0–1	94	98	68	73	90	72	495	Zone 64°–69°.
1–2	34	44	37	42	36	30	223	
2–3	8	20	27	21	16	15	107	
>3	5	20	13	13	11	20	82	
	141	182	145	149	153	137	907	

Table V. is formed to compare the results for all the stars with those made up from B.D. stars only. The B.D. stars have been entered twice—once divided in classes of photographic magnitude and once in classes of visual magnitude. It may be noted that up to the 9^m both classifications run fairly well together, the bulk of the stars of photographic magnitude 9^m to 12^m forming the visual magnitude $9^m{\cdot}0$ to $9^m{\cdot}5$. The means for the B.D. stars show the same particularities as those for all stars, only here again we find for the numbers of the last two sections the proportion 9 : 11.

TABLE V.

m. \ d.	0″–5″.	5″–10″.	10″–15″.	15″–20″.	20″–25″.	25″–30″.	0″–30″.	
12–13	21	28	21	22	31	18	141	Astrographic Cat. 64°–69°.
11–12	44	40	38	43	62	40	267	
10–11	49	52	42	39	35	35	253	
9–10	21	39	25	26	15	17	243	
8– 9	7	18	10	14	7	15	71	
<8	1	3	13	2	5	8	32	
	143	180	149	146	155	133	1007	
11–12	5	4	2	2	1	3	17	B.D. Stars of Zone 64°–69° phot. magn.
10–11	16	27	18	21	17	18	117	
9–10	9	37	20	21	14	17	128	
8– 9	7	18	10	13	7	15	70	
<8	1	3	11	2	5	8	30	
	38	89	61	59	44	61	362	
9·0–9·5	36	59	40	40	26	34	235	Visual magn.
8·0–8·9	10	20	8	14	13	17	82	
<8	2	10	13	5	5	10	45	
	48	89	61	59	44	61	362	

Table VI. gives the results for proper motion shared by the two components. This table needs no comment.

TABLE VI.

d. / *m.*	0″–5″.	5″–10″.	10″–15″.	15″–20″.	20″–25″.	25″–30″.	0″–30″.	
>11	10	3	2	1	0	1	17	Zone 64°–69°.
9–11	12	16	2	5	0	2	37	
<9	1	5	5	1	4	2	18	
	23	24	9	7	4	5	72	
	16	13	6	5	2·5	3·8	8	Per cent. of all Cat. Stars.

Lastly, we would call attention to Table VII., which gives the connection between m and Δm. Now Δm is not altered by the parallax of the system, and therefore one perhaps would have expected an equal distribution of Δm over all magnitudes. But on second thoughts it will be seen that this expectation is illegitimate; as, for example, for a magnitude of 12^m no components showing a difference of 2^m will occur, because of the limiting magnitude of practically 13^m of the Catalogue. Perhaps it will be feasible to reverse this argument and so to get an estimation of the number of double stars of a magnitude of 12^m which is missing because of the faintness of one component. But the present material is not ample enough to permit trustworthy results, therefore it seems better to wait * till the other Zones have been finished.

TABLE VII.

m. \ Δm.	0–1.	1–2.	2–3.	>3.		
12–13	125	16	0	0	141	Zone 64°–69°.
11–12	196	65	6	0	267	
10–11	101	88	48	7	254	
9–10	41	41	33	26	141	
8–9	16	9	18	32	75	
<8	6	4	2	17	29	
	485	223	107	82	907	

I wish to thank Sir F. W. Dyson for his kind help to me in the preparation of this paper.

* Dr. E. A. Kreiken tells me that he intends to follow a similar course for his researches on the statistical properties of the double stars from the Vatican and Potsdam Catalogues, on which he is engaged.

Bussum : 1927.

The Distribution of Stars of Known Parallax. By R. A. Sampson.

A paper was published in *Monthly Notices*, **86**, 1926, p. 390, under the title "The Structure of the Solar Cluster." This paper was based on a collection of trigonometrical parallaxes, comprising over 1200 stars; in fact, practically complete. When these were divided according to spectral class and luminosity, or as was used in that paper, and which comes to the same thing, according to temperature and density, they exhibited clearly marked structures, of which the central feature was a conglomeration in our own neighbourhood, with a progressive fall that made the total numbers of any type finite; in other words, the existence and structure of a solar cluster.

Numerous objections to this view suggested themselves, some of which were dealt with in the paper and some in response to criticisms by the referees, but I was unable to agree that any of them could upset the plain deductions from the collection of data which the paper contained, which had this importance, that they represented facts and not collateral inductions. But a further analysis of the material from a point of view not previously considered (*loc. cit.*, p. 557) showed that it was progressively more and more partial in its relation to the outer regions, so that the conclusions assumed the form of an extrapolation, which was only valid if the partial data were fully representative of the whole. Under these circumstances, while not withdrawing the paper, I said it was not unreasonable to suspend judgment until the matter was examined further with data which were demonstrably free from selection.

In a later issue in the same volume, H. Kienle and P. ten Bruggencate (*M.N.*, **86**, 1926, p. 651), to whom I am indebted for a searching and courteous examination of my paper, made independently much the same objection.

A treatment of spectroscopic parallaxes offered an obvious method of approach. These possess the advantage that they are selected, if at all, by quite a different method; further, though based necessarily upon the trigonometrical determinations, and therefore incapable of carrying conviction in regions beyond the reach of the latter, their probable errors are upon quite a different system and become of less and less importance when the parallax diminishes; so that for statistical purposes their indications can be relied upon considerably further.

The following pages contain the outcome of an investigation of the distribution of the stars as shown by a collection of spectroscopic parallaxes. It appears that such a collection is particularly suitable for disposing of matters of opinion and judgment, for it includes so large a proportion of all the stars down to the 6th magnitude, that questions of selection do not enter. From the 7th magnitude onwards it becomes partial, and later strongly selective, and is therefore impossible to use

demonstratively. It is, of course, a pity that it does not go further, but it is a great advantage that it is complete, for practical inferences, over most of its field.

The conclusions from the examination present some interest, but are chiefly remarkable because they are direct and certain, so far as they go. We are able to infer with reasonable closeness the number of stars per million cubic parsecs for each spectral type and each absolute magnitude at a succession of distances from the Sun. The information attains a certain point definitely and then breaks off.

The conclusions are given on p. 76 in connection with Table IV. Briefly, the consequence is that my previous conclusions must be withdrawn. The clustering found there appears to be a consequence of assuming that the material was representative; the clustering is fictitious, and the regularities which it displays are imported by the method of study.

That so extensive and even imposing a structure should all develop out of one obscure assumption is worth noting, and the author may be permitted to remark, it is a little absurd.

The collection of spectroscopic parallaxes comprises the following sources :—

Mount Wilson Observatory, W. S. Adams and others, *Astrophysical Journal*, **53** (1921), 13; **56** (1922), 242; **57** (1923), 294; **64** (1926), 225.

" R. Oss. Astrofisico di Arcetri," G. Abetti, **41** (1924), 20.*

Norman Lockyer Observatory, W. B. Rimmer, *Mem. R.A.S.*, **62** (1923), 123; D. L. Edwards, *M.N.R.A.S.*, **84**, 366; **85**, 439.

Dominion Astrophysical Observatory, R. K. Young and W. E. Harper, *Publications*, **3** (1924), 1.

Yerkes Observatory, A. Vibert Douglas, *R. Ast. Soc. Canada, Journal*, **20** (1926), 265.

Harvard College Observatory, H. Shapley and others, *H.C. Circulars*, No. 228 (1921), No. 232 (1922), No. 243 (1923), No. 246 (1923).

A card catalogue was formed, based upon one commenced and in large measure executed by Dr. Gorakh Prasad while at the Observatory; most of the stars were found in more than one source, and sometimes in as many as five sources. The agreement is, on the whole, very close. In cases where more than one determination was given, the mean of the recorded parallaxes was taken, without any attempt to consider or remove differences of system otherwise. The apparent magnitude adopted is that of the first authority abstracted, and usually therefore the Mount Wilson system, but for this investigation differences of system hardly enter. The same applies to the spectral class. The absolute magnitude at 10 parsecs distance was computed from the apparent magnitude as adopted and the mean of the parallaxes recorded.

Table I. shows the numbers of stars observed in each spectral class

* Abetti's second paper, **42** (1925), 11, was overlooked in making the collection. It contains 116 additional stars, of which 50 have not been observed elsewhere.

and each apparent magnitude. In this collection, B includes all stars B 0 to B 5, A from B 6 to A 5 (with a few that are classed merely A), and so on, M including from K 6 on and all that are classed as M. In the same way 2·0 mag. includes from 1·8 to 2·2, 2·5 includes from 2·3 to 2·7, and so on.

TABLE I.

Apparent Magnitude.	Oe.	B	A.	F.	G.	K.	M.	Totals.
⩽1·7	..	7	5	2	1	6	2	23
2·0	..	8	7	1	2	7	1	26
2·5	..	5	9	2	1	11	2	30
3·0	1	21	13	6	14	23	5	83
3·5	1	14	22	13	14	43	5	112
4·0	1	18	26	25	30	82	8	190
4·5	1	34	59	27	42	112	20	295
5·0	3	65	119	67	84	167	48	553
5·5	1	57	209	91	88	248	72	766
6·0	..	33	125	103	86	250	69	666
6·5	1	9	50	65	94	155	41	415
7·0	..	..	10	17	41	40	19	127
7·5	..	..	2	16	35	54	17	124
8·0	..	1	1	13	31	68	17	131
8·5	..	..	..	8	16	44	22	90
9·0	..	..	1	2	8	22	35	68
9·5	..	..	..	..	2	3	35	40
10·0	..	..	..	2	..	..	9	11
10·5	..	..	..	1	..	..	1	2
11·0	..	..	..	..	..	..	1	1
Totals	9	272	658	461	589	1335	429	3753

This table is a mere enumeration and calls for only one remark. It will be seen that the succession of stars observed shows at first an increase with each half-magnitude, but this soon turns into a decrease, which is very marked from 6·0 mag. on. Thereafter the proportion observed for successive magnitudes becomes less and less. This factor must be properly allowed for in drawing any conclusion about the distribution of the stars as a whole. The method of treatment will be found later (p. 73).

The absolute magnitude of each star at 10 parsecs distance having been computed, the data were then arranged as in Table II., showing for each spectral class and each absolute magnitude the number of stars found *for each apparent magnitude* within a succession of shells, distant 0–20 ps., 21–40 ps., 41–60 ps., 61–80 ps., 81–100 ps., 101–200 ps., and beyond 200 ps. Alongside each entry in this table a second number is given in brackets, the meaning of which is explained later. Only those

apparent magnitudes are marked which have observations, and, except for Class M, the collection is not continued beyond 7·5 mag., as indeed before this point the observations are so few in proportion to the whole as to carry no authority in a description of the general distribution. Hence also, and because too of certain transfers, the total of observations in Table II. does not strictly correspond with the totals of Table I.

TABLE II.

Class B. (with Oe).

Absolute Magnitude 4^M.

m.	ps. 0–20.	ps. 21–40.	ps. 41–60.	ps. 61–80.	ps. 81–100.	ps. 101–200.	ps. >200.
2·0	..	..	..	..	..	1 (3)	..
3·0	..	..	..	..	..	..	1 (3)
3·5	..	..	..	..	..	..	1 (3)
4·0	..	..	..	..	..	..	1 (3)
Totals	..	..	..	..	..	1 (3)	3 (9)

Absolute Magnitude 3^M.

2·0	..	..	..	2 (6)	5 (17)	..	..
2·5	..	..	..	..	..	4 (13)	..
3·0	..	..	..	..	..	4 (13)	..
3·5	..	..	..	..	..	2 (7)	1 (3)
4·0	..	..	..	..	..	..	2 (7)
4·5	..	..	..	..	..	..	1 (2)
5·0	..	..	..	..	..	..	5 (7)
5·5	..	..	..	..	..	..	2 (14)
6·0	..	..	..	..	..	..	5 (165)
Totals	..	..	..	2 (6)	5 (17)	10 (33)	16 (198)

Absolute Magnitude 2^M.

2·0	..	..	2 (7)	2 (7)	..	..	..
3·0	..	..	..	..	5 (17)	4 (13)	..
3·5	..	..	..	..	..	6 (20)	..
4·0	..	..	..	..	..	6 (20)	..
4·5	..	..	..	..	..	8 (18)	4 (9)
5·0	..	..	..	..	..	..	16 (23)
5·5	..	..	..	..	..	..	8 (57)
6·0	..	..	..	..	..	..	11 (363)
6·5	..	..	..	..	..	..	3
Totals	..	..	2 (7)	2 (7)	5 (17)	24 (71)	42

TABLE II.—*continued.*

Class B.—continued.

Absolute Magnitude 1^M.

m.	ps. 0–20.	ps. 21–40.	ps. 41–60.	ps. 61–80.	ps. 81–100.	ps. 101–200.	ps. >200.
2·0	..	2 (7)	..	..	..	..	..
2·5	..	..	1 (3)	..	..	..	..
3·0	..	..	..	3 (10)	..	..	..
3·5	..	..	..	2 (7)	1 (3)	..	..
4·0	..	..	..	2 (7)	3 (10)	1 (3)	..
4·5	..	..	..	..	..	..	16 (37)
5·0	..	..	..	..	..	..	28 (39)
5·5	..	..	..	..	..	..	28 (200)
6·0	..	..	..	..	..	..	9
6·5	..	..	..	..	..	..	4
Totals	..	2 (7)	1 (3)	7 (24)	4 (13)	1 (3)	85

Absolute Magnitude 0^M.

2·0	..	1 (3)	..	..	..	..	..
3·0	..	2 (7)	1 (3)	..	..	..	..
3·5	..	..	..	1 (3)	..	..	..
4·0	..	..	..	2 (7)	..	..	..
4·5	..	..	..	1 (2)	3 (5)	..	..
5·0	..	..	..	..	2 (3)	8 (11)	..
5·5	..	..	..	..	..	19 (136)	..
6·0	..	..	..	..	..	2	..
6·5	..	..	..	..	..	1	..
Totals	..	3 (10)	1 (3)	4 (12)	5 (8)	30 (147+)	..

Absolute Magnitude 1^M.

4·5	..	..	1 (2)	..	..	..	..
6·0	..	..	..	..	..	1 (7)	..
Totals	..	..	1 (2)	..	..	1 (7)	..

Class A.

Absolute Magnitude 1^M.

5·0	..	..	..	..	..	1 (3)	..
5·5	..	..	..	..	..	..	1 (3)
6·0	..	..	..	..	..	2 (13)	1 (7)
Totals	..	..	..	..	..	3 (16)	2 (10)

TABLE II.—*continued.*

Class A.—continued.

Absolute Magnitude 0M.

m.	ps. 0–20.	ps. 21–40.	ps. 41–60.	ps. 61–80.	ps. 81–100.	ps. 101–200.	ps. >200.
2·0	..	1 (3)	..	..	..	..	..
2·5	..	2 (5)	..	..	..	..	..
3·0	..	..	..	..	..	..	..
3·5	..	..	7 (18)	..	..	..	..
4·0	..	..	3 (8)	2 (5)	..	..	..
4·5	..	..	1 (3)	8 (22)	2 (6)	..	..
5·0	..	..	..	1 (3)	14 (39)	2 (6)	..
5·5	..	..	..	..	14 (36)	46 (118)	..
6·0	..	..	..	..	..	17 (113)	..
6·5	..	..	..	..	..	6 (176)	..
7·0	..	..	..	..	..	..	1 (36)
Totals	..	3 (8)	11 (29)	11 (30)	30 (81)	71 (413)	1 (36)

Absolute Magnitude 1M.

2·0	5 (13)	..	..	..	..	..	..
2·5	3 (8)	2 (5)	..	..	..	..	..
3·0	..	7 (18)	..	..	..	..	..
3·5	..	12 (30)	1 (3)	..	..	..	..
4·0	..	10 (25)	10 (25)	..	..	..	..
4·5	..	1 (3)	25 (70)	2 (6)	..	..	..
5·0	..	..	17 (47)	42 (117)	3 (8)	..	..
5·5	..	..	1 (3)	34 (87)	63 (161)	..	..
6·0	..	..	..	3 (20)	37 (247)	25 (167)	..
6·5	..	..	..	..	4 (118)	17 (500)	..
7·0	..	..	..	..	..	5 (179)	..
Totals	8 (21)	32 (81)	54 (148)	81 (230)	107 (534)	47 (667+)	..

Absolute Magnitude 2M.

2·0	3 (8)	..	..	..	..	..	..
2·5	2 (5)	..	..	..	..	..	..
3·0	6 (15)	..	..	..	..	..	..
3·5	..	2 (5)	..	..	..	..	..
4·0	..	1 (3)	..	..	..	..	..
4·5	..	17 (47)	..	..	..	..	..
5·0	..	11 (31)	19 (53)	..	..	..	..
5·5	..	2 (5)	31 (79)	12 (31)	..	..	..
6·0	..	..	9 (60)	25 (167)	3 (20)	..	..
6·5	..	..	..	8 (235)	12 (353)	..	..
Totals	11 (28)	33 (91)	59 (192)	45 (433)	15 (373)	..	..

TABLE II.—*continued.*

Class A.—continued.

Absolute Magnitude 3M.

m.	ps. 0–20.	ps. 21–40.	ps. 41–60.	ps. 61–80.	ps. 81–100.	ps. 101–200.	ps. ≥200.
2·0	1 (3)	..	..	..	..	..	..
4·5	..	1 (3)	..	..	..	..	..
5·0	..	5 (14)	..	..	..	..	..
5·5	..	2 (5)	1 (3)	..	..	..	..
6·0	..	3 (20)	1 (7)	..	..	..	..
6·5	..	1 (29)	1 (29)	..	..	..	..
7·0	..	..	..	..	1 (36)	..	..
Totals	1 (3)	12 (71)	3 (39)	..	1 (36+)	..	..

Class F.

Absolute Magnitude 2M.

3·5	..	..	..	..	..	1 (2)	..
5·5	..	..	..	..	..	..	1 (2)
6·0	..	..	..	..	..	..	1 (3)
Totals	..	..	..	..	..	1 (2)	2 (5)

Absolute Magnitude 1M.

2·0	..	1 (2)	..	..	..	..	..
2·5	..	..	1 (2)	..	..	..	..
3·0	..	..	1 (2)	..	..	..	..
4·0	..	..	..	..	1 (2)	..	..
6·5	..	..	..	..	..	..	1 (9)
Totals	..	1 (2)	2 (4)	..	1 (2)	..	1 (9)

Absolute Magnitude 0M.

3·0	..	1 (2)	..	..	..	..	..
3·5	..	..	1 (2)	..	..	..	..
4·0	..	..	1 (2)	..	..	..	..
4·5	..	..	..	1 (3)	..	..	..
5·0	..	..	..	1 (2)	1 (2)	1 (2)	..
5·5	..	..	..	..	..	1 (2)	..
6·0	..	..	..	..	..	3 (10)	..
6·5	..	..	..	..	..	1 (9)	..
7·5	..	..	..	..	..	..	1 (71)
Totals	..	1 (2)	2 (4)	2 (5)	1 (2)	6 (23)	1 (71)

TABLE II.—*continued.*

Class F.—continued.

Absolute Magnitude 1M.

m.	ps. 0–20.	ps. 21–40.	ps. 41–60.	ps. 61–80.	ps. 81–100.	ps. 101–200.	ps. >200.
2·0	1 (2)	..	..	..	..	..	..
3·5	..	1 (2)	..	..	..	..	..
4·0	..	1 (2)	2 (3)	..	..	..	..
4·5	..	..	2 (5)	2 (5)	..	..	..
5·0	..	..	3 (6)	2 (4)	..	..	..
5·5	..	..	..	4 (9)	2 (5)	..	..
6·0	..	..	..	..	3 (10)	4 (14)	..
6·5	..	..	..	..	..	2 (18)	..
7·0	..	..	..	..	..	2 (71)	..
7·5	..	..	..	..	..	1 (71)	..
Totals	1 (2)	2 (4)	7 (14)	8 (18)	5 (15)	9 (103+)	..

Absolute Magnitude 2M.

2·5	1 (2)	..	..	..	..	..	..
3·0	2 (3)	..	..	..	..	..	..
3·5	2 (3)	2 (3)	..	..	..	..	..
4·0	..	12 (20)	..	..	..	..	..
4·5	..	7 (18)	1 (3)	..	..	..	..
5·0	..	14 (26)	12 (22)	..	..	..	..
5·5	..	5 (12)	28 (65)	3 (7)	..	..	..
6·0	..	..	..	16 (55)	..	..	..
6·5	..	..	..	8 (73)	9 (82)	..	..
7·0	..	..	..	..	5 (179)	1 (36)	..
Totals	5 (8)	40 (79)	41 (90)	27 (135)	14 (200+)	1	..

Absolute Magnitude 3M.

3·0	1 (2)	..	..	..	..	..	..
3·5	3 (5)	..	..	..	..	..	..
4·0	2 (3)	..	..	..	..	..	..
4·5	2 (5)	3 (8)	..	..	..	..	..
5·0	..	22 (41)	..	..	..	..	..
5·5	..	25 (58)	1 (2)	..	..	..	..
6·0	..	17 (59)	18 (62)	..	..	..	..
6·5	..	4 (36)	19 (173)	2 (18)	..	..	..
7·0	..	..	4 (143)	2 (71)	..	..	..
7·5	..	..	..	4 (285)	8 (571)	..	..
Totals	8 (15)	71 (202)	42 (350+)	8 (350+)	8	..	..

TABLE II.—*continued.*

Class F.—continued.

Absolute Magnitude 4M.

m.	ps. 0–20.	ps. 21–40.	ps. 41–60.	ps. 61–80.	ps. 81–100.	ps. 101–200.	ps. >200.
3·5	2 (3)	..	..	..	..	..	..
4·0	1 (2)	..	..	..	..	..	..
4·5	1 (3)	..	..	..	..	..	..
5·0	2 (4)	1 (2)	..	..	..	..	..
5·5	..	5 (12)	..	..	..	..	..
6·0	..	19 (66)	..	..	..	..	..
6·5	..	11 (100)	..	..	..	..	..
7·0	..	0 (0)	3 (107)	..	..	..	..
7·5	..	..	2 (143)	..	..	..	..
Totals	6 (12)	36 (180)	5 (250+)	..	..	..	..

Absolute Magnitude 5M.

6·0	1 (3)	..	..	..	..	..	..
Totals	1 (3)	..	..	..	..	..	..

Class G.

Absolute Magnitude 4M.

4·0	..	..	..	..	..	..	1 (1)
4·5	..	..	..	..	..	..	1 (1)
Totals	..	..	..	..	..	..	2 (2)

Absolute Magnitude 3M.

4·0	..	..	..	..	..	..	3 (3)
4·5	..	..	..	..	..	..	1 (1)
5·0	..	..	..	..	..	..	3 (4)
5·5	..	..	..	..	..	..	2 (4)
6·0	..	..	..	..	..	..	1 (4)
6·5	..	..	..	..	..	..	1 (7)
7·0	..	..	..	..	..	..	1 (36)
7·5	..	..	..	..	..	..	1 (71)
Totals	..	..	..	..	..	..	13 (130+)

Absolute Magnitude 2M.

3·0	..	..	..	..	..	1 (1)	..
3·5	..	..	..	..	..	2 (2)	..
4·0	..	..	..	..	..	2 (2)	..
4·5	..	..	..	..	..	1 (1)	2 (3)
5·0	..	..	..	..	..	..	3 (4)
6·0	..	..	..	..	..	..	2 (8)
6·5	..	..	..	..	..	..	2 (13)
7·0	..	..	..	..	..	..	1 (36)
Totals	..	..	..	..	..	6 (6)	10 (44+)

TABLE II.—*continued.*

Class G.—continued.

Absolute Magnitude 1^M.

m.	ps. 0–20.	ps. 21–40.	ps. 41–60.	ps. 61–80.	ps. 81–100.	ps. 101–200.	ps. >200.
3·0	..	..	..	1 (1)	..	..	..
3·5	..	..	..	2 (2)	..	..	..
4·0	..	..	..	..	2 (2)	2 (2)	..
4·5	..	..	..	..	..	4 (5)	..
5·0	..	..	..	..	..	6 (7)	..
5·5	..	..	..	..	..	2 (4)	..
6·0	..	..	..	..	..	..	1 (4)
6·5	..	..	..	..	..	..	4 (27)
7·0	..	..	..	..	..	..	1 (36)
Totals	..	..	..	3 (3)	2 (2)	14 (18)	6 (67+)

Absolute Magnitude 0^M

3·0	..	4 (4)	..	..	..	..	..
3·5	..	..	3 (3)	1 (1)	..	..	..
4·0	..	..	1 (1)	2 (2)	..	..	..
4·5	..	..	..	1 (1)	9 (11)	..	..
5·0	..	..	..	1 (1)	8 (10)	10 (12)	..
5·5	..	..	..	..	2 (4)	13 (29)	..
6·0	..	..	..	..	..	6 (23)	..
6·5	..	..	..	..	..	7 (47)	..
7·0	..	..	..	..	..	..	1 (36)
Totals	..	4 (4)	4 (4)	5 (5)	19 (25)	36 (111)	1 (36+)

Absolute Magnitude 1^M.

3·0	..	3 (3)	..	..	..	..	..
3·5	..	3 (3)	..	..	..	..	..
4·0	..	2 (2)	3 (3)	..	..	..	..
4·5	..	..	3 (4)	3 (4)	..	..	..
5·0	..	..	3 (4)	8 (10)	..	..	..
5·5	..	..	..	6 (13)	13 (29)	..	..
6·0	..	..	..	..	7 (27)	6 (23)	..
6·5	..	..	..	..	..	7 (47)	..
7·0	..	..	..	..	..	1 (36)	..
Totals	..	8 (8)	9 (11)	17 (27)	20 (56)	14 (100+)	..

TABLE II.—*continued.*

Class G.—continued.

Absolute Magnitude 2^M.

m.	ps. 0–20.	ps. 21–40.	ps. 41–60.	ps. 61–80.	ps. 81–100.	ps. 101–200.	ps. >200.
3·0	1 (1)	..	..	..	..	..	..
3·5	..	1 (1)	..	..	..	..	..
4·0	..	3 (3)	..	..	..	..	..
4·5	..	2 (3)	..	..	..	..	..
5·0	..	2 (2)	3 (4)	..	..	..	..
5·5	..	..	..	2 (4)	..	..	..
6·0	..	..	..	8 (31)	..	..	..
6·5	..	..	..	1 (7)	4 (27)	..	..
7·0	..	..	..	..	1 (36)	..	..
7·5	..	..	..	..	..	1 (71)	..
Totals	1 (1)	8 (9)	3 (4)	11 (42)	5 (60+)	1	..

Absolute Magnitude 3^M.

2·5	1 (1)	..	..	..	..	..	..
3·0	1 (1)	..	..	..	..	..	..
3·5	2 (2)	..	..	..	..	..	..
4·0	2 (2)	..	..	..	..	..	..
4·5	1 (1)	2 (3)	..	..	..	..	..
5·0	..	4 (5)	..	..	..	..	..
5·5	..	12 (27)	..	..	..	..	..
6·0	..	10 (39)	1 (4)	..	..	..	..
6·5	..	1 (7)	3 (20)	2 (13)	..	..	..
7·0	..	..	4 (143)	3 (107)	..	..	..
7·5	..	..	..	4 (286)	2 (143)	..	..
Totals	7 (7)	29 (81)	8 (150+)	9	2	..	..

Absolute Magnitude 4^M.

3·5	1 (1)	..	..	..	..	..	..
4·0	4 (4)	..	..	..	..	..	..
4·5	7 (9)	..	..	..	..	..	..
5·0	13 (16)	3 (4)	..	..	..	..	..
5·5	8 (27)	5 (11)	..	..	..	..	..
6·0	..	22 (85)	..	..	..	..	..
6·5	..	30 (200)	2 (13)	..	..	..	..
7·0	..	8 (286)	6 (214)	..	..	..	..
7·5	..	1 (71)	8 (571)	..	..	..	..
Totals	33 (57)	69 (600+)	16	..	..	..	..

TABLE II.—*continued.*

Class G.—continued.

Absolute Magnitude 5^M.

m.	ps. 0–20.	ps. 21–40.	ps. 41–60.	ps. 61–80.	ps. 81–100.	ps. 101–200.	ps. >200.
3·5	1 (1)	..	..	..	..	..	..
4·5	2 (3)	..	..	..	..	..	..
5·0	7 (9)	..	..	..	..	..	..
5·5	7 (16)	..	..	..	..	..	..
6·0	13 (50)	..	..	..	..	..	..
6·5	8 (53)	6 (40)	..	..	..	..	..
7·0	1 (36)	8 (286)	..	..	..	..	..
7·5	..	7 (500)	3 (214)	..	..	..	..
Totals	39 (150+)	21	3	..	..	..	..

Absolute Magnitude 6^M.

4·5	1 (1)	..	..	..	..	..	..
5·5	1 (2)	..	..	..	..	..	..
6·5	3 (20)	..	..	..	..	..	..
7·0	4 (143)	1 (36)	..	..	..	..	..
7·5	..	6 (428)	..	..	..	..	..
Totals	9 (150+)	7	..	..	..	..	..

Class K.

Absolute Magnitude 4^M.

5·0	..	..	..	..	..	..	1 (2)
6·0	..	..	..	..	..	..	1 (4)
Totals	..	..	..	..	..	..	2 (6)

Absolute Magnitude 3^M.

3·5	..	..	..	..	..	..	1 (1)
4·5	..	..	..	..	..	..	1 (1)
5·0	..	..	..	..	..	..	2 (3)
Totals	..	..	..	..	..	..	4 (5)

Absolute Magnitude 2^M.

2·0	..	..	1 (1)	..	..	..	..
3·0	..	..	..	..	1 (1)	..	..
4·0	..	..	..	..	..	2 (2)	..
6·0	..	..	..	..	..	..	1 (4)
6·5	..	..	..	..	..	..	1 (10)
Totals	..	..	1 (1)	..	1 (1)	2 (2)	2 (14)

TABLE II.—*continued.*

Class K.—continued.

Absolute Magnitude 1^M.

m.	ps. 0–20.	ps. 21–40.	ps. 41–60.	ps. 61–80.	ps. 81–100.	ps. 101–200.	ps. >200.
2·5	..	..	1 (1)	..	..	..	..
3·0	..	..	1 (1)	..	..	..	..
3·5	..	..	..	..	1 (1)	..	..
4·5	..	..	..	..	..	2 (2)	..
5·0	..	..	..	..	..	6 (10)	..
5·5	..	..	..	..	..	7 (14)	2 (4)
6·0	..	..	..	..	..	2 (7)	11 (41)
6·5	..	..	..	..	..	..	7 (70)
Totals	..	..	2 (2)	..	1 (1)	17 (33)	20 (115)

Absolute Magnitude 0^M.

2·0	..	3 (4)	..	..	..	..	..
2·5	..	3 (4)	..	..	..	..	..
3·0	..	6 (7)	1 (1)	..	..	..	..
3·5	..	1 (1)	10 (12)	1 (1)	..	..	..
4·0	..	..	14 (17)	11 (13)	..	..	..
4·5	..	..	1 (1)	20 (24)	10 (12)	..	..
5·0	..	..	..	8 (13)	28 (47)	10 (17)	..
5·5	..	..	..	..	10 (20)	59 (116)	..
6·0	..	..	..	..	..	59 (218)	..
6·5	..	..	..	..	..	26 (260)	..
Totals	..	13 (16)	26 (31)	40 (51)	48 (79)	154 (611)	..

Absolute Magnitude 1^M.

2·0	4 (5)	..	..	..	..	..	..
2·5	3 (4)	3 (4)	..	..	..	..	..
3·0	..	14 (17)	..	..	..	..	..
3·5	..	20 (24)	4 (5)	..	..	..	..
4·0	..	20 (24)	22 (26)	..	..	..	..
4·5	..	..	41 (50)	14 (17)	..	..	..
5·0	..	..	26 (43)	54 (90)	11 (18)	..	..
5·5	..	..	5 (10)	43 (84)	82 (161)	..	..
6·0	..	..	..	..	58 (215)	55 (204)	..
6·5	..	..	..	..	7 (70)	61 (210)	..
7·0	..	..	..	..	..	9 (231)	..
7·5	..	..	..	..	..	7 (500)	3 (214)
Totals	7 (9)	57 (69)	98 (134)	111 (191)	158 (464)	132 (1000+)	3

TABLE II.—*continued.*

Class K.—continued.

Absolute Magnitude 2M.

m.	ps. 0–20.	ps. 21–40.	ps. 41–60.	ps. 61–80.	ps. 81–100.	ps. 101–200.	ps. >200.
3·0	1 (1)	..	..	..	..	..	..
3·5	1 (1)	..	..	..	..	..	..
4·0	..	12 (14)	..	..	..	..	..
4·5	..	12 (15)	2 (2)	..	..	..	..
5·0	..	3 (5)	3 (5)	..	..	..	..
5·5	..	0 (0)	11 (22)	7 (14)	..	..	..
6·0	..	..	9 (33)	25 (93)	5 (19)	..	..
6·5	..	..	1 (10)	6 (60)	9 (90)	..	..
7·0	..	..	..	1 (36)	3 (107)	1 (36)	..
7·5	..	..	..	..	..	10 (714)	..
Totals	2 (2)	27 (34)	26 (72)	39 (180+)	17	11	..

Absolute Magnitude 3M.

2·0	1 (1)	..	..	..	..	..	..
3·5	3 (4)	..	..	..	..	..	..
4·0	1 (1)	..	..	..	..	..	..
4·5	..	1 (1)	..	..	..	..	..
5·0	..	5 (8)	..	..	..	..	..
5·5	..	3 (6)	1 (2)	..	..	..	..
6·0	..	0 (0)	3 (11)	..	..	..	..
6·5	..	1 (10)	3 (30)	..	..	..	..
7·5	..	..	..	1 (71)	2 (143)	..	..
Totals	5 (6)	10 (25)	7 (43)	1 (71+)	2	..	..

Absolute Magnitude 4M.

4·0	1 (1)	..	..	..	..	..	..
5·5	1 (2)	2 (4)	..	..	..	..	..
6·0	..	3 (11)	..	..	..	..	..
6·5	..	4 (40)	..	..	..	..	..
7·0	..	1 (36)	..	..	..	..	..
Totals	2 (3)	10 (80+)	..	..	..	..	..

Absolute Magnitude 5M.

5·0	2 (3)	..	..	..	..	..	..
5·5	4 (8)	..	..	..	..	..	..
6·0	4 (15)	..	..	..	..	..	..
6·5	5 (50)	5 (50)	..	..	..	..	..
7·0	..	4 (143)	..	..	..	..	..
7·5	..	8 (571)	..	..	..	..	..
Totals	15 (76)	17 (500+)	..	..	..	..	..

TABLE II.—*continued.*

Class K.—continued.

Absolute Magnitude 6M.

m.	ps. 0–20.	ps. 21–40.	ps. 41–60.	ps. 61–80.	ps. 81–100.	ps. 101–200.	ps. >200.
3·5	1 (1)	..	..	..	..	..	..
4·0	1 (1)	..	..	..	..	..	..
4·5	3 (4)	..	..	..	..	..	..
5·0	2 (3)	..	..	..	..	..	..
5·5	5 (10)	..	..	..	..	..	..
6·0	6 (22)	..	..	..	..	..	..
6·5	9 (90)	..	..	..	..	..	..
7·0	13 (464)	1 (36)	..	..	..	..	..
7·5	11 (785)	5 (357)	..	..	..	..	..
Totals	51 (1000+)	6	..	..	..	..	..

Absolute Magnitude 7M.

5·5	1 (2)	..	..	..	..	..	..
6·0	4 (15)	..	..	..	..	..	..
6·5	6 (60)	..	..	..	..	..	..
7·0	4 (143)	..	..	..	..	..	..
7·5	3 (214)	..	..	..	..	..	..
Totals	18 (400+)	..	..	..	..	..	..

Absolute Magnitude 8M.

7·5	1 (71)	..	..	..	..	..	..
Totals	1 (71+)	..	..	..	..	..	..

Class M.

Absolute Magnitude 3M.

4·5	..	..	..	..	..	..	1 (2)

Absolute Magnitude 2M.

2·0	..	..	..	1 (5)	..	..	..
4·5	..	..	..	..	..	1 (2)	..
5·0	..	..	..	..	..	..	1 (1)
5·5	..	..	..	..	..	..	1 (2)
6·0	..	..	..	..	..	..	3 (11)
Totals	..	..	..	1 (5)	..	1 (2)	5 (14)

TABLE II.—*continued.*

Class M.—continued.

Absolute Magnitude 1^M.

m.	ps. 0–20.	ps. 21–40.	ps. 41–60.	ps. 61–80.	ps. 81–100.	ps. 101–200.	ps. >200.
3·0	..	..	..	2 (10)	..	..	..
3·5	..	..	..	..	1 (5)	..	..
4·5	..	..	..	..	..	3 (7)	..
5·0	..	..	..	..	..	9 (13)	..
5·5	..	..	..	..	..	6 (12)	2 (4)
6·0	..	..	..	..	..	3 (11)	5 (19)
6·5	..	..	..	..	..	..	10 (89)
7·0	..	..	..	..	..	..	3
7·5	..	..	..	..	..	..	1
8·0	..	..	..	..	..	..	4
8·5	..	..	..	..	..	..	1
9·0	..	..	..	..	..	..	1
Totals	..	..	..	2 (10)	1 (5)	21 (43)	27 (112+)

Absolute Magnitude 0^M.

2·5	..	2 (10)	..	..	..	..	..
3·0	..	1 (5)	..	..	..	..	..
3·5	..	1 (5)	..	..	..	..	..
4·0	..	..	1 (5)	1 (5)	..	..	..
4·5	..	..	..	7 (16)	3 (7)	..	..
5·0	..	..	..	5 (7)	18 (27)	11 (16)	..
5·5	..	..	..	..	14 (29)	36 (75)	..
6·0	..	..	..	..	..	36 (138)	..
6·5	..	..	..	..	..	15 (133)	3 (26)
7·0	..	..	..	..	..	3	13
7·5	..	..	..	..	..	..	11
8·0	..	..	..	..	..	..	5
8·5	..	..	..	..	..	..	3
9·0	..	..	..	..	..	..	5
9·5	..	..	..	..	..	..	2
Totals	..	4 (20)	1 (5)	13 (28)	35 (63)	101 (362+)	42

Absolute Magnitude 1^M.

3·5	..	1 (5)	..	..	..	..	..
4·5	..	..	..	2 (5)	..	..	..
5·0	..	..	2 (3)	2 (3)	1 (1)	..	..
5·5	..	..	..	1 (2)	9 (19)	..	..
6·0	..	..	..	..	1 (4)	10 (38)	..
6·5	..	..	..	..	..	8 (71)	..
7·0	..	..	..	..	..	2	..
7·5	..	..	..	..	..	..	2
8·0	..	..	..	..	..	..	3
Totals	..	1 (5)	2 (3)	5 (10)	11 (24)	20 (109)	5

Absolute Magnitude 2^M.

7·5	..	..	..	..	..	1	..

TABLE II.—*continued.*

Class M.—continued.

	Absolute Magnitude 7M.		Absolute Magnitude 8M.	
m.	ps. 0–20.	ps. 21–40.	ps. 0–20.	ps. 21–40.
5·0	..	..	1	..
6·5	..	..	1	..
7·0	..	..	1	..
7·5	..	..	..	..
8·0	1	..	..	..
8·5	..	..	2	..
9·0	..	1	7	..
9·5	..	..	3	1
10·0	..	..	..	2
10·5	..	..	..	1
Totals	1	1	15	4

	Absolute Magnitude 9M.		Absolute Magnitude 10M.	
6·5	1	..	..	..
7·0	..	..	1	..
7·5	1	..	..	..
8·0	1	..	..	..
8·5	6	..	2	..
9·0	10	..	4	..
9·5	15	..	10	..
10·0	2	..	4	..
10·5	..	1	..	..
Totals	36	1	21	..

	Absolute Magnitude 11M.		Absolute Magnitude 12M.	
7·5	1	..	..	..
9·0	3	..	1	..
9·5	3	..	2	..
10·0	1	..	..	..
10·5	..	..	2	..
Totals	8	..	5	..

In reading Table II. it will be recognised that the proportion of stars observed, out of the whole number present, is different with different magnitudes, and diminishes sharply from about the 6th magnitude onwards. To estimate what proportion is found for each spectral class, I work from the counts of the Henry Draper Catalogue, given in *Harvard Circulars*, No. 226, Table II., where the actual numbers are given for each class for visual magnitudes brighter than 6·25, 6·75, . . . 9·25. The collection starts almost at the point where my data begin to fail, but, calling any of these numbers Nm, it will be found that $\log_{10} Nm$, charted against m, gives over most of its course a straight line, declining slightly at the faintest magnitudes, owing no doubt to incompleteness of the material at that point. Continuing this straight line backwards as far as magnitudes brighter than 4·25, I obtain a series

of numbers which may be taken as sufficiently reliable for the total numbers present in each class, for each magnitude. Comparing these numbers with the numbers actually observed for parallaxes in the present list, a factor is found representing the proportion present in my list. The factor is taken as the same for any stars brighter than the fourth magnitude. I apply to each number entered in Table II. its appropriate factor, and thus obtain the numbers given in that table in brackets ; thus, for example, the entry under Class B, absolute magnitude 3^M, 101–200 ps., $2^m.5$, 4 (13) means that four stars are found in the list of parallaxes, of absolute magnitudes 3^M, at distances between 100 and 200 parsecs, and of visual magnitude classed as 2·5, while the appropriate factor for stars of 4th magnitude or brighter gives $4 \times 3{\cdot}3 = 13$ as the estimated number of stars of the same type to be found in the whole sky.

The factors employed are shown in Table III.

TABLE III.

Proportions Observed out of Whole Numbers.

		$4^m.0$.	$4^m.5$.	$5^m.0$.	$5^m.5$.	$6^m.0$.	$6^m.5$.	$7^m.0$.	$7^m.5$.	$8^m.0$.
B and Oe	Whole	213	75	84	153	194	265	..	..	
	Observed	70	32	59	57	28	8	..	..	
	Ratio	·30	·43	·70	·37	·14	·03	..	..	
	Factor	3·33	2·33	1·41	2·63	7·14	33	..	..	
A	Whole	200	160	310	530	818	1460	2426	3422	
	Observed	79	57	115	209	126	49	7	..	
	Ratio	·40	·36	·36	·39	·15	·03	..	..	
	Factor	2·50	2·78	2·78	2·56	6·67	29·4	..	..	
F	Whole	68	47	109	176	280	520	960	1464	
	Observed	40	19	59	75	82	57	17	..	
	Ratio	·59	·40	·54	·43	·29	·11	·02	..	
	Factor	1·70	2·50	1·85	2·33	3·45	9·09	56	..	
G	Whole	50	50	91	164	301	528	1272	1896	
	Observed	55	40	74	73	77	81	41	..	
	Ratio	1·10	·80	·81	·45	·26	·15	·03	..	
	Factor	·91	1·25	1·24	2·22	3·85	6·67	31	..	
K	Whole	200	131	272	469	912	1512	2648	5536	
	Observed	168	107	161	240	246	151	44	..	
	Ratio	·84	·82	·60	·51	·27	·10	·02	..	
	Factor	1·19	1·22	1·67	1·96	3·70	10·00	60	..	
M	Whole	54	39	73	143	229	337	578	1078	
	Observed	11	17	49	69	60	38	..	..	
	Ratio	·20	·44	·67	·48	·26	·11	..	..	
	Factor	4·90	2·29	1·49	2·07	3·82	8·87	..	..	

In this table the apparent magnitudes are given in the top line. The entries below these give the corresponding numbers of stars, *e.g.* under Class B and Oe the whole number of stars to be found brighter than $4^{m}{\cdot}25$ is estimated from the Harvard counts, as just explained, to be 213; the additional number, brighter than $4^{m}{\cdot}75$, is estimated at 75, and so on. The numbers observed are shown beneath, and finally the factors required to raise the latter figure to equal the former. In one case—Class G—the estimated number up to mag. 4·25 is 50, while the number observed exceeds this, amounting to 55. But this is of no importance, since the individual numbers concerned are not large.

At the other end of the table, however, we find that one-thirtieth or less, out of the whole number, have been observed. To infer the whole number from the proportion observed becomes then very doubtful. But before this, when as much as one-sixth, one-seventh, or even one-tenth of the whole has been observed it is considered that quite a reliable figure can be got by employing the factor recorded.

Thus making the totals of the numbers in brackets in any column of Table II., I find an estimate of a number of stars of any class and any absolute magnitude, occurring within specified distances from the Sun. Thus, for example, Class A, absolute magnitude 1^{M}, within the shell from 61 to 80 parsecs distant, 81 stars were observed and 230 are estimated to occur. It will be seen that the estimation proceeds without the use of large factors of extrapolation up to a certain definite distance for each group; up to this point the conclusions may be considered as sure and representative, the anomalies that occur belonging to the material itself more than to the treatment.

The volumes through which are spread the numbers of stars thus estimated differ, of course, progressively; they are the following :—

	ps. 0–20.	ps. 21–40.	ps. 41–60.	ps. 61–80.	ps. 81–100.	ps. 101–200
$\times 10^{6}$ cu. ps.]	·0335	·234	·637	1·239	2·044	29·31

Dividing, then, by these volumes we get the density, or number of stars per million cubic parsecs, for each group of stars.

The results are shown in Table IV.

TABLE IV.

Number of Stars per Million Cubic Parsecs.

Class B and Oe.	ps. 0–20.	ps. 21–40.	ps. 41–60.	ps. 61–80.	ps. 81–100.	ps. 101–200.
M.						
3	..	..	..	6	8	1
2	..	..	11	6	8	2
1	..	29	5	19	6	0·1
0	..	43	5	10	4	4+
Class A.						
M.						
0	..	34	46	24	40	14
1	627	346	232	186	262	23+
2	836	389	301	349	183	..
3	90	303	61	..	..	..

TABLE IV.—*continued.*

Class B and Oe.	ps. 0–20.	ps. 21–40.	ps. 41–60.	ps. 61–80.	ps. 81–100.	ps. 101–200.
Class F.						
M.						
1	..	9	6	..	1	..
0	..	9	6	4	1	0·8
1	60	17	22	15	7	3+
2	239	333	145	68	7+	..
3	449	863	550+	172+	..	..
4	359	803	393+	..	..	..
5	90	..	..	..	..	..
Class G.						
M.						
2	..	..	..	..	..	0·2
1	..	..	..	2	1	0·6
0	..	17	6	4	12	4
1	..	34	17	22	27	3+
2	30	38	6	34	30+	..
3	209	346	236+	..	..	..
4	1702	2400+	..	..	..	..
5	4477+	..	..	..	..	..
6	4477+	..	..	..	..	..
Class K.						
M.						
2	..	..	2	..	0·5	0·1
1	..	..	3	..	1	1
0	..	68	49	41	39	20
1	269	295	210	154	227	30+
2	60	145	113	145+	..	..
3	179	108	68	57+	..	..
4	90	322+	..	..	..	..
5	2269	2135+	..	..	..	..
6	30000+	..	..	..	..	..
Class M.						
M.						
2	..	..	..	4	..	0·1
1	..	..	..	8	2	1
0	..	89	8	22	31	12+
1	..	21	5	8	12	4

With regard to the interpretation of this table it may be remarked that the mean separation between stars, in parsecs, is related to the number per 10^6 cu. ps. as follows :—

Mean Separation.	Density.	Mean Separation.	Density.	Mean Separation.	Density.
5	8000	20	125	45	11
7	2915	25	64	50	8
10	1000	30	37	60	5
12	694	35	23	80	2
15	296	40	16	100	1

I add a few remarks on the distribution shown in Table IV.

It must be taken as a fairly complete account up to the point to which each type of star has been carried, but not beyond. Thus, for example, *Class A*, 3^M, a large number of stars beyond 6 mag. visual would require to be observed before any conclusion could be drawn as to the density beyond 60 parsecs.

Since the volume 0–20 ps. is only one-thirtieth of a million cubic parsecs, inequalities in the determination of density within this volume are liable to present themselves without any real significance.

The most striking feature of this table in general is the increase in numbers as the stars grow fainter.

A second feature is this : stars of the same type, that is to say of the same spectral class and luminosity, or what comes to the same thing, of the same temperature, mass, and radius—in fact identical stars—are distributed across space up to the distance that this investigation explores, with about the same density. Where any exceptions appear they are mentioned below.

Class B and Oe is confined to great stars of 0^M or brighter, separated by 40–60 parsecs, and extending with roughly uniform density up to a range of 100 ps., beyond which they are notably less numerous.

Class A appears to begin where B leaves off. It is also uniform up to 100 ps. The numbers for 1^M and 2^M are about ten times more numerous than those for 0^M. There is again a considerable falling off at 3^M, after which the group ceases.

Class F definitely separates into two sub-groups, 1^M and brighter and 2^M and fainter, the latter being about ten times as numerous as the former. The former show little condensation up to 100 ps. For 2^M there appears a fairly distinct condensation on the centre, but it is not confirmed as a system by the following magnitudes.

Class G shows the same division, the boundary magnitudes being 2^M and brighter and 3^M and fainter. The latter set show a very rapid increase in numbers as magnitude rises, the mean separation of the stars of 5^M and 6^M not exceeding 6 ps.

Class K will be looked at with interest for an indication of the Giant and Dwarf division, but, except for a slight summit at 1^M, there is little sign of it, so far as this list goes. The K stars are more numerous than any other class, and if we proceed up to 6^M they appear to be separated by not more than 3 ps. or 4 ps.

Class M is represented in Table IV. solely by stars of 1^M and brighter, few and widely separated. For stars fainter than these there is a deficiency. By reference to Table II. it will be seen that small stars occur in large numbers, beginning apparently at 7^M. But the enumeration cannot here be treated as representative, because they form too small a proportion of the visual magnitudes from which they are drawn to serve as a basis for conclusion ; besides, a large number of them are found to be drawn from the *Cincinnati Catalogue of Stars* of large proper motions, and other special sources, probably with a view to securing stars of measurable parallax. The breach, however, between Giant and Dwarf stars appears indubitable.

If Table IV. is taken to show that the density of any type is a function

of the absolute magnitude m alone, it is worth remarking that this fact is sufficient to determine mathematically that density from the counts of apparent magnitude. For let $I(m)dm$ be the number of stars counted between apparent magnitudes m and $m + dm$, $J(m)dm$ the number existing between absolute magnitudes m and $m + dm$, per cubic parsec, which number is taken the same at all distances. Then the numbers found in the shell between distances D and D + dD is

$$4\pi D^2 dD \cdot J(m)dm,$$

which appear as of apparent magnitude m, provided

$$M = m + 5 - 5 \log_{10} D.$$

Hence, changing the variables from M, D to m, D, and integrating with respect to D between appropriate limits,

$$I(m) = \int_0^{D_0} 4\pi D^2 dD J(m + 5 - 5 \log_{10} D),$$

where the upper limit D_0 is given by

$$m + 5 - 5 \log_{10} D_0 = M_0$$

and M_0 is the limit of absolute magnitude of the class.

This equation belongs to the type

$$f(x) = \int_a^x K(x\xi)u(\xi)d\xi,$$

where f, K are known forms and u has to be determined; that is to say, an integral equation of the first type. But I do not pursue this avenue further at present.

In conclusion, reference may be made to the distribution of the observations in regard to direction, the foregoing treatment having massed all directions together. Dividing the sky into twenty-four equal parts as follows :—

I	0h– 4h,	+ 30° to + 90°	VII	0h– 4h,	0° to + 30°
II	4– 8,	,,	VIII	4– 8,	,,
III	8–12,	,,	IX	8–12,	,,
IV	12–16,	,,	X	12–16,	,,
V	16–20,	,,	XI	16–20,	,,
VI	20–24,	,,	XII	20–24,	,,
XIII	0h– 4h,	0° to – 30°	XIX	0h– 4h,	– 30° to – 90°
XIV	4– 8,	,,	XX	4– 8,	,,
XV	8–12,	,,	XXI	8–12,	,,
XVI	12–16,	,,	XXII	12–16,	,,
XVII	16–20,	,,	XXIII	16–20,	,,
XVIII	20–24,	,,	XXIV	20–24,	,,

I have found for each class the number of observations falling in each part and the mean distance for that part : also the general mean of the distances ; except for Class M, in which case the determination is made in two pieces, namely, distances <60 ps. and distances >60 ps. This applies to distances not greater than 200 ps. For greater distances the number of observations is recorded simply.

These results are contained in Table V. The mean distances are given, with the number of observations subscript.

TABLE V.

		0^h.	4^h.	8^h.	12^h.	16^h.	20^h.	24^h.
B	$+90°$							
	$+30°$	214_{39}	200_{7}	150_{1}	138_{22}	235_{32}	158_{19}	
	0	159_{17}	177_{63}	205_{7}	134_{12}	175_{35}	149_{11}	
	$-30°$	50_{1}	150_{4}	183_{4}	100_{12}	164_{6}	83_{3}	
	$-90°$		None			None		
		General mean 176_{295}.						
A	$+90°$							
	$+30$	86_{60}	87_{35}	67_{44}	68_{39}	80_{49}	99_{45}	
	0	79_{40}	74_{65}	70_{39}	81_{38}	78_{47}	79_{30}	
	$-30°$	86_{14}	59_{17}	87_{12}	84_{38}	85_{22}	97_{16}	
	$-90°$	70_{1}	None	None	70_{1}	50_{1}	None	
		General mean 80_{653} ; >200 ps., 4.						
F	$+90°$							
	$+30°$	52_{37}	60_{27}	47_{30}	60_{35}	55_{34}	63_{36}	
	0	45_{44}	47_{52}	56_{31}	50_{45}	51_{41}	45_{42}	
	$-30°$	15_{1}	30_{1}	30_{1}	15_{2}	None		
	$-90°$		None				None	
		General mean 52_{459} ; >200 ps., 9.						
G	$+90°$							
	$+30°$	61_{48}	61_{30}	68_{36}	43_{34}	60_{38}	60_{33}	
	0	61_{48}	56_{32}	49_{52}	45_{51}	77_{53}	59_{47}	
	$-30°$	26_{6}	56_{7}	51_{6}	120_{4}	108_{6}	70_{6}	
	$-90°$		None			None		
		General mean 59_{537} ; >200 ps., 36.						

TABLE V.—*continued.*

		0^h.	4^h.	8^h.	12^h.	16^h.	20^h.	24^h.
K	$+90°$							
	$+30°$	84_{67}	84_{56}	86_{76}	86_{54}	81_{77}	95_{95}	
	0	74_{66}	84_{67}	82_{49}	66_{75}	75_{81}	84_{64}	
	$-30°$	67_{33}	49_{24}	57_{28}	72_{55}	74_{54}	80_{50}	
	$-90°$	75_{33}	72_{29}	88_{30}	78_{35}	77_{37}	96_{39}	

General mean 79_{1274}; >200 ps., 70.

M	$+90°$							
	$+30°$	13_{12}	13_{4}	12_{16}	12_{6}	9_{8}	7_{9}	
	0	20_{3}	33_{2}	5_{2}	19_{9}	16_{7}	18_{3}	
<60 ps.	$-30°$	23_{4}	8_{3}	12_{3}	14_{6}	18_{4}	38_{3}	
	$-90°$	28_{2}	None			None		

General mean 14_{108}.

>60 ps.	$+90°$							
	$+30°$	130_{9}	129_{14}	127_{9}	137_{19}	152_{18}	137_{20}	
	0	138_{10}	120_{20}	138_{19}	112_{11}	130_{17}	112_{9}	
	$-30°$	125_{11}	114_{9}	130_{8}	130_{6}	123_{8}	122_{13}	
	$-90°$		None		None	70_{1}	70_{1}	

General mean 129_{231}; >200 ps., 85.

With respect to this table, I remark that the southern hemisphere, and especially the areas XIX.–XXIV. between $-30°$ and $-90°$, are very imperfectly represented, owing no doubt to want of observations and not to a deficiency of stars. Further, it must be remembered that the collection ceases to be approximately on a level footing after the 6th apparent magnitude, so that the numbers brought under the means are lopped in a systematic way that has not been allowed for. This is especially true of the close-in M stars.

It will be seen that the classes B, A, F have hardly any representatives beyond 200 ps., while G, K, M present numerous examples beyond that distance.

The Milky Way passes down from N. to S. between 4^h and 8^h, and up from S. to N. between 16^h and 20^h, reaching extreme declinations of $+55°$ and $-55°$. The connection, if any, with the numbers of this table is very weakly shown. The large number of B stars in area VIII., namely 63, follows, of course, the position of Orion.

The rough uniformity of the distances corresponding to different areas furnishes a justification of the treatment by whole shells employed in the previous part of the paper.

Stellar Parallaxes Determined at the Royal Observatory, Greenwich.

(*Communicated by the Astronomer Royal.*)

The following list is a continuation of the results obtained with the 26-inch telescope and published annually in the November number of the *Monthly Notices.*

In the column Proper Motion the first value given is from meridian observations ; the second is the relative proper motion derived from the photographs. The motions in both R.A. and Dec. are expressed in arc of a great circle.

In calculating the parallax, the relative proper motion has been used, *not* the meridian proper motion.

The Probable Error has been calculated by the formula

$$r = 0{\cdot}6745 \times \sqrt{\frac{[vv]}{m-\mu}} \times \frac{1}{\sqrt{w}}.$$

The first P.E. given is that of the parallax, the second is the P.E. of the relative proper motion.

Generally six comparison stars of mean magnitude 11–12 have been used, the magnitude of the parallax star being reduced to equality by means of the rotating sector. The parallax as well as the photographic proper motion is relative to these stars.

The observing list has been extended to include all stars brighter than $5^{m}{\cdot}5$ visual. To compare these with comparison stars of magnitude 11–12 it has been necessary to supplement the reduction in magnitude by the variable sector, by staining a central portion of the plate with a solution of copper sulphate as suggested by Professor Schlesinger. A circular area 37 mm. in diameter was bathed with a $\frac{1}{2}$ per cent. solution for three minutes. The excess was then blotted off and the plate dried before an electric fan. The distortion which may arise from this local treatment has been investigated and the central area appears to be free from systematic distortion. To eliminate such accidental distortions as may have been introduced, the procedure adopted is to make four exposures on each plate, the plate being reversed through 180° for the third and fourth exposures. When it has not been possible to complete a plate by reversal, the result has been given half weight. The residuals indicate that the result from a complete stained plate is fully equal to that from an unstained plate.

No.	Name and B.D. No.	Mag. Vis. Photog.	Spectral Type.	R.A. Dec. 1900·0.	Proper Motion. R.A.	Proper Motion. Dec.	Parallax.	P.E.	No. of Plates.
		m		h m s	″	″	″	″	
1	73° 26	9·1		0 33 2	−·204	−·078	−·004	±·009	17
		9·5		+74° 12′	−·206			±·010	
2	Gr. 145	7·8	Ko	0 43 17	+·364	+·200	+·011	±·009	18
	69° 45	8·5		+69° 54′	+·386			±·009	
3	63° 137	8·7	K7	1 0 19	+1·518	+·290	+·043	±·009	20
		9·5		+63° 24′	+1·540			±·010	
4	O.A. 1434	8·7	Ko	1 16 41	+·083	−·094	−·025	±·008	27
	67° 118	9·1		+67° 35′	+·087			±·008	
5	68° 138	9·2		1 50 48	+·321	−·036	−·001	±·004	26
		9·5		+68° 32′	+·347			±·005	
6	O.A. 2526	7·5	Go	2 9 12	−·325	−·338	+·006	±·010	25
	64° 312	8·5		+64° 29′	−·327			±·010	
7	Br. 448	4·5	B3p	3 11 11	+·011	−·005	+·006	±·007	23
	65° 340	5·0		+65° 17′	+·026			±·008	
8	66° 256	9·1		3 11 52	+·142	−·142	+·023	±·005	25
		10·4		+66° 34′	+·082			±·005	
9	O.A. 5021	9·0	Ko	4 35 46	+·104	−·033	+·028	±·005	29
	69° 271	9·3		+69° 54′	+·081			±·004	
10	P. V. 335	4·7	Ao	6 7 50	+·012	−·109	+·011	±·006	22
	69° 371	4·7		+69° 21′	−·002			±·007	
11	O.A. 10680	7·6	Ko	10 10 57	−·087	−·070	+·020	±·009	26
	73° 491	7·6		+72° 56′	−·081			±·008	
12	70° 639	9·5		10 51 1	−·630	+·058	+·048	±·005	23
		11·6		+70° 8′	−·620			±·006	
13	L.F. 2132	8·3	Ko	12 38 20	−·107	+·032	+·003	±·006	25
	76° 464	8·4		+75° 54′	−·099			±·008	
14	9 Dra.	5·8	Ko	12 56 9	−·149	−·014	·000	±·010	24
	67° 773	6·5		+67° 8′	−·123			±·007	
15	Gr. 1971	7·0	Ko	13 9 35	−·178	+·019	+·012	±·008	25
	68° 717	7·8		+67° 50′	−·120			±·006	
16	Gr. 1972	6·7	Ko	13 10 3	−·182	−·003	+·011	±·009	25
	68° 720	7·5		+67° 49′	−·136			±·008	
17	Gr. 2214	5·2	Go	15 13 29	+·217	−·404	+·048	±·007	24
	67° 876	5·7		+67° 44′	+·209			±·001	
18	P. XVI. 182	5·5	A3	16 31 17	−·103	+·104	+·064	±·011	25
	79° 498	6·0		+79° 10′	−·094			±·008	

No.	Name and B.D. No.	Mag. Vis. Photog.	Spectral Type.	R.A. Dec. 1900·0.	Proper Motion. R.A.	Proper Motion. Dec.	Parallax.	P.E.	No. of Plates.
		m		h m s	″	″	″	″	
19	18 Dra.	5·2	K0	16 40 13	+·030	−·017	+·018	±·007	31
	64° 1145	5·9		+64° 46′	+·019			±·005	
20	h^1 Dra.	5·3	F5	16 55 29	+·247	+·049	+·073	±·012	26
	65° 1157	5·4		+65° 17′	+·249			±·008	
21	ζ Dra.	3·0	B5	17 8 30	−·013	+·020	+·044	±·008	30
	65° 1170	3·0		+65° 50′	−·016			±·004	
22	27 Dra.	5·5	K0	17 32 22	−·013	+·137	−·011	±·009	26
	68° 938	5·9		+68° 11′	+·002			±·007	
23	δ U. Mi.	4·5	A0	18 4 33	+·018	+·055	+·015	±·009	32
	86° 269	4·4		+86° 37′	+·010			±·005	
24	43 Dra.	4·7	A0p	18 22 11	−·009	+·030	−·015	±·008	29
	71° 889	4·1		+71° 17′	+·010			±·005	
25	o Dra.	4·3	K0	18 49 44	+·081	+·023	+·003	±·007	34
	59° 1925	5·8		+59° 16′	+·106			±·004	
26	τ Dra.	4·4	K0	19 17 29	−·138	+·110	−·006	±·008	29
	73° 857	5·7		+73° 10′	−·125			±·005	
27	ρ Dra.	5·1	K0	20 2 22	+·017	+·048	−·024	±·009	30
	67° 1222	5·8		+67° 35′	+·027			±·006	
28	75 Dra.	5·8	K0	20 34 32	+·035	+·011	+·008	±·007	24
	80° 659	6·2		+81° 5′	+·030			±·007	
29	6 Cep.	5·5	B3p	21 17 18	+·003	+·001	−·001	±·008	23
	64° 1527	5·0		+64° 27′	+·044			±·007	
30	C. 3269	9·5		21 24 40	−·056	−·036	−·020	±·007	23
	80° 694	10·1		+81° 10′	−·067			±·006	
31	Br. 2993	5·0	A0	22 21 18	+·049	+·042	+·002	±·007	31
	85° 383	5·2		+85° 36′	+·023			±·005	
32	78° 842	9·5		23 33 27	+·265	+·041	+·007	±·007	20
		10·3		+78° 42′	+·262			±·008	
33	L.F. 4652	7·2	K0	23 59 48	+·122	+·062	−·005	±·009	22
	64° 1894	8·1		+64° 52′	+·066			±·009	

No. 12. A previous result, +″·052±″·010 measured on plates taken for Gr. 1697 with the star not in the centre of the field, has been published in the volume of *Stellar Parallaxes*, 1913–24.

No. 20. Other determinations Alleg. +″·088, Gr. +″·029. The result +″·029, depending on a few "Kapteyn" plates, is weak.

No. 30. The value +″·045 published in the volume of *Stellar Parallaxes*, 1913–24 must be considered erroneous. In this determination the star originally appeared as a comparison star to L.F. 3880. It falls some distance from the centre of the plate and the measures are evidently affected by optical distortion.

Mean Areas and Heliographic Latitudes of Sunspots in the Year 1926.

(*Communicated by the Astronomer Royal.*)

The results here given are in continuation of those in the *Monthly Notices*, **87**, 168, and are derived from the measurement of photographs taken at the Royal Observatories of Greenwich and the Cape, and in India at the Kodaikánal Observatory.

Table I. gives the mean daily area of umbræ, whole spots, and faculæ for each synodic rotation of the Sun included in the year 1926, whilst the mean values for each year as a whole from 1923 to 1926 are given in Table II.

Table III. gives for each rotation in the year 1926 the mean daily area of the whole spots (corrected for foreshortening) and the mean heliographic latitude of the spotted areas for both hemispheres, northern and southern. The mean heliographic latitude of the entire spotted area and the mean distance from the equator of all spots are also tabulated. The mean values for the years 1923 to 1926 are given in Table IV. Tables II. and IV. are in continuation of similar tables given in the *Monthly Notices*; for the years 1874 to 1888, **49**, 381 and 382; 1889 to 1902, **63**, 465 and 466; 1901 to 1914, **76**, 402 and 403; 1913 to 1924, **85**, 1007 and 1008.

The rotations in Tables I. and III. are numbered in continuation of Carrington's series (*Observations of Solar Spots made at Redhill*, by R. C. Carrington, F.R.S.), No. 1 being the rotation commencing 1853 November 9. The assumed prime meridian is that which passed through the ascending node at mean noon on 1854 January 1, and the assumed period of the Sun's sidereal rotation is 25·38 days.

The principal features of the record for the year 1926 were as follows :—

1. A large increase, amounting to 50 per cent., in the mean daily area of spots as compared with the mean area for the year 1925.

2. Rotations, Nos. 967–69, which contributed materially to this increase, included several unusually large spots, Group 9861 being the largest spot observed since the inception of the Greenwich observations. Although the mean daily areas, exhibited both for spots and faculæ, in Table I. show a general decrease from the beginning to the end of the year, the number of groups, irrespective of size, showed no corresponding diminution.

3. The number and area of spots contributed by the two hemispheres, northern and southern, were about equal.

4. A large amount of faculæ was measured during the year, especially in connection with the large spots mentioned in (2).

5. The mean latitude of all spots was $18\frac{1}{2}^\circ$ as compared with 20° for the previous year. Irrespective of the size of groups, the average latitude was 18°. The latitudes of individual groups ranged from 2° to 35°.

6. There were only two days without spots, but on these occasions appreciable areas of faculæ were measured.

7. The number of separate groups lasting for at least two days was 299, divided between the northern and southern hemispheres in the ratio 148 : 151. Besides these, there were recorded 150 small groups (mostly consisting of one or two very small spots) visible on one day only; 85 of these were in the northern and 65 in the southern hemisphere.

8. Judging from the average latitude of the spots, the maximum year should be 1928.

TABLE I.

No. of Rotation.	Rotation commenced G.M.T.	No. of Days on which Sun photographed.	Mean of Daily Areas. Projected.* Umbræ.	Whole Spots.	Faculæ.	Corrected for Foreshortening.† Umbræ.	Whole Spots.	Faculæ.
	1925.							
967	Dec. 30·86	27	572	3435	3123	439	2708	3782
	1926.							
968	Jan. 27·19	28	466	2612	2895	362	2077	3268
969	Feb. 23·54	27	345	2131	2825	265	1671	3224
970	Mar. 22·85	27	130	671	2434	103	529	2809
971	Apr. 19·14	27	249	1361	2314	189	1017	2739
972	May 16·37	27	231	1314	2427	169	954	2962
973	June 12·58	28	267	1440	2141	206	1095	2562
974	July 9·77	27	215	1280	1646	168	990	1973
975	Aug. 5·99	27	163	956	1519	126	752	1876
976	Sept. 2·23	28	309	1730	1509	227	1273	1798
977	Sept. 29·50	27	298	1873	1455	240	1492	1760
978	Oct. 26·79	27	136	736	1553	97	531	1864
979	Nov. 23·09	27	316	1971	2086	222	1371	2483

TABLE II.

Year.	No. of Days. Photographed.	Without Spots.	Mean Daily Areas. Projected.* Umbræ.	Whole Spots.	Faculæ.	Corrected for Foreshortening.† Umbræ.	Whole Spots.	Faculæ.
1923	365	171	15	74	189	10	55	222
1924	366	97	62	361	498	46	276	575
1925	365	19	189	1102	1508	141	830	1750
1926	365	2	284	1651	2154	217	1262	2551

* Expressed in millionths of the Sun's disc.
† Expressed in millionths of the Sun's hemisphere.

TABLE III.

No. of Rotation.	Rotation commenced G.M.T.	Spots NORTH of the Equator. Mean Daily Area.	Spots NORTH of the Equator. Mean Heliographic Latitude.	Spots SOUTH of the Equator. Mean Daily Area.	Spots SOUTH of the Equator. Mean Heliographic Latitude.	Mean Latitude of entire Spotted Area.	Mean Distance from Equator of all Spots.
	1925.		°		°	°	°
967	Dec. 30·86	1932	21·12	776	19·84	+ 9·38	20·76
	1926.						
968	Jan. 27·19	876	19·71	1201	18·21	− 2·22	18·84
969	Feb. 23·54	365	20·18	1306	24·13	−14·47	23·27
970	Mar. 22·85	267	22·12	261	20·32	+ 1·15	21·23
971	Apr. 19·14	292	15·81	725	19·71	− 9·51	18·59
972	May 16·37	392	13·90	562	17·30	− 4·47	15·90
973	June 12·58	945	20·17	150	18·31	+14·90	19·92
974	July 9·77	195	18·60	796	12·92	− 6·73	14·04
975	Aug. 5·99	120	19·03	633	17·50	−11·68	17·74
976	Sept. 2·23	1059	23·30	214	14·79	+16·89	21·87
977	Sept. 29·50	1225	17·97	266	13·54	+12·34	17·18
978	Oct. 26·79	223	17·61	308	13·75	− 0·59	15·37
979	Nov. 23·09	722	12·64	649	13·62	+ 0·21	13·10

TABLE IV.

Year.	No. of Days on which Sun photographed.	Spots NORTH of the Equator. Mean Daily Area.	Spots NORTH of the Equator. Mean Heliographic Latitude.	Spots SOUTH of the Equator. Mean Daily Area.	Spots SOUTH of the Equator. Mean Heliographic Latitude.	Mean Latitude of entire Spotted Area.	Mean Distance from Equator of all Spots.
			°		°	°	°
1923	365	33	13·88	22	17·32	+ 1·34	15·26
1924	366	232	22·19	45	25·54	+14·49	22·73
1925	365	517	20·70	313	19·37	+ 5·60	20·20
1926	365	664	19·26	599	17·98	+ 1·60	18·65

Royal Observatory, Greenwich :
1927 *November* 1.

The Orbit of Comet 1927 *f* (*Gale*) : *An Interesting Case of Double Solution.* By A. C. D. Crommelin, D.Sc.

It has long been known that there are occasionally two solutions of the problem of finding an elliptical orbit from three observations. Prof. C. V. L. Charlier investigated the locus of the boundary that separates the two-solution region from the one-solution one (*M.N.*, **71**, 120 and 454). The curve is repeated with some further discussion in Prof. H. C. Plummer's *Dynamical Astronomy*, p. 78. It is, however,

exceptional for any serious doubt to occur as to which is the orbit to select. In fact, the present case is the first that I have met with that has two closely adjacent solutions; further, the solution that proved to be the wrong one seemed at first sight far more probable, since the period 13·1 years is similar to those of Peters 13·4 and Tuttle 13·5 years; whereas there have hitherto been no known periods between 8·9 years (Swift, 1889, vi.) and the above 13·4 years. My first ellipse was based on observations from June 22 to August 9; the comet was in the two-solution region for a large portion of the arc used; but the later Johannesburg observations, extending up to September 2, by which time the comet had passed far outside the two-solution region, with their rapidly increasing residuals, soon convinced me that my orbit was wrong, and led me to the second and third solutions. The existence of two neighbouring solutions greatly increases the difficulty of the problem; it renders the convergence of certain auxiliary quantities, *e.g.* P, Q of Watson, ν_1 ν_3 of Merton, extremely slow. These are functions of the ratios of sector to triangle for the different arcs; a very large number of successive approximations was necessary in the present case.

The following tables give (1) the observations which have come to hand; (2) my three orbits, of which the first is wrong; (3) the residuals, observed *minus* computed, for the different dates. The orbits are all referred to the equinox of 1927·0.

Time of Observation.	R.A. 1927·0.	Decl. 1927·0.	Place.
1927 June 22·97519 U.T.	344° 35′ 48″·0	−33° 12′ 28″·7	Cape Obs.
23·99531	345 41 31·2	−33 16 18·2	,,
24·99329	346 44 5·4	−33 19 42·5	,,
July 8·00609	357 29 42·9	−33 44 10·5	Union Obs., Johannesburg.
20·93160	3 24 1·35	−33 58 53·8	,,
23·97708	4 10 31·95	−34 2 52·5	,,
Aug. 9·05351	4 59 2·55	−34 18 2·3	,,
19·86026	3 8 57·0	−34 5 47·2	,,
29·90227	0 27 29·25	−33 24 31·4	,,
Sept. 2·87612	359 17 0·75	−32 58 29·3	,,

Dates used.	First Orbit. Jun. 22, Jul. 20, Aug. 9.	Second Orbit. Jun. 22, Jul. 20, Sept. 2.	Third Orbit. Jun. 22, Jul. 20, Sept. 2.
T(1927) U.T.	June 14·44366	June 14·57540	June 14·56894
ω	209° 32′ 37″·79	209° 49′ 35″·65	209° 50′ 36″·80
Ω	67 25 39·40	67 5 33·03	67 5 6·70
i	11 47 30·47	11 36 24·09	11 36 44·01
φ	51 21 3·65	49 5 19·21	49 8 20·06
log a	0·7446081	0·6959489	0·6970694
Period (years)	13·08917	11·06428	11·10719
log q	0·0850784	0·0838297	0·0839287

Residuals : Observed – Computed.

	R.A.			Decl.		
	First.	Second.	Third.	First.	Second.	Third.
June 22	− 4″·57	″·00	+ ″·19	− 2″·42	″·00	+ ″·15
23			− 2·81			+ ·85
24			+ ·66			−1·29
July 8		−24·12	− 5·09		+ 2·73	+2·64
20	− 2·30	−22·06	− ·88	+ 1·70	+ 1·29	+ ·45
23		−19·23	+ 1·88		+ 3·80	+2·50
Aug. 9	− 12·15	− 5·35	−11·19	− ·04	+11·21	−4·88
19	− 88·12	+10·24	+20·22	+ ·56	+ 2·63	− ·08
29	−219·18	+20·60	+22·28	+27·38	− 7·17	−8·37
Sept. 2	−299·33	·00	− ·60	+59·45	·00	+ ·68

Extrapolation from the residuals of July 8, 20, 23, August 9, indicates the period 11·1190 years as that which best satisfies the combined observations. This happens to be very close to the period 11·1 years indicated by Dr. Innes as that which would bring about a near approach of the comet to Jupiter in 1917. My own computations, however, indicate a period some two months longer as necessary for this purpose. From my third orbit I have computed the longitude and latitude of the comet and its radius vector as follows :—

1917·805	comet, longitude	56° 49′·81,	latitude − 2° 4′·11,	log r ·70303
	Jupiter	63 6	− 0 47·1	·70200
1917·813	comet	56 59·60	− 2 2·13	·70448
	Jupiter	63 21	− 0 46·4	·70207

The distance of the comet from Jupiter was of the order of half a unit ; a closer approach occurred one revolution earlier. There will now be no more close approaches till the comet has gained a revolution on Jupiter. Other values found for the period are 16·28 years by Dr. Innes (*Astr. Nach.*, 5525) and 11·86 years by Mr. H. E. Wood ; both of these are derived from June observations only ; the comet was observed at Johannesburg on 12 days in June, but these observations have not yet been communicated.

I take this opportunity to express my appreciation of the very useful tables of elliptic motion published by Dr. Innes as a supplement to *U.O. Circular*, 71 ; they enable a close solution to be obtained of Kepler's problem in orbits of any eccentricity, and at any distance from perihelion ; their use means a great saving of time.

On the Perturbations of the Major-Axis of the Orbit of a Satellite or Planet. By L. Becker, Ph.D., Regius Professor of Astronomy in the University of Glasgow.

1. This paper treats of the integration of the differential equation for the major-axis (I.) of a satellite's orbit as disturbed by the sun, and (II.) of the orbit of a planet as disturbed by other planets. The positions of the perturbing bodies are assumed to be known. In both cases (I.) and (II.) the differential equations of motion are

$$\ddot{x} = \frac{\partial U(x, y, z, t)}{\partial x}, \quad (x, y, z)$$

$$U = f(m_0 + m)r^{-1} + \Omega$$

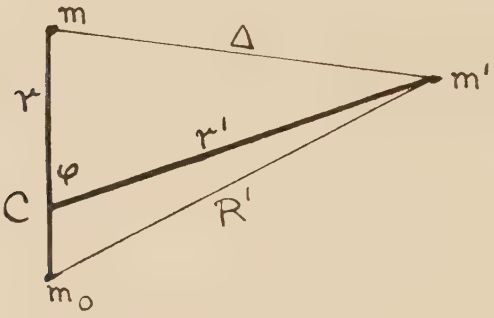

Fig. 1.

where (I.) x, y, z are the co-ordinates of satellite "m" referred to planet "m_0" and the co-ordinates of the sun, m', are known relatively to the centre, C, of inertia of m_0 and m as functions of the time, t, and constants, c, and

$$(1) \quad . \quad . \quad \Omega = fm'\left(\frac{1}{\sigma}\frac{1}{R'} + \frac{1}{1-\sigma}\frac{1}{\Delta}\right) \quad \text{(see fig. 1)},$$

$$\sigma = m/(m_0 + m),$$

and (II.) x, y, z are the co-ordinates of planet "m" referred to sun "m_0" and the co-ordinates of the disturbing planets m_i are given as functions of t and constants, C.

$$(2) \quad . \quad . \quad \Omega = \Sigma f m_i\left(\frac{1}{\Delta_i} - \frac{1}{r_i} - \frac{r}{r_i^2}\cos\psi_i\right) \quad \text{(see fig. 2)}.$$

In case (I.), R′ and Δ depend on (fig. 1) r, ϕ, $r'(t, c)$, and in case (II.) Δ_i is a function of r, ψ_i, $r_i(t, C)$.

The Hamiltonian function is $H = \frac{1}{2}V^2 - U$, V designating the velocity of m relatively to m_0.

2. *H for Polar Co-ordinates.*—On the Celestial Sphere (fig. 3) the

position M_0 defines the direction from m_0 to m, and M'_c represents (I.) the direction to m' from the centre, C, of inertia of m_0 and m, or, (II.),

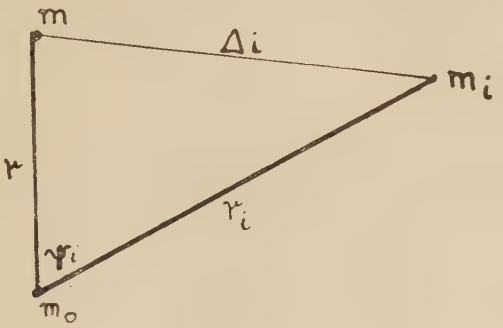

Fig. 2.

the direction from m_0 to m_i. The positions on the C.S. are referred to a great circle whose pole is P; this reference great circle might conveniently represent (I.) a plane through C lying near the path of

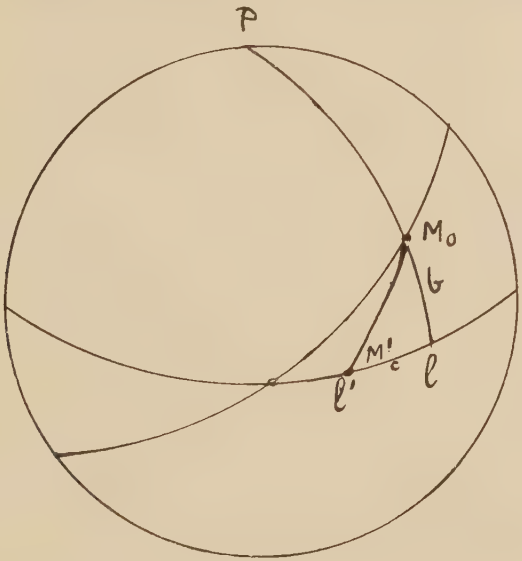

Fig. 3.

m', or (II.) a plane through m_0 near the paths of the masses m_i. The arc $M_0M'_c$ is designated by ϕ in case (I.) and by ψ_i in case (II.). The polar co-ordinates of M'_c, (I.) $l'b'$, or (II.) l_ib_i are known as functions of t and constants.

I designate the polar co-ordinates of M_0 by r, l, b (fig. 3), and the

co-ordinates canonically conjugated to them R, L, B. The Hamiltonian function then becomes

$$H = \tfrac{1}{2}[R^2 + L^2/r^2 \cos^2 b + B^2/r^2] - f(m_0 + m)/r - \Omega.$$

3. Consider the two-body problem, represented by the Hamiltonian function

$$H_0 = \tfrac{1}{2}[R^2 + L^2/r^2 \cos^2 b + B^2/r^2] - f(m_0 + m)/r.$$

The integrals are the well-known formulæ of Keplerian motion. They express l, b, r as functions of t and the canonic constants of integration, a_1, a_2, a_3, and those respectively conjugated to them, A_1, A_2, A_3. The time, t, and A_1 enter these formulæ only through the mean anomaly, M.

$$M = n(t - A_1),$$

where the mean motion, n, depends on the major-axis, $2a$, of the elliptic orbit :

$$n^2a^3 = f(m_0 + m)$$
$$a_1 = f(m_0 + m)/2a.$$

4. $H = H_0 - \Omega$. To integrate the differential equations belonging to the problem defined in the first paragraph, introduce the six new co-ordinates, (a_k), (A_k), $k = 1, 2, 3$, instead of l, b, r, L, B, R, where $l = l[t, (a_k), (A_k)]$, etc. are, apart from brackets, the same formulæ, $l = l(t, a_k, A_k)$, etc., as were mentioned in the preceding paragraph. Hence

$$\frac{\partial r[t, (a_k), (A_k)]}{\partial t} = \frac{\partial H_0[r, R, \ldots]}{\partial R},$$

and similarly for l and b.

The equations of motion for the new co-ordinates, (a_k), (A_k), are again canonic,

$$(\dot{a}_k) = \frac{\partial \Omega[t, (a_k), (A_k), c]}{\partial (A_k)}$$
$$(\dot{A}_k) = -\frac{\partial \Omega[t, (a_k), (A_k), c]}{\partial (a_k)}.$$

5. Integration of

$$(\dot{a}_1) = \frac{\partial \Omega[t, (a_k), (A_k), c]}{\partial (A_1)}.$$

Ω depends only on the relative positions of the three bodies and not on the orientation of their configuration.

Ω is a function of r, ϕ, r' in case (I.), and of r, ψ_i, r_i in case (II.), where ϕ depends on l, b, l', b' (fig. 3) and ψ_i on l, b, l_i, b_i. r, l, b are functions of t, (a_k), (A_k), and r', l', b' of t and c, and r_i, l_i, b_i, of t and C.

Therefore

$$\frac{\partial \Omega[t, (a_k), (A_k), c]}{\partial (A_1)} = \frac{\partial \Omega[r, \phi, r']}{\partial r} \frac{\partial r[t, (a_k), (A_k)]}{\partial (A_1)} + \frac{\partial \Omega}{\partial \phi} \frac{\partial \phi[t, (a_k), (A_k)c]}{\partial (A_1)},$$

and an analogous equation found by changing ϕ into ψ_i.

According to §§ 3 and 4

$$\frac{\partial r[t,(a_k),(\mathrm{A}_k)]}{\partial(\mathrm{A}_1)} = -\frac{\partial r[t,(a_k),(\mathrm{A}_k)]}{\partial t} = -\frac{\partial \mathrm{H}_0(r,\mathrm{R},\ \ldots\ )}{\partial \mathrm{R}}$$

$$\frac{\partial \phi[t,(a_k),(\mathrm{A}_k)c]}{\partial(\mathrm{A}_1)} = -\frac{\partial \phi[t,(a_k),(\mathrm{A}_k)l',b']}{\partial t} = -\frac{\partial \phi[l,b,l',b']}{\partial l}\frac{\partial \mathrm{H}_0}{\partial \mathrm{L}} - \frac{\partial \phi}{\partial b}\frac{\partial \mathrm{H}_0}{\partial \mathrm{B}}.$$

In the corresponding equation for ψ_i, l_i, and b_i replace l', b'. But

$$\frac{\partial \mathrm{H}_0}{\partial \mathrm{R}} = \frac{\partial \mathrm{H}}{\partial \mathrm{R}},$$

and similarly for L and B. Further, from § 4

$$\frac{\partial \mathrm{H}}{\partial \mathrm{R}} = \dot{r}, \qquad \frac{\partial \mathrm{H}}{\partial \mathrm{L}} = \dot{l}, \qquad \frac{\partial \mathrm{H}}{\partial \mathrm{B}} = \dot{b},$$

whereby the equations become

$$\frac{\partial r[t,(a_k),(\mathrm{A}_k)]}{\partial(\mathrm{A}_1)} = -\dot{r}$$

$$\frac{\partial \phi[t,(a_k),(\mathrm{A}_k),c]}{\partial(\mathrm{A}_1)} = -\frac{\partial \phi[l,b,l',b']}{\partial l}\dot{l} - \frac{\partial \phi}{\partial b}\dot{b} = -\dot{\phi} + \frac{\partial \phi[l,b,l',b']}{\partial l'}\dot{l}' + \frac{\partial \phi}{\partial b'}\dot{b}'.$$

Substitute these values in the differential equation given in the heading

$$(\dot{a}_1) = -\frac{\partial \Omega[r,\phi,r']}{\partial r}\dot{r} - \frac{\partial \Omega[r,\phi,r']}{\partial \phi}\phi + \frac{\partial \Omega[r,\phi,r']}{\partial \phi}\left(\frac{\partial \phi[l,b,l',b']}{\partial l'}\dot{l}' + \frac{\partial \phi}{\partial b'}\dot{b}'\right),$$

the integral of which is

$$(a_1) = a_1 - \Omega - \delta\Omega,$$

a_1 is the constant of integration and

$$\text{(I.)}\quad \delta\Omega = -\int\left\{\frac{\partial \Omega[r,\phi,r']}{\partial \phi}\left(\frac{\partial \phi[l,b,l'b']}{\partial l'}\dot{l}' + \frac{\partial \phi}{\partial b'}\,b'\right) + \frac{\partial \Omega[r,\phi,r']}{\partial r'}\dot{r}'\right\}dt,$$

$$\text{(II.)}\quad \delta\Omega = \sum_i \int\left\{\frac{\partial \Omega[r,\psi_i,r_i]}{\partial \psi_i}\left(\frac{\partial \psi_i[l,b,l_ib_i]}{\partial l_i}l_i + \frac{\partial \psi_i}{\partial b_i}\dot{b}_i\right) + \frac{\partial \Omega[r,\psi_i,r_i]}{\partial r_i}\dot{r}_i\right\}dt.$$

Instead of the canonic variable (a_1) and the canonic constant a_1 introduce the semi-major axis (a), of the osculating ellipse and the constants a and n (see § 3):

$$\frac{1}{(\mathrm{a})} = \frac{1}{\mathrm{a}} - \frac{2}{\mathrm{f}(\mathrm{m}_0+\mathrm{m})}(\Omega + \delta\Omega).$$

Apart from $\delta\Omega$ the integration has been effected.

6. $\delta\Omega$ *for a Satellite.*—I shall consider only terms of zero order in the eccentricities of the planet's and satellite's orbits. I shall further neglect the effect on $\delta\Omega$ of the perturbation of the inclination, i, of the satellite's orbit and assume M'_c to move in a plane.

I choose as reference plane the orbit plane of M'_c. Then $r = a$,

$l' = n'$, $b' = 0$, $\dot{b}' = 0$, $\dot{r}' = 0$. Further, according to the spherical triangles in fig. 4,

$$\cos\phi = \cos b \cos(l - l'),$$
$$\frac{\partial\phi}{\partial l'}[l, b, l'] = -\cos\theta,$$
$$d\nu = (n + \dot{\omega})dt + \ldots,$$
$$d\nu' = (n' - \dot{\Omega})dt + \ldots$$

The perturbative function may be developed here into a power series in $\frac{r}{r'}$, $(n'^2a'^3 = f(m_0 + m + m'))$,

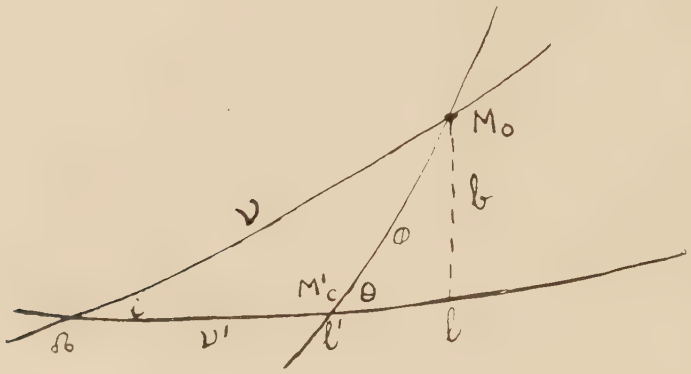

FIG. 4.

the well-known formula being

$$\Omega = \frac{m'}{m' + m_0 + m} n'^2 \left(\frac{a'}{r'}\right)^3 r^2 \left[\frac{1}{4} + \frac{3}{4}\cos 2\phi + \frac{r}{r'}\left(\frac{3}{8}\cos\phi + \frac{5}{8}\cos 3\phi\right)(1 - 2\sigma) + \ldots\right].$$

Thence from (I.), § 5,

$$\delta\Omega = -\frac{3}{2}\frac{m'}{m' + m_0 + m} n'^3 a^2 \int \sin 2\phi \cos\theta dt (1 + e(\ldots) + e'(\ldots) + \ldots).$$

Substitute

$$\cos\phi = \cos\nu\cos\nu' + \sin\nu\sin\nu'\cos i,$$
$$\cos\theta\sin\phi = -\cos\nu\sin\nu' + \sin\nu\cos\nu'\cos i,$$
$$\cos\theta\sin 2\phi = -\tfrac{1}{2}\sin^2 i \sin 2\nu' + \cos^4\tfrac{1}{2}i \sin 2(\nu - \nu') - \sin^4\tfrac{1}{2}i \sin 2(\nu + \nu'),$$

$$\delta\Omega = \frac{m'}{m' + m_0 + m} n'^2 a^2 \left[-\frac{3}{8}\frac{n'}{n' - \dot{\Omega}}\sin^2 i \cos 2\nu' + \frac{3}{4}\frac{n'}{n - n' + \dot{\omega} + \dot{\Omega}}\cos^4\frac{1}{2}i \cos 2(\nu - \nu') - \frac{3}{4}\frac{n'}{n + n' + \dot{\omega} - \dot{\Omega}}\sin^4\frac{1}{2}i \cos 2(\nu + \nu')\right] + \ldots$$

In the case of the moon, $i = 5°$, the second term is the only zero-order term and it may be combined with the corresponding term in Ω.

Hence

$$\frac{1}{(a)} = \frac{1}{a} - \frac{m'}{m' + m_0 + m}\left(\frac{a'}{r'}\right)^3\left(\frac{r}{a}\right)^2\left(\frac{n'}{n}\right)^2\frac{1}{a}$$
$$\left[\frac{1}{2} + \frac{3}{2}\left(1 + \frac{n'}{n - n' + \dot{\omega} + \dot{\Omega}}\right)\cos 2\phi + \ldots\right].$$

It is perhaps unnecessary to write out the complete value of Ω, since terms arising from $\delta\Omega$ of the order $e\frac{n'}{n}$ have been neglected in the bracket. The formula is the equation to the so-called "variational" curve.

For the outer satellites of Jupiter, where i is not small, the three terms of $\delta\Omega$ must be used, whereby terms of the order $e\sin^2 i$, and $e\frac{n'}{n}\cos^4\frac{1}{2}i$, $e\frac{n'}{n}\sin^4\frac{1}{2}i$ are neglected in the formula for $a/(a)$.

The Effect of Finite Velocity of Transmission of Gravity on the Motion of the Planets. By L. Becker, Ph.D., Regius Professor of Astronomy in the University of Glasgow.

Equations of Motion (fig. 1).—Consider two bodies, m_0 and m, whose co-ordinates at time t are ξ_0, η_0, ζ_0, and ξ . . ., as referred to a fixed system of axes. The acceleration of the velocity of m at t originated at time $t - \Delta t_0$, when m_0 had the co-ordinates $\xi_0 - \Delta\xi_0$. . . . The ξ-component of this acceleration is $-fm_0(\xi - \xi_0 + \Delta\xi_0)r_1^{-3}$, where

(1) . . . . $r_1^2 = (\xi - \xi_0 + \Delta\xi_0)^2 + \ldots$

Similarly the acceleration of m_0 at time t was caused by m at time $(t - \Delta t)$, when the co-ordinates of m were $\xi - \Delta\xi$ . . ., and the ξ-component of this acceleration is $+fm(\xi - \xi_0 - \Delta\xi)r_2^{-3}$, where

(2) . . . . $r_2^2 = (\xi - \xi_0 - \Delta\xi)^2 + \ldots$

Next refer m at t to m_0 at t by means of the relative co-ordinates x, y, z. $x = \xi - \xi_0$ . . ., and obtain

$$\ddot{x} = -fm_0(x + \Delta\xi_0)r_1^{-3} - fm(x - \Delta\xi_0 - \Delta x)r_2^{-3}.$$

The space travelled by m_0 is $C\Delta t = Cr_1/G = \gamma r(1 + \rho_1)$ (whose components are $\Delta\xi_0$ . . .), where C designates the velocity of the solar system towards the apex, A, G the velocity of transmission of gravity, $\gamma = C/G$, and $r_1 = r(1 + \rho_1)$. The space travelled by m relatively to m_0 is $V\Delta t = Vr_2/G = \nu r(1 + \rho_2)$, and its components are Δx . . ., in which $\nu = V/G$, $r_2 = r(1 + \rho_2)$.

Choose as XY-plane the plane (r, V) at time t, and as X-axis the

direction from m_0 to m, both at time t. The accelerations at time t then become

$$(3)\quad \begin{cases} \ddot{r} &= -fm_0r_1^{-3}(r+\Delta\xi_0) - fmr_2^{-3}(r-\Delta\xi_0-\Delta x) \\ \ddot{y} &= -fm_0r_1^{-3}\Delta\eta_0 \qquad\quad - fmr_2^{-3}(-\Delta\eta_0-\Delta y) \\ \ddot{z} &= -fm_0r_1^{-3}\Delta\zeta_0 \qquad\quad - fmr_2^{-3}(-\Delta\zeta_0). \end{cases}$$

The accelerations at time t for instantaneous action of gravity are

$$(4)\quad \ddot{r} = -fm_0r^{-2} - fmr^{-2}, \qquad \ddot{y} = 0, \qquad \ddot{z} = 0.$$

The differences (3) minus (4) are the components R, U, Z of the perturbative acceleration due to the velocity of transmission of gravity. I calculate these up to second order terms in γ and ν. The equations

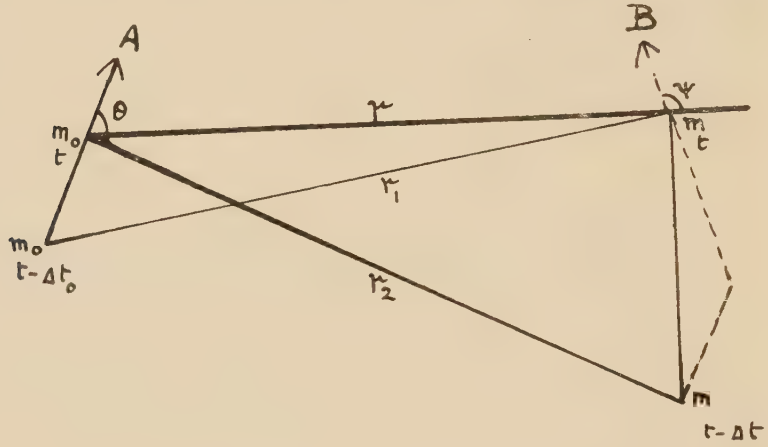

FIG. 1.

for x . . . agree in their first order terms with those used by Lehmann-Filhès *, who, however, omits from the outset those terms which alone produce secular perturbations in the Keplerian elements.

Let ψ be the angle (r, V) and θ, θ', θ'' designate respectively the angles (A, r), (A, Y), (A, Z), then

$$(5)\quad \begin{cases} \Delta\xi_0 = \gamma r(1+\rho_1)\cos\theta \\ \Delta x = \nu r(1+\rho_2)\cos\psi, \end{cases}$$

and corresponding four other formulæ for ($\Delta\xi_0$, $\Delta\eta_0$, $\Delta\zeta_0$) and (θ, θ', θ''), (Δx, Δy, Δz) and (ψ, $90^\circ-\psi$, 90°).

From (1), (2), and (5) find

$$(6)\quad \begin{cases} r_1^2 = r^2(1+2\gamma\cos\theta(1+\rho_1)+\gamma^2) \\ r_2^2 = r^2[1-2\gamma\cos\theta(1+\rho_1) - 2\nu\cos\psi(1+\rho_2)+\gamma^2+\nu^2 \\ \qquad\qquad + 2\gamma\nu(\cos\theta\cos\psi+\cos\theta'\sin\psi)]; \end{cases}$$

* Tisserand, *Mécanique Céleste*, **4**, p. 496, and *A.N.*, **2630**, 1884.

hence

$$(7)\qquad \rho_1 = \gamma\cos\theta + \ldots \text{ and } \rho_2 = -\gamma\cos\theta - \nu\cos\psi + \ldots,$$

and, apart from periodical terms with arguments θ, θ', θ'', which cannot produce secular terms in the elements since these arguments do not occur in (9), (10), or (11),

$$(8)\quad \begin{cases} r_1^{-3} = r^{-3}(1 + \frac{3}{4}\gamma^2 + \ldots) \\ \Delta\xi_0 r_1^{-3} = r^{-2}(-\gamma^2 + \ldots) \\ r_2^{-3} = r^{-3}(1 + \frac{15}{4}\gamma^2 - \frac{3}{2}\nu^2 + 3\nu\cos\psi + \frac{9}{2}\nu^2\cos^2\psi + \ldots) \\ \Delta\xi_0 r_2^{-3} = r^{-2}(2\gamma^2 + \ldots) \\ \Delta x r_2^{-3} = r^{-2}(\nu\cos\psi + 2\nu^2\cos^2\psi + \ldots). \end{cases}$$

The differences (3) minus (4) become with regard to (8),

$$(9)\quad \begin{cases} \mathrm{R} = \frac{1}{4}fm_0 r^{-2}\dfrac{\mathrm{C}^2}{\mathrm{G}^2} + fmr^{-2}\left[-2\dfrac{\mathrm{V}\cos\psi}{\mathrm{G}} - \dfrac{5}{2}\dfrac{\mathrm{V}^2\cos^2\psi}{\mathrm{G}^2} + \dfrac{3}{2}\dfrac{\mathrm{V}^2}{\mathrm{G}^2} \quad \dfrac{7}{4}\dfrac{\mathrm{C}^2}{\mathrm{G}^2}\right] + \ldots \\ \mathrm{U} = fmr^{-2}\left[\dfrac{\mathrm{V}\sin\psi}{\mathrm{G}} + 2\dfrac{\mathrm{V}\sin\psi}{\mathrm{G}}\dfrac{\mathrm{V}\cos\psi}{\mathrm{G}}\right] + \ldots, \end{cases}$$

in which I have omitted terms that cannot give rise to secular terms. The Keplerian co-ordinates (elliptic elements) are connected with r, V, ψ by the formulæ

$$(10)\qquad \mathrm{V}\sin\psi = na^2\cos\phi r^{-1} \quad \text{and} \quad \mathrm{V}\cos\psi = nae\sec\phi\sin v,$$

and are defined by the differential equations

$$(11)\quad \begin{cases} e\dot{\pi} = -\dfrac{1}{na}\cos\phi\,\mathrm{R}\cos v + \dfrac{2\sin v + \frac{1}{2}e\sin 2v}{na^2\cos\phi}\mathrm{U}r \\ \dot{e} = \dfrac{\cos\phi}{na}\mathrm{R}\sin v + \dfrac{1{\cdot}5e + 2\cos v + 0{\cdot}5e\cos 2v}{na^2\cos\phi}\mathrm{U}r \\ \dot{a} = \dfrac{2e}{n\cos\phi}\mathrm{R}\sin v + \dfrac{2a\cos\phi}{n}\dfrac{\mathrm{U}}{r}. \end{cases}$$

Notation:

$2a$ = major axis, e = eccentricity,
π = longitude of perihelion, n = mean motion,
v = true anomaly, $r = a\cos^2\phi/(1 + e\cos v)$, $a^3n^2 = f(m_0 + m)$.

With the above values of R and U the secular terms become

$$(12)\quad \begin{cases} \dfrac{\dot{\pi}}{n} = -\frac{1}{4}\sec^3\phi\left[\dfrac{m_0}{m_0+m} - \dfrac{7m}{m_0+m}\right]\dfrac{\mathrm{C}^2}{\mathrm{G}^2} - \dfrac{m}{m_0+m}\left(\dfrac{na}{\mathrm{G}}\right)^2\sec^5\phi(1+e^2) \\ \dfrac{\dot{e}}{e} = \dfrac{5n}{2}\dfrac{m}{m_0+m}\dfrac{na}{\mathrm{G}}\sec^4\phi(1+\frac{1}{4}e^2) \\ \dfrac{\dot{a}}{a} = 2n\dfrac{m}{m_0+m}\dfrac{na}{\mathrm{G}}\sec^6\phi(1+2e^2+\frac{1}{8}e^4). \end{cases}$$

Substitute $n^2 = k^2\left(1 + \frac{m}{m_0}\right)a^{-3}$ and integrate the equation for $\dot{a}$ from zero value of a, then

$$T = \frac{a^2 G}{4k^2}\frac{m_0}{m}$$

is the time required by the planet to travel from the sun to its present distance. The eccentricity, e, has been neglected, since it would also have been increasing if our hypothesis about gravity were correct.

According to the first formula under (12) the secular change in the longitude of the perihelion of Mercury, which is positive, cannot be explained in this way.

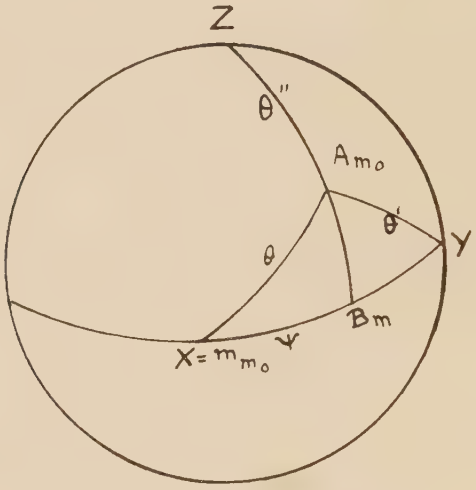

FIG. 2.

The table below contains the numerical values of the secular changes per century, the velocity, G, of gravity being replaced by x times the velocity, L, of light. The following data were employed: C = 20 km./sec., L = 300000 km./sec., L = 86400/498 astronomical units per day, $na = 2\pi a/P$, P being the period in days.

	$\dot{\pi}x^2$.	$\dot{e}x/e$.	$\dot{a}x/a$.	T/x.
Mercury	−0″·64	19 10^{-8}	17 10^{-8}	360 million years.
Venus	−0·25	73	58	85 ,,
Earth	−0·14	47	37	133 ,,
Mars	−0·08	2	2	2900 ,,
Jupiter	−0·01	552	445	11 ,,
Saturn	−0·005	49	40	130 ,,
Uranus	−0·002	2	2	3400 ,,
Neptune	−0·001	1	1	7000 ,,

If gravitation were propagated at finite velocity, G = xL, L being the velocity of light, this would have caused Jupiter to leave the sun about 11x million years ago ; indeed, so much later than the other planets, that at time of departure these planets would have almost arrived at their present distances and orbits. Thus Jupiter would have crossed successively the orbits of Mercury, Venus, Earth, Mars, and the minor planets, and remained for ages (of the order of a million years) in the neighbourhood of each orbit. Without special calculations it may be asserted that, under such conditions, the perturbations by Jupiter would have been enormous, and that the eccentricities of the orbits could not be what they actually are at present. I conclude that the conditions in the solar system as at present constituted exclude the possibility that Jupiter has crossed the orbits of the inner planets.

Jupiter must therefore have originated outside the region of the minor planets. Let $2a_0$ be the major axis at time of its formation τ years ago, then the integration of the last equation under (12) gives

$$G = 4k^2 \frac{m}{m_0} \frac{\tau}{(a^2 - a_0^2)}$$

and

$$T = \tau / \left(1 - \frac{a_0^2}{a^2}\right) = x \text{ times } 11 \text{ million years.}$$

There is a wide range for possible values of τ, and $1/\left(1 - \frac{a_0^2}{a^2}\right)$ may lie between infinity and, say, 10. There is therefore also a wide range for possible values of x, *i.e.* of the velocity of propagation of gravity.

The first two columns of the table would permit of a value of x even as low as 1/2.

The outcome of this investigation then is, if only the perturbation under consideration be taken into account, that the solar system furnishes no evidence that gravitation is not propagated at finite velocity.

Note added 1927 *December* 5.—In *A.N.*, 5519, Professor Courvoisier has derived a velocity of our stellar system of the order of 500 km. per second. Such a velocity would diminish the longitude of the perihelion of Mercury by $-400''x^{-2}$ per century, and would require the velocity of gravitation to be a large multiple of the velocity of light.

The Degree of Darkness during the Total Solar Eclipse of 1927 *June* 29. By W. J. S. Lockyer, M.A., Ph.D., Major (late R.A.F.). (Plate 2.)

It is a fact of observation that the darkness which prevails during the total obscuration of the sun does not appear to be equally profound when the observations of different eclipses are compared together, and this is so even at different places where the same eclipse has been observed. Indeed it sometimes becomes so dark during totality that

it is difficult to see small figures or lettering, and it has become routine among eclipse observers to paint all figures, etc., which are required to be seen in large type and even have lanterns ready if necessary.

The degree of darkness or general illumination is usually defined in terms of the light displayed on a full moonlight night. Part of the programme of the Norman Lockyer Observatory's expedition to Olliver Ducket, Richmond, Yorks, was to determine if possible how near to full moonlight the general illumination attained.

The illumination during totality is derived from two sources. The first is that due to the light of the corona and any exposed prominences, and the second that which arises from the light reflected by those regions of the atmosphere which are still lit up by the direct rays of the sun.

Each of these sources of light is variable from one eclipse to another. Taking the case of the corona first, the apparent relative sizes of the sun and moon will cause a considerable difference in the degree of darkness, because the larger the moon, the greater the area of the lower corona that will be covered, and therefore a less amount of light is available for illumination purposes. Further, the corona is not the same brightness at every eclipse, but varies according to the state of the solar activity. Thus the corona is brightest at maximum solar activity, so that at these epochs the illumination from this source should be at a maximum also.

In the case of the illumination due to diffused daylight at any one eclipse this will vary, not only according to the observer's position relative to the central line of totality, but also along the track of the central line. At the sunrise and sunset ends of the track the illumination will be greatest, and it will be least on that portion where the sun is on the meridian during totality. Further, the nearer the sun is to the zenith during totality, the more the illumination will be reduced. At all positions in the zone of totality the amount of diffused daylight will be reduced if the apparent size of the moon is very much larger than that of the sun, because the shadow cone will have a much larger diameter.

There is little doubt that the illumination due to diffused daylight is not only responsible for the greater portion of the light during totality, but its variability from eclipse to eclipse accounts most probably for the changes of the degree of darkness recorded.

The light emitted from the corona is evidently not very great, for the writer can find no record of any shadow being cast by it. In London, at the eclipse of 1715, when totality lasted 3 minutes 23 seconds, Halley recorded that "it was vastly inferior to that of the full moon, and so weak that I did not observe it cast a shade." In the eclipse of June last, as is referred to later on, a stick threw no perceptible shadow on a white sheet, in spite of the fact that the corona was exceedingly bright.

The solar conditions that prevailed on the occasion of the recent eclipse presented nearly an ideal state for a large degree of illumination. Firstly, the moon's disc was only slightly larger than that of the sun, thus exposing during totality nearly the whole area of the lower

corona and several large prominences. Secondly, the corona was nearly of maximum brightness owing to the closeness of the epoch of the eclipse to that of the maximum condition of solar activity, namely, 1928.

From the sky diffusion point of view here again a large degree of illumination was to be expected, because the observing station in Yorkshire was well situated on the western portion of the eclipse track, the sun being only 13 degrees above the horizon at the time of totality. During totality there were both high and low clouds ; the latter would tend to reduce the illumination, but the former would considerably add to it as they would reflect more sunlight into the shadow cone than would blue sky.

A good available standard to use in making the attempt to determine the degree of darkness is to compare the general illumination to that of a night of full moon, when the moon is on the meridian. Here an element of uncertainty arises, because the moon may have a large northerly or southerly declination when the illumination would be very much greater in the former than in the latter case. Naturally only a northern declination should be utilised to make the comparison.

During the last eclipse the following photographic procedure was adopted. It consisted in fixing a camera on a rigid stand and photographing the eastern portion of the eclipse camp which included in the field of view (see Plate 2) an old stone "look-out tower" or "Ducket," some of the instruments, and also the eclipsed sun. The longest exposure was given, namely, 20 seconds, and the full aperture of the lens employed. The main object of this photograph was to find out how much detail in the landscape could be brought out. By comparing this photograph with one taken on a subsequent full moonlight night, using the same camera, aperture, exposure, and similar plates, it was considered that an approximate relative idea of the general illumination could be secured.

The actual photograph taken during the eclipse was accomplished by Miss Lockyer, using a 5×4 Kodak at full aperture (*f*/8) on Kodak film. In order to record exactly all the details in the view under full illumination, another photograph was taken from exactly the same position at 10 o'clock G.M.T. on the morning of the day previous to the eclipse, using the same aperture but giving an exposure of one-hundredth of a second. Thus these two exposures were in the relation of 2000 to 1. On both occasions the sky was about equally cloudy, and while the eclipse photograph was greatly underexposed and required longer development, that on the previous day was almost correct.

Reproductions of these two photographs are shown in Plate 2. In order to illustrate the relative densities of the two negatives, the films were placed side by side in one printing frame and a print made from them *on one sheet* of velox paper, the exposure and development being naturally identical in each case. *One block* of this plate has been made for this illustration and it brings out well the differences in the original. The upper figure is from the negative taken the day before the eclipse, and the lower one that taken during totality.

It will be at once noticed that the eclipse photograph is much more

than a mere silhouette, and shows many details in the structure of the " Ducket " and in the tube of the large coronagraph. Both the operators of this coronagraph are seen one on each side of the tube, and these remained for the most part stationary during the exposure. On the other hand, the two ghost-like figures to the left are the images of Sir Francis McClean, who was evidently only stationary in these positions for a few seconds during the exposure. The two time-callers on the " Ducket " are clearly seen and can only have moved very slightly during the interval.

The opportunity to test what actually could be photographed on a full moonlight night did not occur until the nights about the full moon of October, because the moon's declination was southerly in the preceding months at these epochs. The programme arranged was to take two photographs on each of the nights of the 9th, 10th, and 11th when the moon was on the meridian. Full moon occurred at about 21 hours on the 10th, and was at an altitude of 41 degrees when on the meridian.

The camera faced north, and the view photographed was a country house at a distance of 150 feet, the same distance as the " Ducket " was away from the camera in the eclipse photograph. This house was a much more striking object to photograph than the dull appearance of the stone " Ducket," having numerous windows with white frames, gables, and a long verandah.

The same camera, aperture, and similar films were used, and all the nights were cloudless and very bright. With exposures of 20 seconds not a single trace of any record could be found on any of the negatives. On the last night exposures of 60 and 120 seconds were given in addition, and these negatives also declined to show any record.

Thus an exposure, on a bright moonlight night, six times longer than that given during the eclipse fails to give any record.*

The only conclusion that can be drawn, therefore, is that the illumination during totality was very much more intense than that on a bright moonlight night.

In this connection it is interesting to mention the observations made at Ringebu, Norway, by G. Armellini and G. Conti of the Campidoglio Observatory, Rome, during the last eclipse.

According to them * the illumination during totality was much greater than that of full moon. It is stated that Signor Armellini could read type 0·5 mm. high, while 2 mm. was the minimum in full moonlight. They remark also that most of the light during totality was diffused skylight and not that of the corona, since a stick 4 cm. in diameter threw no perceptible shadow on a white sheet.

Note added November 25.—The above photographs were repeated on November 7, two nights before the next full moon, with exposures of 30 and 90 minutes, the moon being near the meridian. The first of these photographs approximates more closely to that taken during the eclipse, but probably an exposure of 50 minutes would have secured the desired effect.

* *Astr. Nach.*, No. 5519.

A Statistical Study of Binary Stars.

By Dr. E. A. Kreiken.

(*Communicated by the Secretaries.*)

A number of investigations have been made to ascertain whether the orbit-planes of the visual binary stars exhibit a random distribution or whether there is a tendency to parallelism to a certain plane, as, for example, the plane of the Milky Way. These investigations have, as a rule, been based upon the systems whose orbits are known, although the fact that the orbit elements do not define the plane uniquely presents a serious difficulty.

The results obtained by various authors are very different.* R. G. Aitken has summarised them in his well-known work, *The Binary Stars* (pp. 218 and 219). For an exact knowledge of the dynamical laws in our stellar system this problem is of great importance.

At present our data, though far from being complete, are more reliable than those used by previous authors. Therefore I have tried a new solution, in which I have investigated the space distribution of the major-axes of the known systems.

TABLE I.

Distribution of the Inclinations.

Angle.	Numbers Observed.	Percentage O.	Arbitr. Distr. C.	O–C.
°				
+90				
	5	3·1	6·7	−3·6
+60				
	14	6·9	11·1	−4·2
+40				
	26	17·0	15·0	+2·0
+20				
	29	17·6	17·1	+0·5
0				
	38	22·7	17·1	+5·6
−20				
	30	19·5	15·0	+4·5
−40				
	10	6·3	11·1	−4·8
−60				
	12	7·6	6·7	+0·9
−90				

In the following we have to consider two directions of the major-axis of each binary, of which one is real, the other spurious. The lack of radial velocity observations makes it impossible to discriminate between those two. Even when taking into account two values for each binary

* A. Everett, *M.N.*, **56**, 462, 1896 ; T. J. See, *Evolution of Stellar Systems*, **1**, 247, 1896 ; W. Doberck, *A.N.*, 147, 251, 1898, and *A.N.*, 179, 199, 1908 ; T. Lewis and H. H. Turner, *M.N.*, **67**, 498, 1907 ; K. Bohlin, *A.N.*, 176, 197, 1907 ; J. M. Poor, *Astron. Journ.*, **28**, 145, 1914.

it is directly evident from Tables I. and II. that the space distribution is by no means haphazard. Of the two tables the first one gives the numbers of axes having an inclination between 0° and 20°, 20° and 40°, etc., with the plane of the Milky Way. The second column contains the corresponding percentages. If the distribution was haphazard these percentages should be proportional to the areas covered by the successive galactic belts, and would be equal to the numbers in the next column. For the smaller values of β the difference Obs.-Comp. is positive, so we conclude that there is a concentration towards the plane of the Milky Way. Fig. 1 is drawn according to the data of Table I. The dotted curve indicates the random distribution, while the full-drawn gives the observed distribution. (There are three stars for which we

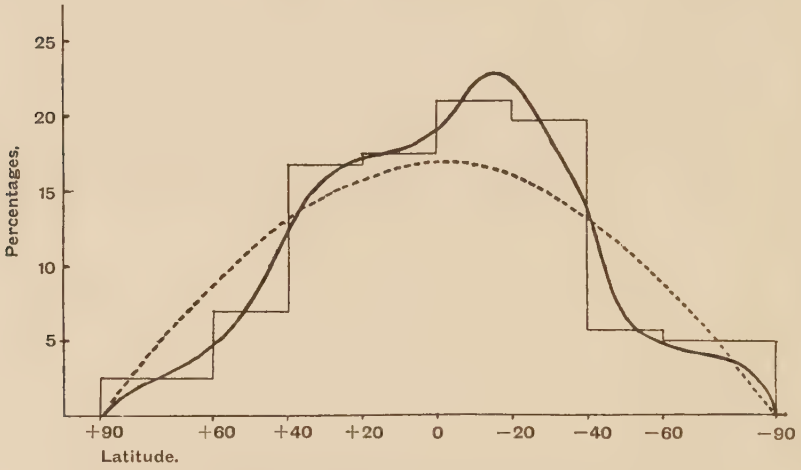

Fig. 1.—Distributions of the inclinations. The dotted curve indicates the random distribution.

have radial velocity measures. In these cases the correct value was inserted with double weight.)

Table II.

Distribution over the Different Longitudes.

Longitude.	0°.	30°.	60°.	90°.	120°.	150°.	180°.	210°.	240°.	270°.	300°.	330°.	360°.
Numbers.	13	7	15		8	8	14	8	11	20	15	29	16
			35			30			39			59	

Table II. was drawn up in the same manner as Table I. It contains the numbers of major-axes, of which the projection on the plane of the Milky Way is between the longitudes 0° to 30°, 30° to 60°, etc. The excess in the longitudes between 300° and 330° is very apparent. This appears also from fig. 2. In this figure the circle indicates the random distribution.

We may expect that the actual concentration of the major-axes towards a direction parallel with the plane of the Milky Way and in the longitudes 300° to 330° is larger than the ones found above. It is obvious that part of these actual concentrations are obliterated by the spurious directions of the axes. Still, these real concentrations are the important ones. We can only find them when we consider the distribution of the true direction alone. We know that there is no direct method by which we may discriminate between the true values and the spurious ones. Therefore I tried to find an indirect one. This, of course, is a rather dangerous proceeding, and it will be necessary to control our results. The different binary systems were arranged into three groups. The first contains all systems with galactic latitude

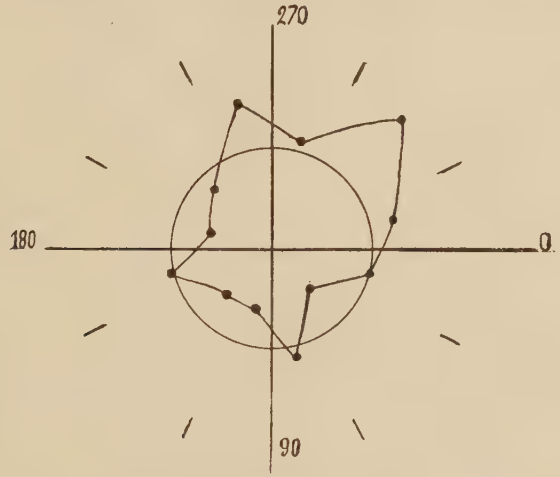

Fig. 2.—Distribution in longitude. The circle indicates the random distribution.

$<30°$, the second those with $30°<\beta<60°$, the third those with $60°<\beta<90°$. For each group the distribution curves of the supposed true directions were derived. The general shape of the curves we expect to be the same. We will also compare the distribution curves of the supposed wrong directions. We now expect to find large differences.

Several methods have been tried, but had to be rejected, as they gave unsatisfactory results. A good result was obtained by taking into account the sense of rotation of the different binaries. This rotation is either L (left) or R (right). In the case L the rotation of the component is such that when it passes between us and the main star its longitude (galactic) decreases. In the case R, on the other hand, its longitude increases.

In the following the directions of the major-axes corresponding to the cases R and L will be called the R and L direction.

It appears that for the majority of the binary systems the inclination of the L direction with the plane of the Milky Way is smaller than

the inclination of the R direction. Out of 81 cases, 51 give a smaller L value, while 30 cases give a smaller inclination for the R direction.

The best way to prove the importance of the designations L and R is to consider the general distribution curves derived from them.

TABLE III.

Distribution of the Inclinations in Different Latitudes.

Latitude. / Angle. °	0–30°.		30–60°.		60–90°.		0–90°.	
	L.	R.	L.	R.	L.	R.	L.	R.
+90								
	1	3	1	0	0	0	2	3
+60								
	5	5	1	2	0	2	6	9
+40								
	7	7	2	5	1		10	16
+20								
	6	10	5	4	4	0	14	14
0								
	14	5	8	7	3	3	25	15
−20								
	8	12	5	3	2	2	15	17
−40								
	2	2	1	5	1	0	4	7
−60								
	4	3	4	1	0	0	8	4
−90								

In the first place, we consider the inclinations of the L and R directions relative to the galactic plane. For both cases Table III. gives the number of systems whose inclinations are between the limits 90° and 60°, 60° and 40°, etc. With the numbers of Table III. we drew fig. 3.

Comparing them we see that the general aspect of the different L curves is the same. They all have a tendency to a pronounced maximum near zero latitude. In the curve for 30° to 60° we remark a relative large number of axes in the direction of the southern galactic pole. The other local disturbances are of no importance. This is very remarkable, as the total number of all known binaries is only 81. On the other hand, the R curves show large differences. They all show a minimum at zero inclination and two maxima each.

This is just what we should have expected. Suppose that the major-axes of all known binary systems are parallel to the plane of the galaxy, we would have to choose between two directions of the major-axis of each binary. The correct axis would then always be parallel to the Milky Way, while the spurious one would deviate from it. The sign and amount of this deviation ought to depend on the galactic latitude of the stars. The correct distribution-curve would show a maximum at the zero-inclination. The wrong curves should then be resolved into two separate curves, each with its own maximum. The inclination of the one maximum will be negative, that from the other one positive.

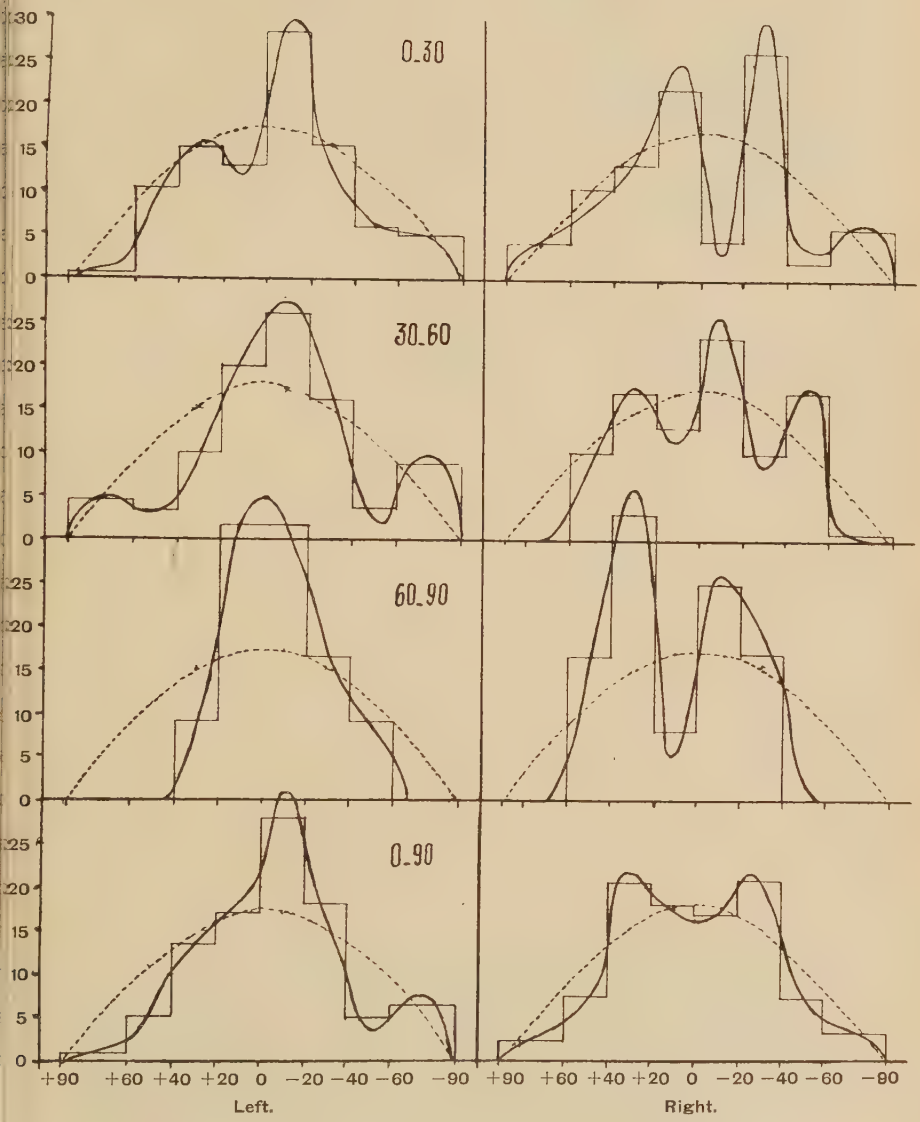

Fig. 3.—The distribution of the inclinations. The dotted curve indicates the random distribution.

In reality the major-axes of the binaries are not exactly parallel to the plane of the Milky Way, but are scattered round it. It is evident that less pronounced maxima are found in the correct as well as in the spurious distribution curves. This will, however, not greatly affect the shape of the curves.

Undoubtedly the L curves in fig. 3 are the correct ones, while the R curves are the spurious ones. From the figure it appears that the probable error of the distribution curves L is rather on the large side, and that there are several systems with a large deviation. For the latter the inclination of the R direction may be smaller than the inclination of the L direction.

TABLE IV.

Longitude Distribution for Different Latitudes.

Latitude. / Longitude.	0°–30°.		30°–60°.		60°–90°.		0°–90°.	
	L.	R.	L.	R.	L.	R.	L.	R.
0°	3	7	2	1	1	0	6	8
30°	6	3	1	0	0	0	7	3
60°	2	4	4	3	2	2	8	9
90°	2	2	1	4	0	0	3	6
120°	2	1	1	1	1	2	4	4
150°	4	3	1	2	2	1	7	6
180°	2	4	2	0	1	1	5	5
210°	2	3	3	3	1	0	6	6
240°	4	9	1	1	1	2	6	12
270°	5	2	1	5	1	1	7	8
300°	11	6	6	2	1	1	18	9
330°	3	3	4	5	0	1	7	9
360°								

Our results are confirmed by considering the longitude distribution of the L and R directions which are given in Table IV. and in fig. 4. The arrangement of the tables and of the figures need not be more fully explained. From fig. 4 we see that the general aspect of the different L curves is the same. In all three curves a well-pronounced maximum is found in the direction $\lambda = 330°$; that is the direction in which probably lies the centre of our stellar system.* On the other hand, we find large differences between the three R curves. They are all very irregular and rather improbable.

* E. A. Kreiken, *M.N.*, 1926, pp. 665–686; J. Oort, *B.A.N.*, pp. 120 and 132, 1927.

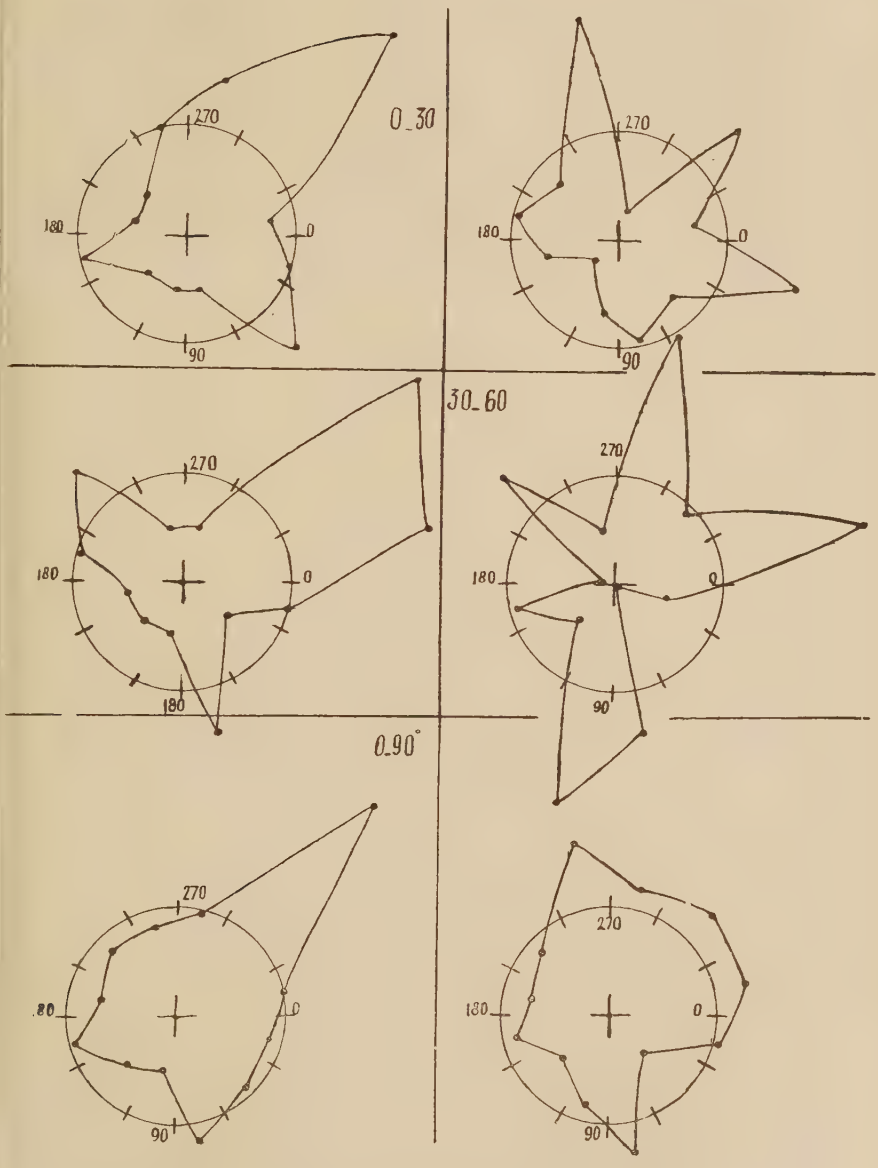

Fig. 4.—The longitude distribution in the cases L and R. The random distribution is indicated by a circle.

I have summarised my results as follows :—

1°.—The space distribution of the major-axes is not a haphazard one.

2°.—There is a strong tendency to parallelism with the plane of the Milky Way.

3°.—A maximum frequency is found in the direction $\lambda = 330°$.

4°.—It is probable that all binaries have a rotation in the same direction, viz. the one which has been called the rotation L.

Further observational evidence is wanted as the definite proof of the fourth statement. As it is, it is still more or less hypothetical.

We must remark that the three binaries, for which we have spectroscopic measures, all have a L rotation. Therefore I think that the observation of a few more pairs would settle this point definitely.

I would be greatly pleased if observers would pay some attention to this case.

Haarlem :
1927 *October.*

κ *Pavonis.* By A. W. J. Cousins.

(*Communicated by Dr. A. W. Roberts.*)

General.—The short-period variable star κ Pavonis is perhaps the most interesting southern variable star of its class. Its brightness led to an early discovery by Thome in 1872,[1] and since then it has been the object of a good deal of investigation.

Approximate elements were published by Gould in the *Uranometria Argentina*, and these were confirmed by Roberts in 1891.[2] From this time on κ Pavonis has been fairly continuously observed ; preliminary results being published in 1893,[3] followed by more accurate elements in 1901.[4] In his notes on the star, Roberts refers to the approximate equality of the ascending and descending branches of the light curve, which is particularly marked in the case of this star.

Some doubt was shed on these elements by Chandler in the revision of his third catalogue, but all uncertainty was cleared up by Roberts in 1904.[5] In this paper a secular variation in the period was brought to light. The period of this inequality is eight years and the amplitude a little over half a day, and hence the period calculated from observations extending over only a few years may differ appreciably from the mean period deduced from a more extended series.

The determination of the variable radial velocity of κ Pavonis by Wright in 1904 led to a more careful investigation of its light variation by Roberts, some results of which were published in 1910.[6] In this paper he draws attention to a secondary phase in the light curve, taking the form of a pause during the rise to maximum. This peculiarity is shown by several distinct series of observations, and is not dependent on the choice of comparison stars.

The present paper serves rather to confirm previous investigations than to extend them in other directions.

Observations.—The present series covers the period 1920 to 1924 with a total of 380 observations, made partly at Pretoria and partly at Johannesburg. The greater number were made with the naked eye, but binoculars were also frequently used when observations were made

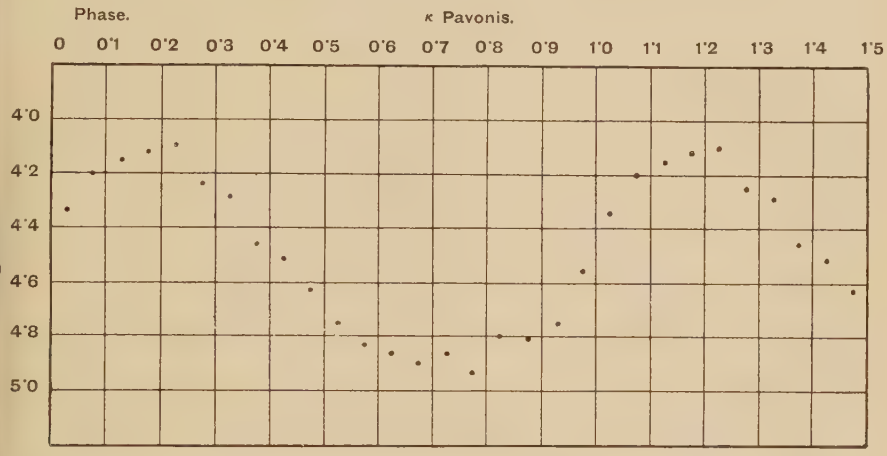

in bright moonlight, since the variable then becomes rather faint for naked-eye observation.

The " step " method has always been used, and in making reductions the value of the step has been assumed 0·1 magnitude for all ranges. The magnitudes of the comparison stars were obtained from the Henry Draper Catalogue. (See Table I.)

TABLE I.

Comparison Stars (Draper Catalogue).

Star.	R.A. (1900). h m	Decl. (1900). ° ′	Phtm. Mag.	Spect.
δ Pavonis	19 59·0	−66 27	3·64	G5
ζ „	18 31·3	−71 31	4·10	Ko
ξ „	14·0	−61 32	4·25	K2
λ „	42·9	−62 18	4·42	B2
ν „	22·0	−62 20	4·81	B8
(3)	35·6	−64 58	4·90	A2
(2)	59·2	−68 35	5·30	Ko
θ Pavonis	18 38·8	−65 14	5·89	A3

The treatment of the observations is similar to that applied to *l* Carinæ.[7]

The "Observed Maxima and Minima" (Table II.) cannot be given much weight individually, and it would not therefore be wise to draw

TABLE II.

Observed Maxima and Minima.

1920.

Maxima.				Minima.			
Date.	J.D. 242–	O–C.	Mag.	Date.	J.D. 242–	O–C.	Mag.
July 31·8	2537·8	+0·3	4·1	Sept. 1·0	2569·0	−0·4	5·2
Aug. 9·3	2546·3	−0·3	4·1	11·3	2579·3	+0·8	5·2
27·7	2564·7	−0·1	4·1	19·4	2587·4	−0·2	5·2
Sept. 5·9	2573·9	0·0	4·0	Oct. 7·4	2605·4	−0·3	5·1
15·3	2583·3	+0·3	4·1	Mean	2551·2	±0·5	
Mean	2546·6	±0·3					

1921.

June 23·6	2864·6	−0·2	4·1	June 29·2	2870·2	0·0	5·0
July 2·8	2873·8	−0·1	4·2	July 8·2	2879·2	−0·1	4·9
11·7	2882·7	−0·3	4·1	16·3	2887·3	−1·1	4·9
30·3	2901·3	+0·1	4·1	27·3	2898·3	+0·8	4·9
Aug. 8·3	2910·3	0·0	4·1	Aug. 4·3	2906·3	−0·3	4·9
17·8	2919·8	+0·4	4·1	14·5	2916·5	+0·8	4·9
26·2	2928·2	−0·3	4·0	24·1	2926·1	+1·3	4·9
Sept. 23·5	2956·5	+0·8	4·0	31·2	2933·2	−0·7	5·0
Oct. 1·8	2964·8	0·0	4·0	Sept. 18·9	2951·9	−0·2	4·8
Mean	2901·2	±0·2		27·5	2960·5	−0·6	5·0
				Oct. 7·2	2970·2	0·0	4·9
				25·5	2988·5	+0·1	4·9
				Mean	2906·6	±0·4	

1922.

June 23·3	3229·3	+0·3	4·0	June 28·1	3234·1	+0·2	5·1
July 1·8	3237·8	−0·3	4·1	July 7·0	3243·0	0·0	4·9
11·2	3247·2	0·0	4·2	16·2	3252·2	+0·1	4·9
29·3	3265·3	−0·1	4·1	24·3	3260·3	−0·9	5·0
Sept. 22·1	3320·7	+0·2	4·1	Sept. 18·0	3316·0	+0·3	5·0
Oct. 28·2	3356·2	−0·1	4·1	Oct. 6·3	3334·3	+0·4	5·0
Mean	3229·0	±0·2		Mean	3233·9	±0·3	

TABLE II.—*continued.*

1923.

Date.	Maxima. J.D. 242–	O–C.	Mag.	Date.	Minima. J.D. 242–	O–C.	Mag.
July 28·0	3629·0	+0·1	4·1	July 15·3	3616·3	−0·4	5·0
Sept. 2·3	3665·3	0·0	4·2	Sept. 8·3	3671·3	+0·1	4·9
11·2	3674·3	−0·1	4·1	Nov. 29·3	3753·3	+0·3	4·9
Mean	3665·3	±0·5		Dec. 8·3	3762·3	+0·1	5·0
				Mean	3671·2	±0·4	

1924.

July 7·3	3974·3	−0·4	4·1	July 21·9	3988·9	0·0	5·1
Sept. 27·3	4056·3	−0·2	4·2	Oct. 2·3	4061·3	−0·3	5·0
Nov. 21·5	4111·5	+0·5	4·1	Nov. 17·4	4107·4	+0·4	5·0
30·3	4120·3	+0·2	4·1	Mean	4052·5	±0·5	
Mean	4047·4	±0·5					

any definite conclusions from them. The residuals have been obtained by applying the mean period to the mean maximum and minimum for the year. In all probability these are principally errors of observation.

In reducing the observations to a mean epoch for each year, or to the mean epoch for the series, the reciprocal period has been used, the value 0·110005 being adopted. The mean light curve thus obtained is shown in the figure.

The "Mean Maxima and Minima" (Table III.) have been determined by two distinct methods: those obtained by a discussion of

TABLE III.

Mean Maxima and Minima.

Maxima.

Year.	A. J.D. 242–	B. J.D. 242–	Mean. J.D. 242–	J.D. 242–
1920	2546·6±0·3	2546·6	2546·6±0·3	3228·5
1921	2901·2±0·2	2901·4	2901·3±0·2	3228·6
1922	3229·0±0·2	3228·9	3229·0±0·2	3229·0
1923	3665·3±0·5	3665·4	3665·3±0·3	3228·9
1924	4047·4±0·5	4047·3	4047·3±0·3	3229·2
			Mean	3228·8±0·2

Minima.

1920	2551·2±0·5	2551·4	2551·3±0·5	3233·2
1921	2906·6±0·4	2906·7	2906·6±0·4	3233·9
1922	3233·9±0·3	3234·2	3234·0±0·3	3234·0
1923	3671·2±0·4	3670·9	3671·1±0·4	3234·9
1924	4052·5±0·5	4052·8	4052·7±0·4	3234·6
			Mean	3234·1±0·3

Table II. are given at A, and those obtained from the annual mean light curves are given at B. These have been combined to give the mean maxima and minima for the series.

Results.—An inspection of the light curve shows a distinct pause during the rise in brightness at the same point as that found by Roberts. The amplitude of variation is, however, considerably less than that found by him, and the pause is hence less pronounced.

An approximate harmonic analysis of the actual (unsmoothed) light curve gives the following expression :—

$$\begin{aligned} M = 4{\cdot}555 &+ 0{\cdot}400 \sin (39^\circ{\cdot}6t + 161^\circ{\cdot}3) \\ &+ 0{\cdot}050 \sin (79^\circ{\cdot}2t + 191^\circ{\cdot}2) \\ &+ 0{\cdot}014 \sin (118^\circ{\cdot}8t + 217^\circ{\cdot}0) \\ &+ 0{\cdot}012 \sin (158^\circ{\cdot}4t + 14^\circ{\cdot}2) \\ &+ 0{\cdot}020 \sin (198^\circ{\cdot}0t + 46^\circ{\cdot}0) \\ &+ 0{\cdot}016 \sin (237^\circ{\cdot}6t + 340^\circ{\cdot}4) \end{aligned}$$

where

M = Magnitude at any instant,

t = Time (in days) after any computed maximum.

Three decimals have been retained in the constant terms, but not more than two can be relied on.

The smallness of the second harmonic (0·125 of fundamental) indicates an unusually symmetrical light curve.

Several attempts were made to improve the value for the period of the star. A discussion of Table III. gives 9·098 days ± ·003 ; and a correlation of the two light curves obtained by grouping the early and later observations separately, gives 9·096 days ± ·004, indicating a period of about 9·097 days, which is not in agreement with the period of 9·091 days obtained from observations of the star made between 1890 and 1910. Assuming this latter period, and using the elements

$$\begin{aligned} T_M &= 2415029{\cdot}5 + 9{\cdot}0910E \\ T_m &= 2415034{\cdot}3 + 9{\cdot}0910E \end{aligned}$$

as an extension of Roberts' paper of 1904, and comparing with the observed mean maxima (Table III.), the residuals are found to be of the same order as those found by him. It would, therefore, appear that the cause of the discrepancy is the secular inequality in the period of the star.

The eight-year cycle does not, however, quite fit the case, and it would be very interesting to extend the investigation to observations made between 1904 and 1920, if such were available.

TABLE IV.

Mean Maxima and Minima.

Maxima.

E.	Date.	Observed.	Calculated.	O–C.
827	1920 Aug. 9·6	242 2546·6	242 2547·8	−1·2
866	1921 July 30·3	2901·3	2902·3	−1·0
902	1922 June 23·0	3229·0	3229·6	−0·6
950	1923 Sept. 2·3	3665·3	3666·0	−0·7
992	1924 Sept. 18·3	4047·3	4047·8	−0·5

Minima.

827	1920 Aug. 14·3	242 2551·3	242 2552·6	−1·3
866	1921 Aug. 4·6	2906·6	2907·1	−0·5
902	1922 June 28·0	3234·0	3234·4	−0·4
950	1923 Sept. 8·1	3671·1	3670·8	+0·3
992	1924 Sept. 23·7	4052·7	4052·6	+0·1

REFERENCES.

(1) *Uranometria Argentina.*
(2) *B.A.A. Memoirs*, **1**, 62, 63.
(3) *A.J.*, 295, April 1893; *B.A.A. Journal*, **3**, 427.
(4) *A.J.*, 491–492, February 1901.
(5) *A.J.*, 563, June 1904.
(6) *Ap. J.*, **34**, 164–171.
(7) *M.N.R.A.S.*, **84**, 621.

An Observational Test of the Accuracy of Mr. Denning's Ephemeris of the Perseid Radiant-point. By A. King.

In the *Monthly Notices* of 1901 December, at p. 169, Mr. W. F. Denning gave an ephemeris of the shifting radiant-point of the Perseid meteor-stream, covering the period July 15 to August 20. He expressed (p. 168) the hope that its correctness would be tested by accurate observations, and further states: "I think it is quite possible that the radiant should be placed a little farther north, particularly at about the period of the maximum, for the presence of the stars γ and η Persei just south of the radiant must probably have exercised a slight influence in leading observers to place the centre too far south."

The following table contains the radiant-points of the Perseid shower derived by the writer from his observations during the years 1898–1927 inclusive, together with comparisons with Mr. Denning's ephemeris. In the fourth column are given the residuals on subtracting observed positions from the corresponding ephemeris-positions, after correcting

the latter for precession to date, the ephemeris being taken as for 1902.* Owing to the lapse of a day in 1900, radiants determined before that year have been advanced a day in working out the mean residuals.

Since the ephemeris gives *average* places, that is, no account was taken of *epoch*, or position, in the cycle of years beginning with leap year, the same course has been followed here.

One radiant deduced from the real path of a shooting star has been added. This was accurately marked by two well-observed apparent tracks mapped by Mr. J. P. M. Prentice at Stowmarket, and by the writer at Ashby.

Date.	Position. α.	Position. δ.	No. of ↓'s.	E−O. $\Delta\alpha$.	E−O. $\Delta\delta$.	
	°	°		°	°	
July 23–24, 1900–1920	23½	+52	6	0·0	0·0	
24, 1920 & '27	24	+52	6	0·0	+0·3	
25, 1925	24½	+52½	5	+0·8	+0·1	Means, $\Delta\alpha$, +0°·0; $\Delta\delta$, +0°·1.
1926	26	+52½	4	−0·7	+0·1	
26–27, 1922–27	27	+53	5	−0·1	+0·1	
27, 1911	27½	+53½	4	−0·3	−0·3	
27–28, 1902	28	+53	4	−0·35	+0·35	
28, 1902 & '25	28	+53½	5	+0·35	0·0	
29, 1922 & '26	29½	+53½	5	+0·2	+0·4	
30, 1911	30	+55	4	+0·6	−0·9	
1922 & '26	31	+55	4	−0·1	−0·8	Means, $\Delta\alpha$, +0°·8; $\Delta\delta$, −0°·9.
1924	30	+55½	5	+0·9	−1·3	
1925	30	+55	4	+0·9	−0·8	
31, 1899–1922	31½	+54½	5	+0·3	−0·05	
1924	33	+54 S.S.P.		−1·0	+0·4	Means, $\Delta\alpha$, +0°·4; $\Delta\delta$, 0°·0.
1926	30¼	+54¾	4	+1·8	−0·3	
Aug. 1, 1899–1924	33	+56	4	−0·1	−1·3	Means, $\Delta\alpha$, 0°·0; $\Delta\delta$, −0°·75.
1926	33	+55	6	+0·1	−0·2	
2, 1919	34	+55	5	+0·2	+0·1	
1920	37	+55	4	−2·8	+0·1	Means, $\Delta\alpha$, −0°·3; $\Delta\delta$, +0°·2.
1922	33	+54½	9	+1·2	+0·6	
1924	34	+55	5	+0·3	+0·1	
3, 1903	34	+55½	6	+1·1	−0·2	
1911	35½	+56½	5	−0·2	−1·2	
1914–23	36	+55	4	−0·6	+0·4	Means, $\Delta\alpha$, −0°·2; $\Delta\delta$, −0°·2.
1926	37½	+55½	4	−2·0	−0·1	
1927	35	+55½	7	+0·5	−0·1	

* So considered by Mr. Denning, in a letter to the writer.

	Date.	Position.		No. of ↓'s.	E−O.		
		α.	δ.		$\Delta\alpha$.	$\Delta\delta$.	
Aug.	3–4, 1900–04	36°	+55°½	5	−0°·25	−0°·1	
	4, 1903	36	+57	7	+0·4	−1·5	Means, $\Delta\alpha$, +0°·2; $\Delta\delta$, −0°·2.
	1923	35	+54	7	+1·8	+1·6	
	1926	38	+56	12	−1·2	−0·4	
	1927	37	+56	8	−0·2	−0·4	
	5, 1919	38	+55	5	−0·1	+0·8	Means, $\Delta\alpha$, +0°·2; $\Delta\delta$, +0°·3.
	1924	37½	+56	8	+0·5	−0·2	
	6, 1904	38	+56½	10	+0·9	−0·5	Means, $\Delta\alpha$, 0°·0; $\Delta\delta$, +0°·4.
	1919	40	+55½	7	−0·8	+0·6	
	1923	39	+55	4	+0·3	+1·1	
	1924–5	39	+56	5	+0·3	+0·1	
	1926	40	+55½	6	−0·7	+0·6	
	7, 1919	41	+57	8	−0·5	−0·7	Means, $\Delta\alpha$, −0°·2; $\Delta\delta$, +0°·2.
	1924	40½	+55½	12	+0·1	+0·8	
	1926	40·6	+56	7	0·0	+0·3	
	1927	41·0	+56·0	8	−0·3	+0·3	
	8, 1904, etc.	41¼	+57	5	+0·25	−0·5	Means, $\Delta\alpha$, +0°·1; $\Delta\delta$, 0°·0.
	1918	42	+57	6	−0·25	−0·4	
	1921	41	+57	11	+0·8	−0·4	
	1923	42	+56	4	−0·1	+0·6	
	1924	42	+56	8	−0·1	+0·6	
	9, 1902	42	+57	4	+0·9	−0·3	Means, $\Delta\alpha$, +0°·3; $\Delta\delta$, −0°·45.
	1901–20	43	+57	5	+0·15	−0·25	
	1918	43	+58	6	+0·2	−1·3	
	1921	43	+57	5	+0·2	−0·2	
	1923	43¼	+57	7	0·0	−0·2	
	9, 1899	44	+57	11	+0·2	−0·1	Means, $\Delta\alpha$, +0°·15; $\Delta\delta$, −0°·2.
	10, 1902	44	+58	9	+0·3	−1·1	
	1907	45	+57	8	−0·6	−0·1	
	1909	44	+57	7	+0·4	−0·1	
	1915	44	+56½	6	+0·5	+0·45	
	1917–18	45	+58	12	−0·4	−1·0	
	1919 & '27	45	+56	4	−0·3	+1·0	
	1923	44½	+57	15	+0·2	0·0	
	1924	44½	+57	8	+0·2	0·0	
	1925	44	+58	8	+0·7	−1·0	
	1926	44⅓	+57	13	+0·4	0·0	

Date.	Position. α.	Position. δ.	No. of ↓'s.	E−O. $\Delta\alpha$.	E−O. $\Delta\delta$.	
	°	°		°	°	
Aug. 10, 1898	45	+57½	4	+0·7	−0·4	
1899	45	+57	29	+0·7	+0·1	
11, 1901	46½	+57	14	−0·8	+0·1	
1904	45½	+57½	32	+0·2	−0·4	
1907	46	+57½	6	−0·3	−0·4	
1914	45	+59	7	+0·9	−1·9	
1917	45⅓	+58½	23	+0·65	−1·3	
1919	46	+57½	7	0·0	−0·3	Means, $\Delta\alpha$, +0°·1; $\Delta\delta$, −0°·3.
1921	46	+58½	45	0·0	−1·3	
1922	46·1	+57	18	0·0	+0·2	
1923	46	+57	16	+0·1	+0·2	
1924	46	+57	16	+0·1	+0·2	
1925	46¼	+57	19	−0·2	+0·2	
1926	46	+57	15	+0·1	+0·2	
1927	46¼	+57	18	−0·1	+0·2	
11, 1898	46½	+58	34	+0·4	−0·7	
1899	46	+57	20	+1·0	+0·3	
12, 1900	48	+58	12	−0·9	−0·7	
1901	47	+58	13	+0·1	−0·7	
1902	48	+56½	6	−0·9	+0·8	
1904	46½	+57½	13	+0·6	−0·2	Means, $\Delta\alpha$, +0°·3; $\Delta\delta$, −0°·2.
1914	46	+56½	9	+1·3	+0·8	
1915	48	+58½	14	−0·7	−1·2	
1918	47	+57½	44	+0·4	−0·2	
1919	46	+58	13	+1·4	−0·6	
1922	47	+57½	7	+0·5	−0·1	
12, 1899	48	+58	7	+0·4	−0·5	
13, 1903 & '11	50	+59	3	−1·4	−1·5	
1914	47	+58½	7	+1·7	−1·0	
1915	49	+58⅔	7	−0·25	−1·1	
1918	49	+57	6	−0·2	+0·5	Means, $\Delta\alpha$, 0°·07; $\Delta\delta$, −0°·7.
1923	48½	+58½	14	+0·4	−0·9	
1925	49	+58½	8	−0·1	−0·9	
1926	49	+58	4	0·0	−0·4	
13, 1899	49	+57	6	+0·9	+0·7	
14, 1903	48	+59½	6	+2·0	−1·8	
1904	50½	+58½	4	−0·5	−0·8	Means, $\Delta\alpha$, +0°·9; $\Delta\delta$, −0°·6.
1914	48	+58	5	+2·2	−0·3	
1926	50½	+58½	12	0·0	−0·7	

Date.	Position. α.	Position. δ.	No. of ↓'s.	E−O. Δα.	E−O. Δδ.	
	°	°		°	°	
14, 1898	51	+58	5	+0·4	−0·2	
1899	50	+59	3	+1·3	−1·2	
15, 1901	51	+58	4	+0·4	−0·2	
1904	52	+57½	4	−0·6	+0·3	Means, Δα, +0°·4; Δδ, −0°·5.
1910	50	+58½	4	+1·6	−0·7	
1920	52	+58	5	−0·25	−0·1	
1923	52	+59	6	−0·2	−1·1	
16, 1925	53½	+59	6	−0·1	−0·9	
1926	53½	+58½	5	−0·1	−0·4	Means, Δα, 0°·0; Δδ, −0°·7.
1927	53·3	+59	8	+0·1	0·9	
17, 1922	55	+60	6	−0·2	−1·7	
17, 1898	56	+59	6	−0·2	−0·6	Compare ephem., Aug. 18.
18–19, 1904–17	57	+59	6	−0·1	−0·55	
19, 1927	58	+59	4	−0·1	−0·5	
21–22, 1900	61	+59	5	+0·2	0·0	(By extension of ephemeris.)
23, 1927	64	+59½	5	..	..	
25, 1927	67½	+60	5	..	..	
26, 1927	69	+60	5	..	..	

Total number of meteors, 1046; of radiants, 121.

Plotting the declination residuals on squared paper, and drawing a smooth curve through them, I find the following *observational* corrections to the ephemeris (epoch 1902):—

Date.	Corr. in Decl.	Date.	Corr. in Decl.
	°		°
July 24	−0·15	Aug. 13	+0·4
Aug. 2	0·0	14	+0·5
6	+0·1	16	+0·6
9	+0·2	18	+0·7
11	+0·3	20	+0·8

Similarly, the following corrections in R.A. were found: July 23–26, 0°·0; Aug. 4, −0°·1; Aug. 14, −0°·2; Aug. 20, −0°·3 (?). These decreases of R.A. are at least in part accounted for by the increase of latitude of the corrected ephemeris.

In *M.N.*, 1892 March, Mr. Joseph Kleiber gave the theoretical places of the cometary radiant as:

July 8, 9°, +46°. Aug. 9·5, 43°·58, +57°·08. Aug. 16, 54°, +59°.

When the corrections given above are applied, it will be seen that the agreement between the ephemeris-places and those based on the cometary radiant is very close. It must be borne in mind that Mr. Denning based his ephemeris entirely on observation, without reference to theoretical considerations.

Conclusions.

1. When the indicated corrections are applied the ephemeris very accurately represents the observational facts.

2. The present series of observations confirms the duration of the shower over the period July 23 to August 26.*

Ashby, Scunthorpe, Lincs:
1927 November 10.

Observations of the Transit of Mercury on 1927 November 10, made at the Royal Observatory, Greenwich.

(Communicated by the Astronomer Royal.)

On the morning of 1927 November 10 the sky was perfectly clear from sunrise at $7^h\ 8^m$ till a short time before egress. A small cloud began to pass over the sun about 5 minutes before third contact and passed off just after third contact. The observations of this contact were made through the thin edge of the cloud, while the fourth contact took place in better conditions. The definition throughout was poor. On account of the low altitude of the sun several instruments could not be used. Visual observations were made with the 28-inch refractor stopped down to 15 inches, the Corbett of aperture 6 inches, and a detached telescope of aperture 4 inches. With the Thompson photo-heliograph a photograph was taken by Mr. Newton about 10 minutes before egress, and three others at 30^s intervals, beginning as soon as the sky was sufficiently clear after third contact.

Dr. Crommelin observed the transit at his home about $\frac{1}{2}$ mile east of the observatory, where the cloud passed off a minute or two before third contact. His observations are included in the following table:—

	h m s	Observer.	Aperture.
Third contact	8 28 7·7	Mr. Witchell	6 inches.
	8 28 14·1	Mr. Furner	15 ,,
	8 27 41·6	Mr. Jeffries	4 ,,
	8 27 51	Dr. Crommelin	3 ,,
Fourth contact	8 29 48·4	Mr. Witchell	6 ,,
	8 29 54·1	Mr. Furner	15 ,,
	8 29 21·3	Mr. Jeffries	4 ,,
	8 29 17	Dr. Crommelin	3 ,,

On the photograph taken at $8^h\ 19^m\ 48^s$ the centre of the planet was about 5·4 mm. from the edge of the sun, the diameter of the sun being 194 mm. Allowing for the motion of the sun and Mercury given on p. 459 of the *N.A.*, it was estimated that the centre of the planet would be on the limb $9^m\ 14^s$ later, so that if we allow half the computed time

* Since the publication of his ephemeris, Mr. Denning has obtained good reason to believe that the Perseid shower lasts from the end of June to the first few days of September.

between third and fourth contact, *i.e.* $\frac{1}{2} \times 101^{s}\cdot3$, we find from this photograph for the time of third contact $8^{h}\ 28^{m}\ 11^{s}$. A photograph taken at $8^{h}\ 28^{m}\ 53^{s}$ showed Mercury not quite half off the disc, so that from it the time of third contact could be judged to be at $8^{h}\ 28^{m}\ 8^{s}$. The probable error of these observations is about $\pm\ 10^{s}$.

When we consider all the data we may conclude as the best value for the third contact $8^{h}\ 28^{m}\ 11^{s}$, and for fourth contact $1^{m}\ 41^{s}$ later.

From the data given on p. 459 of the *N.A.* the times of third and fourth contact were computed to be

$$8^{h}\ 28^{m}\ 23^{s}\cdot9 \qquad \text{and} \qquad 8^{h}\ 30^{m}\ 5^{s}\cdot2,$$

so that the egress appears to have taken place 13^{s} early.

Observations of the Transit of Mercury, 1927 November 10, made at the Radcliffe Observatory, Oxford. By H. Knox-Shaw and W. H. Robinson.

The last phases of the transit were observed under as good atmospheric conditions as could be expected considering the low altitude of the sun. With the Marlborough telescope, with which observations were made from the east window of the Observatory tower, the seeing was distinctly good, but with the Barclay the sun had risen directly over neighbouring chimneys as recently as $8^{h}\ 15^{m}$ and was still involved in their smoke. The seeing was consequently very unsteady with this instrument. The observed times of the contacts, and their differences from the *N.A.* values, are given below :

Barclay Telescope, Aperture 10-in., Power 90, Observer H. Knox-Shaw.

	G.M.T.	O–C.
	h m s	s
Internal contact	8 28 4	−20
External contact	8 29 37	−29

Times were recorded between which the contacts were considered to have occurred ; they were 10 and 7 seconds apart respectively ; the means were taken and are given above.

Marlborough Telescope, Aperture 3¼-in., Power 54, Observer W. H. Robinson.

	G.M.T.	O–C.
	h m s	s
Internal contact	8 28 1	−23
External contact	8 29 30±	−35±

This last observation must be considered as a mere estimate and is deserving of very little weight, owing to serration of the sun's limb and bad definition due to proximity of the line of sight to a wall.

To both observers Mercury's image was round, black and well defined, without any trace of a halo.

Radcliffe Observatory, Oxford
1927 *November* 10.

Observations of the Transit of Mercury, 1927 *November* 10, *made at Cambridge Observatory.*

Dr. Smart and the following members of his practical class—G. J. Nash, B.A. (St. Catherine's), G. Thomerson (Trinity), W. C. G. Knowles (Trinity), J. C. P. Millar (Trinity), F. M. Redington (Magdalene), T. W. Agley (Corpus Christi), C. R. Danham (King's), L. C. Young (Trinity)—attempted the observations of third and fourth contact by means of a projected image formed by the $3\frac{1}{2}$-inch Cooke equatorial. At G.M.T. $8^h\ 27^m\ 38^s$, noted by Mr. Agley—estimated to be within a few seconds of third contact—the phenomenon was lost in clouds. Mr. Green, with the Northumberland telescope, succeeded in observing third contact only, the G.M.T. being $8^h\ 28^m\ 0^s$.

Transit of Mercury observed at Herne, 1927 *November* 10.
By B. M. Peek.

Position of Observatory :

Longitude 1° 6′ 56″ E.
Latitude 51 21 18 N.

Instrument, 150 mm. Zeiss equatorial refractor.

The sky was clear from dawn until after the end of the transit. Mercury was seen on the sun as soon as the telescope could be directed to it, but definition was bad, and on the whole there was little improvement, except for a few isolated moments, one of which was, fortunately, about the time of third contact.

Nothing unusual was observed.

At third contact a " black drop " was seen to form for a few seconds, but it was low and wide, and might have escaped detection had it not been to some extent anticipated.

Third contact was observed with a power of 315, during a temporary improvement in the seeing, as follows :—

	h	m	s
Black drop	8	28	2
Estimated geometrical contact	8	28	6
Calculated from *N.A.*	8	28	24
O–C			− 18

After third contact seeing became exceedingly bad, and the estimated time of $8^h\ 29^m\ 42^s$ for fourth contact can be regarded as little more than a guess.

Although the seeing conditions did not justify it, an attempt was made to measure the diameter of the planet, while on the disc, with the Cooke filar micrometer belonging to the Society.

Four groups of settings were made, but for only one of these could the highest power (315) be used ; neglecting the others, which gave even smaller values, the diameter comes out at only $8''{\cdot}1$—a surprisingly low value even when due allowance is made for irradiation. In such seeing, however, little accuracy could be expected.

Observation of the Transit of Mercury, 1927 *November* 10, *made at Birmingham.* By J. Young.

The following observations of the transit of Mercury were made by Miss M. Rider and Mr. J. Young at the Birmingham University Observatory :—

Phase.	G.M.T. h m s	Instrument.	Observer.
3rd contact	8 28 7	3½-inch refractor	M. R.
3rd ,,	8 28 8	7 ,, ,,	J. Y.
4th ,,	8 29 38	3½ ,, ,,	M. R.
4th ,,	8 29 38	7 ,, ,,	J. Y.

The position of the observatory is—

W. Long. $0^h\ 7^m\ 42^s{\cdot}49$.
N. Lat. $52^\circ\ 26'\ 58''{\cdot}3$.

Egress was observed in a clear sky, but the unsteadiness of the images made the times of contact difficult to estimate. The probable error of internal contact is about 5 seconds, while that of external contact is very much greater.

Observations of the Transit of Mercury, 1927 *November* 10, *near Frome, Somerset.* By C. S. Saxton.

Latitude N.	51° 13′ 24″	
Longitude W.	2 22 16·7	
Altitude 360 feet.		
		h m s
Computed time of third contact (from *N.A.* formula)		8 28 24·6
Observed time		8 28 6·5

Instruments used : 3-inch refractor, power 120, with a stop-watch which was started in agreement with a marine chronometer and stopped at the contact about two minutes later. The chronometer was checked by wireless time-signals at $18^h\ 30^m$ on November 9, and again at $10^h\ 30^m$ on November 10. In stating the above time of observed contact an allowance has been made for an estimated error of one second by delay in stopping the watch owing to the unexpectedly early occurrence of the contact.

An equatorial reflector with 8½-inch mirror could not be used owing to obstructed view, but in any case is not very satisfactory for solar observations.

No black drop was seen.

Weather conditions very good.

Observer, C. S. Saxton.

Observations of the Transit of Mercury, on 1927 November 10, at the Astronomical Observatory, Kiew. By Professor S. D. Tscherny.

(*Communicated by the Secretaries.*)

1. *Observers and Instruments.*—Professor S. D. Tscherny (T): Merz-Repsold refractor, aperture 243 mm., stopped down to 125 mm., magnifying power 145.

O. Fialkowskaja (F): Goerz refractor, aperture 70 mm., magnifying power 58.

N. Pisarenko (P): Utzschneider and Fraunhofer refractor, aperture 70 mm., magnifying power 74.

2. *Observations of Contacts.*

	h m s	Obs.	O−N.A. s	O−C.d.T. s	Remarks.
Third Contact : Greenwich Mean Time	8 27 45·03	T	−28·46	−28·54	
	8 28 5·37	F	− 8·12	− 8·20	
	8 28 5·01	P	− 8·48	− 8·56	
Bisection of Mercury : Greenwich Mean Time	8 28 41·87	T	−22·25	−22·13	Windy. Clouds.
Fourth Contact : Greenwich Mean Time	8 29 18·77	T	−35·99	−35·67	
	8 29 12·69	F	−42·07	−41·75	
	8 29 13·83	P	−40·93	−40·61	

3. *Observations with the Filar Micrometer.*—The atmosphere was very unsteady, and the clouds interfered with the observations. The diameter of Mercury was measured by Professor Tscherny ten times, with the following results :—

	r
	0·271
	0·269
	0·255
	0·261
	0·250
	0·268
	0·301
	0·253
	0·273
	0·269
Mean	0·2670

The value of one revolution of the micrometer screw for the temperature at the time of observation (+ 10°·0 R.) is 28″·3565, and therefore we have for the diameter of Mercury (the differential refraction is taken into consideration) 7″·59, with the probable error ± 0″·086. The diameter of Mercury given in the *Nautical Almanac* is 9″·86, and therefore O − C = − 2″·27. During the transit of Mercury on 1924 May 7, we obtained (*M.N.*, **84**, 544) 10″·33 ± 0″·170 and O − C = − 1″·65.

For unit distance we obtain from our observations the following values of the diameter of Mercury :—

		Bessel (1832).	O−B.
1924 May 7	5″·76	6″·68	−0″·92
1927 Nov. 10	5·13	6·68	−1·55

Our values of the diameter of Mercury are near the following values :—

Gambart	(1832)	− 5″·18
Maclear	(1868)	− 5·65
Duner	(1868)	− 5·95
Bruhns	(1878)	− 5·90
Peter	(1878)	− 5·97
Schroeder	(1878)	− 5·92
Copeland	(1878)	− 5·92
Campbell	(1894)	− 5·73
See	(1901)	− 5·90

Astronomical Observatory, Kiew :
1927 *November* 24.